An investigation into the relationship between surface concrete resistivity and chloride conductivity tests

Lombe Mutale

Supervisor: A/Prof. Hans-Dieter Beushausen

Co-Supervisors: Prof. Mark G. Alexander and Mr Mike Otieno

February 2014

Thesis presented for the degree of Masters of Science

In the Department of Civil Engineering

University of Cape Town

DECLARATION

I, Lombe Mutale know the meaning of plagiarism and declare that all the work in the documents, save for which is properly acknowledged is my own.

Signature: _____

ABSTRACT

The chloride conductivity test (CCT) is a South African-developed Durability Index (DI) test used for the evaluation and quantification of the quality of concrete cover. It is also used as an input parameter for service life prediction (SLP) of RC structures in the marine environment, using a modified version of Crank's solution to Fick's second law of diffusion. The surface concrete resistivity test is an electrochemical test that has a good correlation with the concrete chloride diffusion process. The surface concrete resistivity test is used as a quick way to determine the durability of concrete.

The purpose of this study was to provide an in-depth literature review on surface concrete resistivity and investigate its use for the design and prediction of durability in RC structures. The study also compared and contrasted surface concrete resistivity with CCT, using results from previous work, in terms of their application in the design of RC structures. Thereafter, the study investigated the relationship between surface concrete resistivity and CCT.

The study was carried out by comparing laboratory and field surface concrete resistivity with CCT results. Then, corrosion initiation periods (CIP's) and diffusion coefficients were estimated using Mackechnie's (1996) CCT SLP model as well as surface concrete resistivity models by Andrade (2004) and Baroghel-Bouny et al. (2009). Input parameters for the model such as surface concrete resistivity and CCT results were based on measurements from a previous study. It was found that moisture gradients, chloride contamination and temperature gradients easily influence concrete electrical resistivity testing done in-situ. The input parameters for the surface concrete resistivity models were restricted to laboratory results.

The analysis revealed that for blended cement concrete, w/b ratio has a greater influence on chloride conductivity than binder type. It was observed that using a different binder type has a greater influence on surface concrete resistivity at a high w/b ratio than a low one. In addition, decreasing the w/b ratio for GGBS concrete is more effective than decreasing it for FA concrete in influencing the surface concrete resistivity. Andrade's surface concrete resistivity SLP model resulted in similar CIP values as the CCT model for CEM I only concrete and slag concrete at 0.40 w/b. A constant links the diffusion coefficients from surface concrete resistivity and CCT models. An inverse relationship was found between surface concrete resistivity and the diffusion coefficient calculated from the CCT SLP model.

ACKNOWLEDGEMENTS

A/Prof. Hans Beushausen

Prof. Mark Alexander

Mr Mike Otieno

Ms Elly Yelverton

CoMSIRU

Ms Katlego Loeto

Ms Gladwell Nganga

Mr Nicholas Kizito

Mr Matongo Kabani

Mr Sultan Hassan

Family and friends

TABLE OF CONTENTS

LIST OF FIGURES

LIST OF TABLES

1 INTRODUCTION

1.1 Background

Durability refers to the ability of a structure or component to withstand the design environment over the design life, without undue loss of serviceability or need for major repair (Ballim et al., 2009). Baroghel-bouny et al. (2009), assert, "long-term durability of reinforced concrete structures (RC) is a major concern for safety, economic and environmental reasons." There is an increasing number of RC structures and components of infrastructure that are not durable and are failing to realise their design service life (Alexander et al., 2008). Consequently, many resources in form of time and human capital continue to be expended towards their repair and rehabilitation. The public has also continued to suffer from the lack of durability of structures – especially during the closure of roads and bridges during repair, as well as in the event of high maintenance costs. This inability of RC structures to realise their intended service life has necessitated the study of concrete durability and factors that hinder it such as corrosion of steel reinforcement.

Corrosion of reinforcing steel is caused by the ingress, through the concrete cover, of deleterious species such as chloride ions and carbon dioxide. The degree of penetration of these species into the concrete depends on the quality of the construction materials, construction practices and their exposure environment (Otieno et al., 2011b). Knowledge of these factors facilitates accurate prediction of the corrosion rate and consequently the service life, which will lead to more durable concrete structures (Ahmad, 2003). For this reason, performance-based specifications are used whereby relevant material properties are tested to predict the ingress of deleterious substances. This ensures that:

> …the concrete selected for a specified design life achieves the desired quality and chemical resistance to deterioration that was assumed at the design stage (Alexander et al., 2011).

The performance-based approach relies on measuring material potential and construction quality to determine future performance of the concrete structure. An important aspect of the approach is test methods for determining and predicting the durability of RC structures. The test methods measure material potential by linking transport mechanisms and deterioration mechanisms and are then used as input parameters in service life prediction models.

1.2 The use of surface concrete resistivity tests– current trends

Surface concrete resistivity tests are quick and simple tests that assess the resistance of concrete against the ingress of ionic species. The use of surface concrete resistivity tests to supplement existing durability tests has become widespread around the world (Riding et al., 2008). Its

popularity stems from its non-destructive nature, rapidness and ease of use compared to other tests. Another reason is the current trend to shift from the traditional prescriptive-based approach to the performance-based approach for design, making the issue of durability more pertinent than before. Concrete resistivity is linked to durability as many researchers have identified its correlation with diffusion, a prominent parameter in the determination of concrete durability (Kessler et al., 2008; Polder, 1995; Sengul and Gjorv, 2008). Therefore, the test is an ideal candidate for the performance-based design approach.

In South Africa, the performance-based approach makes use of durability index (DI) testing comprising the water sorptivity test, oxygen permeability test and the chloride conductivity test (CCT). While these tests fare well when compared with other durability tests in terms of reproducibility and repeatability (Beushausen and Alexander, 2008), exploration of ways in which the DI can be supplemented with other tests is a worthy endeavour. The CCT in particular produces similar results with other tests with which the surface concrete resistivity test is being compared. Similar to the CCT, surface concrete resistivity test is a handy tool because of the ease with which it can be used to quantify the quality of concrete. While the CCT is characterized as a service life prediction and quality control tool, surface concrete resistivity is traditionally merely a means for condition assessment of RC structures. Surface concrete resistivity is used to assess the capacity of the concrete to allow corrosion to occur and evaluate the rate at which corrosion is occurring in concrete (Alonso et al., 1988; Broomfield, 2007). However, many other uses of surface concrete resistivity have been identified. For instance, currently in the USA, concrete resistivity is replacing the Rapid Chloride Penetrability Test (RCPT) for use as a quality control parameter during construction to test concrete permeability (Kessler et al., 2008; FDOT, 2004). In the Netherlands, it is also used as a means for quality control during construction (Rooij et al., 2007; Polder et al., 2010). Similarly, in Spain, the 28-day concrete resistivity result is being used as a means for service life prediction incorporating both the corrosion initiation and propagation periods (Andrade and Andrea, 2010; Andrade, 2004). Additionally, it can also be used to calculate the effective chloride diffusion coefficient (Baroghel-Bouny et al., 2009).

1.3 Research motivation

According to Icenogle et al. (2012) and Rooij et al. (2007) reasons for the move towards surface concrete resistivity in durability studies and research include its:

- correlation with chloride diffusion
- intuitive nature – a high resistivity indicates better quality concrete than a low resistivity
- simplicity and ease of use – the test is not highly technical and can easily be taught
- rapidness compared to other tests

- non-destructive nature
- small voltage is used when testing resulting in non-destruction of the concrete microstructure
- cheap – substantial cost savings were noticed compared to when the RCPT was used
- accuracy – low standard deviation between tests

Controlling the concrete properties of diffusion and resistivity is linked to improved durability, which diminishes the likelihood of early corrosion (Mackechnie, 1996). On the one hand, there are numerous studies on the use of the CCT to obtain the diffusion coefficient and service life of RC structures, although these are mostly done specifically for South African marine conditions. On the other hand, globally, there is an ongoing shift towards surface concrete resistivity as a rapid means to predict concrete durability. However, there is a lack of research thoroughly investigating how surface concrete resistivity is used in the design of RC structures and its relationship with the CCT.

Although it is intuitive that a correlation exists between the CCT and concrete resistivity, there is insufficient research or literature on the exact nature of the relationship between the two. In fact, there has been no reported attempt to quantify or relate the two. However, some studies have been done that show a good correlation between the results from the RCPT and concrete resistivity (Smith et al., 2004; Feldman et al., 1999). Since RCPT and CCTs also have a good correlation (Beushausen and Alexander, 2008), it is reasonable to propose that there could be a relationship between the CCT and surface concrete resistivity.

1.4 Objectives

The primary objective of this study is to:

i) Investigate the relationship between surface concrete resistivity and CCT.

Other secondary objectives are listed below:

- Carry out a comprehensive literature review of surface concrete resistivity test by:
  - Establishing its properties and theoretical basis
  - Identifying the strengths and limitations of the test method
  - Discussing existing models for service life prediction and design of reinforced concrete structures
- Compare and contrast surface concrete resistivity with CCT, using results from previous work, in terms of their use in the design of RC structures:

1.5 Limitations and scope of the research

The bulk of the thesis will be a literature review and an analysis of surface concrete resistivity and CC results from a previous study by Otieno (2014). The use of another researcher's work is a major limitation because there was no control over the parameters tested. For instance, though not recorded, temperature and porosity would have been useful in this study. This research is limited to:

- Five mixes and three binders namely, CEM I or 100% Portland cement, 50/50 GGBS and 70/30 fly ash.
- Two w/b ratios of 0.40 and 0.55.
- Results for field and lab surface concrete resistivity tested over a period of two years for each mix.
- 28-day and 90-day CCT results for each of the five mixes.

1.6 Thesis outline

The thesis is divided into five chapters with *Chapter 1* introducing the topic and explaining the motivation for the study.

Chapter 2 is a three-part literature review discussing 1) transport mechanisms and chloride ingress in concrete, 2) the various aspects of the CCT including its underlying theory and use in prediction of concrete cover durability and 3) surface concrete resistivity focussing on its fundamental aspects, influencing factors and uses in the concrete industry around the world.

Chapter 3 describes the research methodology followed to achieve the aims of this study. The chapter includes a description of the data and procedures for each of the three models used in the study.

Chapter 4 firstly presents the surface concrete and CCT results from Otieno's (2014) study. This is followed by a presentation and discussion of the model outputs and an investigation into the relationship between surface concrete resistivity and the CCT.

Chapter 5 is a treatise on the conclusions and recommendations that can be drawn from the literature review and data analysis.

2 LITERATURE REVIEW

2.1 INTRODUCTION

It is well known that chloride ingress into concrete is of particular concern in marine environments. The reason for this is that its presence is a major factor in the initiation and propagation of chloride-induced corrosion. The exact nature and characteristics of chloride-induced corrosion are determined by the diffusivity and resistivity capabilities of the concrete. This chapter is a critical synthesis of the available literature on specific aspects of chloride ingress, the surface concrete resistivity and chloride conductivity tests (CCT) to feed into the current study as shown in Figure 2.1. The focus of the study is on how the tests compare in terms of underlying theory, service life prediction, quality control and ease of use.

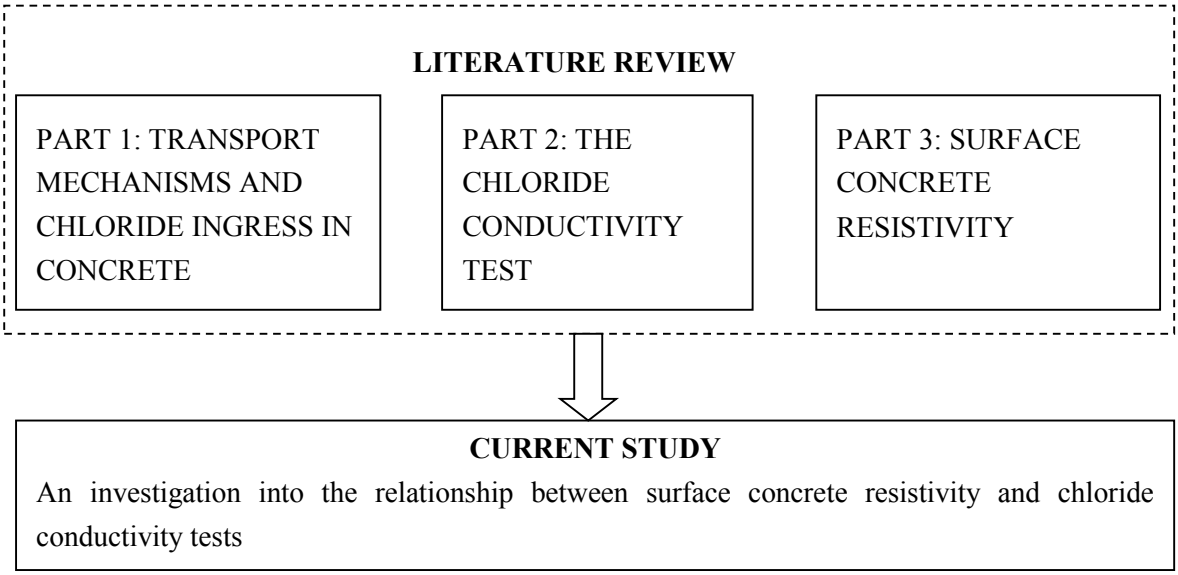

Figure 2.1: Schematic of literature review

In a study of concrete chloride ingress and resistivity, it is imperative to establish the underlying mechanisms and theories that are used in their analysis. This includes the exact nature of the transportation process of species through concrete and the associated test methods. As will be seen, most transport processes can be modelled mathematically using time-dependent equations, thereby making it possible to predict the species behaviour given certain conditions. This is achieved using test methods that are related to transport processes.

Specific test methods used around the world to test chloride ingress in concrete will be described and compared with those of the CCT. The CCT is one of three Durability Index (DI) test methods for quantifying the quality of concrete in South Africa. The CCT includes a service life prediction (SLP) model for the corrosion initiation period (CIP), which will also be discussed.

The chapter also gives an analysis and description of surface concrete resistivity test methods. The focus will be on the Wenner probe as this was found to be the most popular method in practice. Its usage as a quality control parameter during construction and use for SLP purposes will be discussed. There will also be a detailed explanation of theoretical and practical basis of the test and its sensitivity to varied test conditions.

Lastly, all of the above will provide a foundation for the comparison and dissection of the relationship between various components of the two tests in a comprehensive and all-encompassing conclusion. This will pave the way for the current study as depicted in Figure 2.1.

2.2 PART 1: TRANSPORT MECHANISMS AND CHLORIDE INGRESS IN CONCRETE

2.2.1 Transport mechanisms in concrete

To form concrete, binders such as Portland cement, ground granulated blastfurnace slag (GGBS), fly ash (FA) and condensed silica fume (CSF) react with water to produce cementing products. The products of this reaction are the paste that holds aggregates together to form the composite material that is concrete. These binders are mostly composed of the compounds lime, silica and alumina in different proportions as shown below.

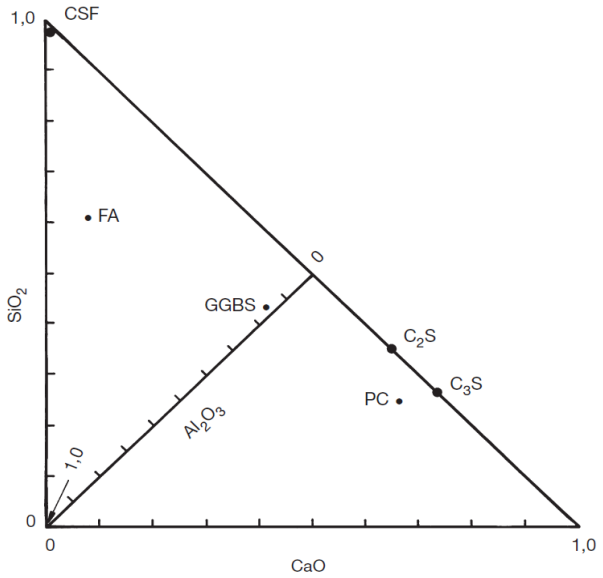

Figure 2.2: Proportions of lime, silica and alumina in binders

(where C_2S, C_3S refer to di- and tri-calcium silicate respectively) (Grieve, 2009b)

The aggregates are usually assumed to be inert so that the paste is the determinant of the reactivity of the concrete. The chemical and physical composition of the concrete will determine its properties such as transport processes. Transport processes in concrete refer to

the means by which deleterious species such as chloride ions, sulphates, oxygen and carbon dioxide move through the concrete and eventually react with the reinforcement. Transportation of these species in concrete occurs through the pore spaces in the cement paste (microstructure) and the inter-facial transition zone (ITZ) (Poulsen and Mejlbro, 2006).

The science of transport processes is studied to understand the mechanisms by which deleterious species from the environment and in the concrete move through the pores in concrete causing deterioration. In marine environments such as Cape Town, chloride-induced corrosion is the major form of deterioration for reinforced concrete structures (Broomfield, 2007). Both the chloride conductivity and surface concrete resistivity tests measure concrete properties linked to transport processes, suggesting that they can be tools for the assessment of concrete durability (Poulsen and Mejlbro, 2006). Examples of transport processes are described below.

2.2.1.1 Permeation

Permeation is the movement of a fluid from a zone of high hydraulic pressure to one of low hydraulic pressure through a porous medium. It is easier to assess the permeability of gases through the fluid such as oxygen and carbon dioxide as opposed to ions such as chlorides and sulphates. The reason for this is that various ions present in concrete make it difficult to isolate the movement of a single ion. The Oxygen Permeability Index (OPI) test is a Durability Index (DI) test for measuring oxygen permeability in South Africa (Alexander et al., 1999a) and the Torrent Permeability Tester is its European counterpart (Lindvall, 1998). The OPI test is based on Darcy's Law and assesses i) the degree of concrete compaction and ii) interconnectedness of the microstructure (Ballim et al., 2009).

2.2.1.2 Absorption

Absorption refers to the pull of water or capillary suction. This occurs when water is drawn into the concrete pores or specifically unsaturated material. Examples of ions that undergo absorption into the concrete include chlorides and sulphates. As one would expect, the capillary suction force decreases rapidly as the degree of saturation increases. The process usually occurs near the surface of the concrete where the degree of saturation is effectively zero (McCarter et al., 1992). It is near the surface (less than a centimetre) that absorption begins as moisture-containing ions are transmitted from the environment into the concrete. Deeper in the concrete, the process is impeded by aggregates and the increased degree of saturation. For this reason at greater concrete depths, the ions are more likely to move through the action of other transport processes such as diffusion (McCarter et al., 1992).

In marine environments, water absorption increases the surface chloride concentration, which subsequently leads to chloride diffusion into the depths of the concrete. A similar situation

occurs under wetting and drying conditions. The water sorptivity test is the (DI) test for the measurement of the concrete absorption process, with a low value indicative of a good quality concrete. Unlike most absorption tests, it can be used to measure both the porosity and the sorptivity (Ballim et al., 2009). More details on the theory and particulars of absorption are available in McCarter et al. (1992).

2.2.1.3 Adsorption

Adsorption is the ion binding process that captures ions from the capillary pores into the concrete microstructure so that they cannot be transferred or react with other materials (Claisse, 2005). Adsorption depends on the matrix chemistry, which is a function of the binder type. Aluminium oxide (Al_2O_3) or alumina is part of the chemical composition of most binders as shown in Figure 2.2 above. Alumina reacts with chlorides to form a compound with the hydration products or chemically bind the chloride (Luo et al., 2003; Thomas et al., 2012). However, the chlorides compete with hydroxides and sulphate ion to react with the alumina so that the more alkaline the concrete the less the bound chlorides.

The adsorption process is important as it determines the number of ions, particularly chloride ions that are either chemically bound or physically bound. The chloride ions that have been adsorbed can be determined by calculation of the acid soluble (total chlorides) and the water soluble (free chlorides). The difference between the two is the adsorbed chlorides (Claisse, 2005).

2.2.1.4 Migration

Migration is the flow of cations or anions towards an applied negative or positive electric field respectively. Consequently, migration only occurs when zones have differing electrical potentials. When an electrical field is applied to the surface of concrete, hydroxides are depleted and chlorides are replenished as chlorides are attracted to the negative electrodes while hydroxides are attracted to the positive electrodes. Illustrated in Figure 2.3 below, migration provides a means to measure the ionic flux through concrete. The cathode is upstream and placed in a catholyte (NaOH) while downstream is the anode placed in an anolyte (NaCl).

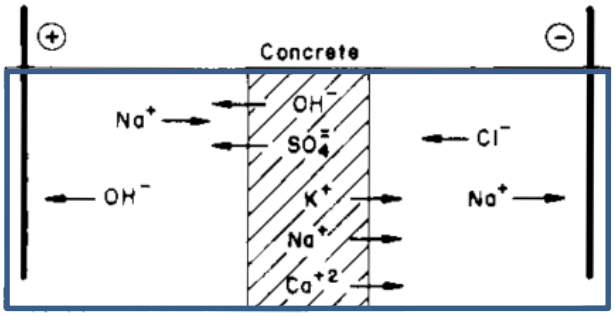

Figure 2.3: Setup for migration of ions in concrete

(Andrade, 1993)

Another type of migration is thermal migration, which occurs due to the presence of a temperature gradient causing ions to flow from a warm region to a cooler region. For instance, marine concrete structures are prone to salt ingress after exposure to warm weather. Due to its rapidness, migration is the usual mechanism by which the transport of species through concrete are measured and related to slower processes such as diffusion using the Nernst-Planck equation (Kropp and Alexander, 2007). The Nernst-Planck equation sums up the equations for convection, electrical migration and diffusion, and equates them to the total ionic species flux. The equation is discussed further in Section 2.2.3.2.

2.2.1.5 Diffusion

Diffusion is a time-dependent process of random particle interaction solely driven by concentration differences between adjacent zones i.e. ions move from zones of high concentration to zones of low concentration (Cerny and Rovnanikova, 2002). Diffusion of ions such as sulphates and chlorides can occur in partially saturated concrete. The process is usually modelled by immersing a concrete in solution with two different concentrations on either side similar to that shown in Figure 2.4.

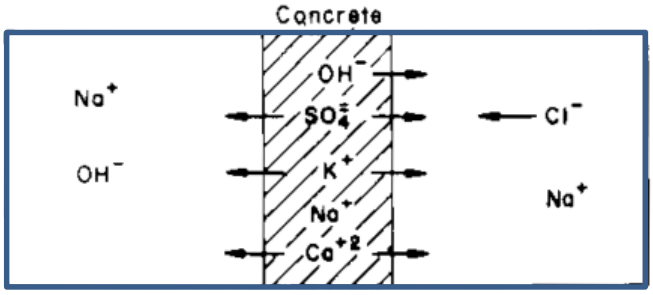

Figure 2.4: Setup for ionic diffusion process in concrete

(Andrade, 1993)

From the figure above, the chloride ions will move from the NaCl solution through the concrete, to the NaOH solution compartment at constant pressure. This setup is used to

determine the concrete resistance to the diffusion of deleterious species. It is known that diffusion is the predominant transport process in concrete when no electric field has been applied and the moisture conditions are steady or when the concrete is fully saturated. In other words, diffusion is the most likely mechanism by which transportation of ions occurs in concrete. Therefore, it is imperative to understand the principles and underlying theory regarding concrete diffusion and its application.

2.2.2 Fick's 1st and 2nd laws of diffusion

Fick's laws of diffusion are used to model the process of diffusion in concrete. The principles of the equations are based on a setup such as the one in Figure 2.4. The underlying theory is valid provided the following assumptions (Lu, 1997) are adhered to:

(i) The fluxing species do not react with the matrix

(ii) The matrix has a homogenous structure and composition

Saturated conditions and a constant pressure must be maintained for the assumptions to remain valid. Fick's first law of diffusion states that the flux of ions diffusing through the matrix is directly proportional to the rate of change of the concentration with distance;

$$F = -D\frac{\partial C}{\partial x} \qquad (2.1)$$

where C is the concentration of the ion at a specific time t and point x; F is the flux; D is the diffusion coefficient

Evidently, a high flux implies a high diffusion coefficient. In comparison, Fick's second law of diffusion (Equation 2.2) is a mathematical description of the change in concentration per unit time equated to the change in flux per unit length.

$$\frac{\partial C}{\partial t} = \frac{-\partial F}{\partial x} \qquad (2.2)$$

where C is the concentration of the ion at a specific time t and point x; F is the flux.

When the concentration increases the flux or diffusion reduces. In other words, the parameters increase in opposing directions and this is the reason for the negative sign in the equation. Taking the derivative of Equation 2.1 and equating it to Equation 2.2 yields a simplified version of Fick's second law:

$$\frac{\partial C}{\partial t} = D\frac{\partial^2 C}{\partial x^2} \qquad (2.3)$$

where C is the concentration of the ion at a specific time t and point x; F is the flux; D is the diffusion coefficient

Although, both ions and gases diffuse through concrete, the modelling of diffusion is usually restricted to saturated conditions, such that only ions are involved. While sulphates and chlorides both diffuse, the focus is primarily on chlorides due to their participation in the steel reinforcement corrosion process. For this reason, the *C* in Fick's laws usually refers to the concentration of chlorides ions in concrete.

Obtaining the diffusion coefficient by means of Fick's 1st law is not favourable due to the stringent requirement of steady state conditions (Andrade, 1993). Consequently, Fick's 2nd law is favoured by most researchers. Crank's solution given in Equation 2.4 is the preferred approach to solving Fick's 2nd law of diffusion.

$$C_x = C_s\left(1 - \mathrm{erf}\left(\frac{x}{\sqrt{4Dt}}\right)\right) \qquad (2.4)$$

where *D* is the diffusion coefficient; C_s is the surface chloride concentration; C_x is the chloride concentration at time *t* and depth *x*; *erf* is the mathematical error function

The use of Crank's solution in SLP is based on work by Collepardi et al. (1972) who showed that it could be applied to chloride diffusion in concrete. Details can be found in Crank (1979). The solution is valid only if the boundary and material properties are constant and the initial conditions are such that: $C_x = 0$ when $x > 0$ and $C_x = C_s$ for $x = 0$. In other words, it is assumed that initially there are no chlorides in the concrete and the only chlorides in the system are the surface chlorides. As will be seen later, this equation is an integral part of the determination of the service life of marine reinforced concrete structures prone to chloride ingress.

Nevertheless, the concrete industry is not unanimous in its decision to use Fick's second law as a basis for modelling diffusion. For example, Marchand & Samson (2009) have raised concerns over assumptions specified in the use of Fick's law. For instance, they state that the assumption of saturated conditions to ensure that only diffusion occurs is not completely adhered to. In addition, it is suggested that the simplified chemical interactions in the diffusion of concrete setup (Figure 2.4) do not accurately represent the cementitious compounds and environment of RC structures. Furthermore, they found that dependence on the environment makes the equation unsuitable for relating laboratory measured concrete to site exposed concrete. Instead of Fick's law, the use of more complex models with a wider variety of input parameters is recommended (Marchand and Samson, 2009).

While the concerns raised are valid, most models not only use experiments conducted in the laboratory but also have them validated with existing structures. Consequently, any inherent errors in the equations used are accounted for in this manner, as will become apparent later in this chapter. Furthermore, the large number of input parameters that would be required for the models proposed would not be feasible for practical use (DuraCrete, 1998).

2.2.3 Calculation of diffusion coefficients using chloride profiles

One way of calculating diffusion coefficients from Crank's solution is by fitting chloride profiles obtained through controlled experiments over time to Equation 2.4 (Muigai et al., 2012; Morris et al., 2002; Yuan et al., 2009). A chloride profile (Figure 2.5) is a graph of chloride concentration in percentage mass concrete versus distance from chloride exposed surface concrete. More often than not, the chloride content is higher at the surface and decreases with cover depth as depicted in Figure 2.5. This agrees with the assumption in Equation 2.4.

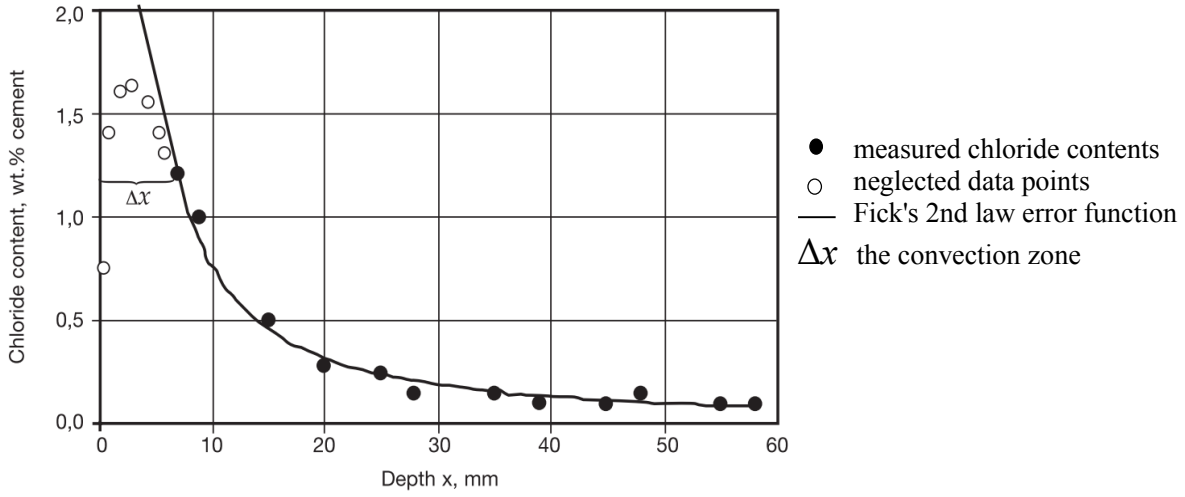

Figure 2.5: Typical measured chloride profiles

(Ballim et al., 2009)

Tests such as the bulk diffusion test are used to establish the chloride profile of a concrete specimen. This is achieved by grinding and testing the specimen for chloride concentration at different depths along the length of the sample. The chloride profile is then fitted into Crank's solution (Equation 2.4) to obtain the two unknowns – the surface chloride concentration and the apparent chloride diffusion coefficient. The best fit is determined using curve fitting software, as done in the figure above, or regression analysis such as a least squares fit.

Chloride profiles are classified as either achieved or potential. The achieved chloride profile results from exposure of a concrete specimen in a certain environment. The potential or estimated chloride profile results from laboratory controlled conditions such as temperature and exposure to a standard solution of chloride (Poulsen and Mejlbro, 2006). Both profiles depend on the initial chloride content of the concrete, the chloride concentration at the surface of the concrete and the chloride diffusion coefficient (Poulsen and Mejlbro, 2006). Given the diffusion coefficient and surface chloride concentration, the chloride profile can be predicted using Fick's second law of diffusion and vice versa.

Rather than using the chloride profile approach, relationships of diffusion coefficients with accelerated migration and diffusion tests have been established (Whiting, 1981; Andrade, 1993). These are divided into two. The main ones are the steady state tests that do not account for binding but focus on ionic chloride transport only, such as the CCT. The less common ones are the non-steady state tests that do such as the Nord Test (Muigai, 2008). Others such as the Multi-Regime Method (MRM) are known to measure both steady state and non-steady state diffusion coefficients (Castellote and Andrade, 2009). These and others will be explored in more detail in the sections that follow.

Heiyantuduwa et al. (2006) and Song et al. (2008) state that when making use of these accelerated test methods it is worth considering the following:

(i) The effect of chloride binding and considering that carbonation reduces the amount of bound chlorides.

(ii) The diffusion of chlorides into concrete and that the buildup of the surface chlorides can be time-dependent. Moreover, both are dependent on binder types and surface treatments. The surface chloride concentration is also dependent on the distance to the sea.

(iii) The effect of the ongoing hydration process, temperature changes and environmental conditions on the concrete.

2.2.3.1 Time-dependent chloride diffusion

The surface chloride concentration increases with time while the diffusion coefficient reduces with time. Usually either the time-dependent aspect of the surface chloride concentration or diffusion coefficient is incorporated into Crank's solution. Researchers usually focus on the time-dependent aspect of the diffusion coefficient (Nokken et al., 2006). The reason for the preference could be that environmental factors affecting the surface chloride concentration are more complex to predict. The reduced diffusion coefficient is linked to the improved microstructure of the concrete with continued hydration as well as chloride binding. Therefore, the time reducing factor depends on the mix proportions of the concrete. It is common practice to lower the measured diffusion coefficient using the following equation:

$$D(t) = D_0 \left(\frac{t_0}{t}\right)^m \tag{2.5}$$

where $D(t)$ is the diffusion coefficient at time t, D_0 is the diffusion coefficient at reference time t_0, m is the reduction factor

The above equation was employed by Mangat and Molloy (1994) who highlighted the exponential relationship in the reduction of the diffusion coefficient with time. Thereafter, they

validated the equation with experimental data. This has been confirmed more recently by various other researchers (Nokken et al., 2006).

Once the diffusion coefficient at the starting time is measured, the apparent diffusion coefficient is plotted with time on a log-log scale. Subsequently, the value of the reduction factor from Equation 2.5 is obtained using linear regression analysis. It is worth noting that methods for the calculation of the reduction factor make use of either the average time, effective or total time of chloride exposure thereby producing different values. The total time gives the least value of reduction factor while the effective time produces the greatest value (Nokken et al., 2006). Details on the latter can be found in Stanish and Thomas (2003).

2.2.3.2 The use of migration to calculate the diffusion coefficient

While diffusion is the main transport mechanism by which chlorides move through concrete, it may take up to a year to reach steady-state conditions. This made it impractical for use as a rapid test method for quickly establishing the quality of concrete.

It is well known that an applied voltage speeds up the movement of ions through a medium by the process of migration. In view of that, migration was identified as a suitable alternative to diffusion, in a quest to establish a rapid test to measure chloride transport through concrete (Whiting, 1981). The Nernst-Planck equation is a description of the transport processes occurring in solution when an electric field is applied. The equation states that the flux is a sum of the migration, diffusion and convection processes as depicted in Figure 2.6. A concrete specimen is immersed in a chloride solution on one side and a sodium hydroxide on the other side forcing the diffusion of chlorides. The application of an electric field leads to migration of the various ions in the solutions to the electrodes.

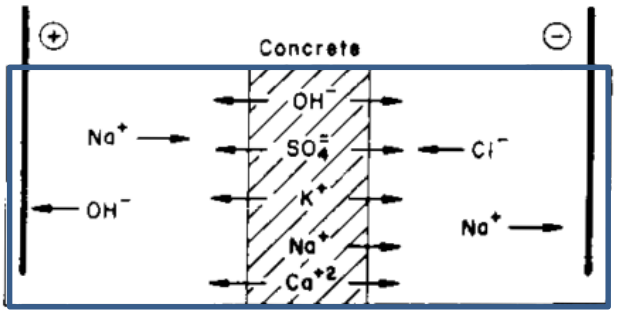

Figure 2.6: Setup for measuring diffusion and migration processes in concrete

(Andrade, 1993)

The Nernst-Planck equation can be simplified using assumptions that render the convection and diffusion terms redundant. To this end, many researchers use the resulting Nernst-Einstein

equation, (Equation 2.6) to establish the relationship between electrochemical properties and diffusion of concrete (Sengul and Gjorv, 2008).

$$D = \frac{J \cdot R \cdot T}{z \cdot F \cdot C_{cl} \cdot \Delta E} \qquad (2.6)$$

where, D is the ion diffusivity $[m^2/s]$; R is the gas constant 8.314 $[J/mol]$; T is the absolute temperature $[K]$; z is the ionic valence; J is the flux $[mol/m^2s]$; F is Faraday's constant 96500 $[C/mol]$; C_{cl} is the concentration of chlorides in the capillary pores $[mol/m^3]$ and ΔE is the energy in $[J/m]$.

The hydroxyl ion contributes to the maintenance of the high pH necessary to sustain the passivation of the concrete. In contrast, the main deleterious species that leads to reinforcement corrosion in concrete is the chloride ion. The danger posed by chlorides at the reinforcement lies in their ability to cause the destruction of the passivation layer. The next section therefore explores the properties and interactions of chlorides in concrete and the role it plays in SLP.

2.2.4 Chloride ingress in concrete

2.2.4.1 Chloride in concrete

There are two types of chloride found in concrete, free chloride and bound chloride. Chloride binding is the process whereby the free chloride ions become bound to hydration products by adsorption, as described previously. Chloride can be bound either chemically or physically to hydration products. The higher the content of bound chlorides, the less chloride content is available to initiate corrosion. This causes a reduction in the free chloride ions thereby lowering the corrosion rate (Shi et al., 2012).

The sum of all the chlorides in concrete is known as the total chloride content. The total amount of chloride ions can be determined by dissolution in an acid solution; usually nitric acid and then potentiometric titration against silver nitrate (Song et al., 2008). The process begins with the grinding of small increments along the depth of the specimen followed by dissolution. Free chloride is found by dissolution into an aqueous solution (Poulsen and Mejlbro, 2006). The chloride bound in the concrete will then be the difference of the two.

It was found that the diffusion coefficient calculated for the total chloride concentration profile is higher than that calculated for the free chloride concentration profile (Castellote et al., 2001). This is in line with the theory of free and bound chlorides. Once the chloride content at the level of reinforcement reaches a certain critical concentration, reinforcement corrosion is initiated. This level is known as the chloride threshold and is discussed next.

2.2.4.2 Chloride threshold

The chloride threshold level is the percentage of chloride by mass of binder at which corrosion is initiated. This idea stems from the simplified service life prediction (SLP) model established by Tuutti (1980). Essentially, the model has two service life phases separated by the point at which the initiation period ends and the propagation period begins, as shown in Figure 2.7.

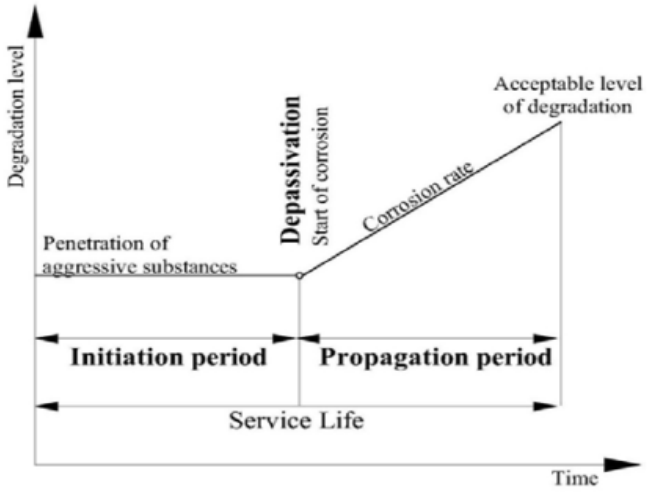

Figure 2.7: Simplified service life prediction model

(Tuutti, 1980)

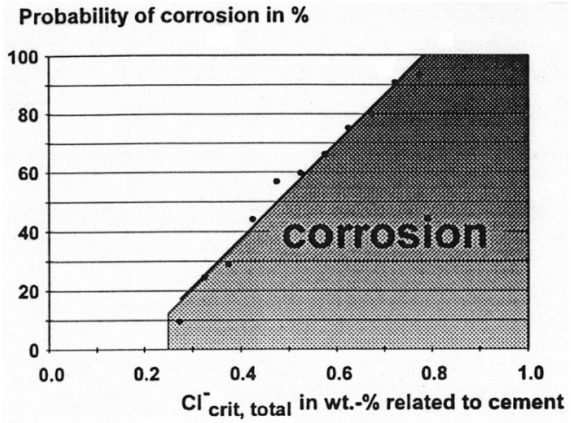

Figure 2.8: Probability of the onset of chloride-induced corrosion

(DuraCrete, 1998)

The chloride level at which corrosion is initiated is usually assumed a constant of 0.4 % by mass of binder (Mackechnie and Alexander, 1997b; Broomfield, 2007). This value is taken from European standards, based on experimental work, that recommend it as the maximum allowable total chloride level in reinforced concrete. The work revealed that, assuming there is enough oxygen and moisture and in the absence of carbonation, the corrosion risk at a chloride content of 0.4% chloride by mass of cement is low to negligible (Broomfield, 2007). Other

researchers reference Figure 2.8 above, which shows that the probability of corrosion is less than 40% when the chloride content is less than 0.4%.

However, the chloride threshold level depends on the binding capabilities of the concrete constituents. It increases with increasing hydroxyl ion concentration, which is also affected by the binder type. Additionally, it increases with the degree of saturation and with decreasing water/cement ratio. Consequently, the assumption of a constant chloride threshold may be an overestimate or underestimate depending on the type of binder (Hobbs and Matthews, 1998).

A review of 20 studies by Glass & Buenfeld (1997) revealed that the total chloride values, measured from structures, for corrosion initiation ranged from 0.17 - 2.5 wt% cement (Glass and Buenfeld, 1997). Similarly, Hobbs and Matthews (1998) conducted a comprehensive literature review on the principle factors influencing the time it takes for chlorides to reach the threshold level and came up with the following list:

- degree of exposure to chlorides
- water-binder ratio
- curing time
- moisture state
- pH of the pore solution
- binder type
- temperature
- concrete cover
- uniformity of bond between concrete and steel

The list covers most of the factors but falls short by excluding carbonation. The interaction of chloride ions and the carbonation front speeds up the destruction of the depassivation layer as carbonation reduces the concrete pH. The reduced pH is more conducive for corrosion to occur. Consequently, when the carbonation front approaches the steel reinforcement, then corrosion initiation can occur at a lower chloride threshold level (Ballim et al., 2009). Moreover, the chloride threshold also varies with cracks in the concrete because they provide a quicker path to the reinforcement (DuraCrete, 1998). Conversely, if the pores are saturated then the oxygen availability will be low and corrosion initiation will be delayed (Bertolini, 2008).

It is evident that the chloride threshold level is a multi-faceted parameter and the assumption of it being a fixed value such as 0.4 % by mass of binder needs confirmation. Others such as Polder (2009) raise the point that 0.4 % has no scientific basis. For instance, different binders under a variety of conditions will have their own particular chloride threshold levels.

Additionally, a lower chloride threshold has been observed for reinforcement bars in concrete with condensed silica fumes than ones produced with PC (Manera et al., 2008).

It has been proposed by Val & Stewart (2009) that the chloride threshold is taken as the free chloride concentration to hydroxyl concentration ratio. This was due to the observation that the corrosion initiation only occurred once a critical ratio of chloride to hydroxyl ions was reached. However, the review by Glass and Buenfeld (1997) showed that there was no justification for using free chloride rather than the total chloride for chloride threshold calculations. This was because evidence showed that bound chlorides could be unbound and partake in corrosion.

2.2.5 Factors affecting chloride ingress in concrete

Uninhibited diffusion and permeation of deleterious species into concrete are likely to lead to reinforcement corrosion. Specifically, chloride ingress as it occurs in concrete depends on a variety of factors. These include the concentration of chlorides that are available in the concrete. Other influences include temperature, carbonation, moisture, porosity, concrete composition, conditions during construction and exposure conditions (Val and Stewart, 2009; Claisse, 2005). These are discussed in more detail in the sections that follow to form a basis on which to compare and relate CCT with the surface concrete resistivity test.

2.2.5.1 Influence of temperature and curing

Temperature and its effect on chloride ingress in concrete are relevant in the study of durability test methods. This allows developers and users of such tests to be cognisant of the most appropriate temperature to carry out tests. To investigate the influence of temperature on concrete chloride ingress, Caré (2008) calculated the diffusion coefficient for cementitious materials before and after heating. Results revealed increased diffusion or chloride ingress with increased temperature, which was attributed to the heat inducing a macroscopic crack network and modifying the pore size distribution. Consequently, the porosity increased and made it easier for chloride and other ions to be transported through the concrete. Another reason for the increase could be that the temperature of concrete increases the mobility of the ions and consequently their diffusion rates (Liu and Beaudoin, 2000). However, the effect of temperature on chloride binding is complex and further study is required to establish any correlation with concrete properties (Yuan et al., 2009).

These results can be used in the selection of a suitable temperature for curing. Even though a recent study revealed that the influence of the period of curing on chloride ingress was found to be complex, some degree of control can be obtained from temperature. Additionally, curing did not exhibit any correlation between chloride ingress and either water/binder ratio or binder (admixture) content (Bertolini et al., 2011). Nevertheless, it is known that water curing gives a higher degree of hydration than air curing thereby improving the impermeability of the

concrete. Therefore, the use of water curing as opposed to air curing can in theory yield higher chloride ingress resisting properties.

2.2.5.2 Influence of different binder types

The binder and consequently the water/binder ratio determine the microstructure and chemical properties of the concrete. For instance, some binders give the concrete a finer pore structure, leading to reduction in the pH value and the total ionic concentration in the pore solution (Liu and Beaudoin, 2000). Other binders with chloride-binding properties, decrease chloride permeability, raise the chloride threshold content and improve the homogeneity of the concrete (Shi et al., 2012). For example, concrete with ground granulated blastfurnace slag (GGBS), fly ash (FA) and condensed silica fume (CSF) is known to exhibit better resistance to chloride ingress compared to Portland cement (Mackechnie and Alexander, 1997a; Luo et al., 2003; Ampadu et al., 1999; Song et al., 2008). Therefore, the time-dependent factor *'m'* is invariably lower for PC than for pozzolans (Nokken et al., 2006). Fly ash and GGBS also improve the pore structure of the concrete in what is known as the "fine filler" effect (Luo et al., 2003). The fine filler effect improves the homogeneity of the concrete and strengthens the ITZ, making it less permeable. This results in lower chloride conductivity, depending on the concrete grade, as illustrated in Figure 2.9 below.

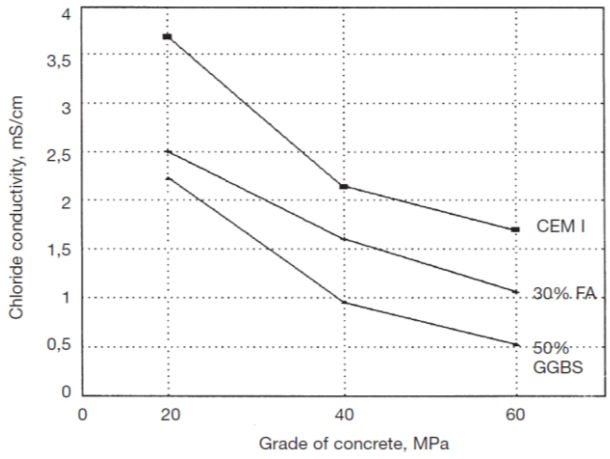

Figure 2.9: Effect of FA and GGBS in reducing the chloride conductivity

(Mackechnie, 1996)

The improvements in performance of the concrete with the addition of GGBS are possibly due to its chloride binding ability. However, the inclusion of sulphates with GGBS renders these chloride-binding capabilities of GGBS ineffective (Luo et al., 2003). Another example of the superior impermeability of slag compared to PC is shown in Figure 2.10.

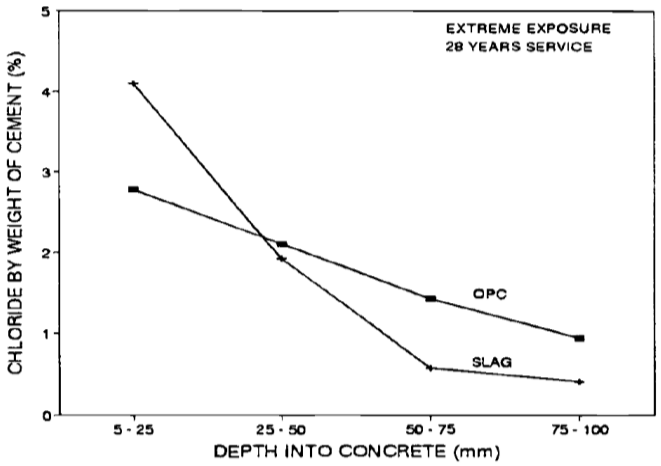

Figure 2.10: Average chloride profiles for PC and slag concrete

(Mackechnie and Alexander, 1997a)

The chloride content in the concrete cover depth is much less for GGBS than for PC. These results are consistent with those found in related binder experiments conducted by Song et al. (2008). Furthermore, it is worth noting that the content of cement extender added to the concrete also affects the extent of improved performance (Hobbs and Matthews, 1998). Generally, increasing the content of cement extenders in concrete guarantees better performance. For instance, replacement of Portland cement with at least 50% of GGBS is required for a substantial improvement in the properties of concrete but only 30 % is required for fly ash and less than 10% for CSF. Moreover, blended cements results in a higher surface chloride concentration compared to PC (Song et al., 2008). This is possibly due to their high chloride binding capacity (Poulsen and Mejlbro, 2006).

In contrast to CSF, GGBS and FA, when limestone is blended with cement, the resulting diffusion coefficient is much higher than that for PC, irrespective of the water/binder ratio (Bertolini et al., 2011). Therefore, limestone does not improve the resistance of concrete to chloride ingress because less hydration products are formed when it replaces cement.

2.2.5.3 Influence of carbonation

Carbonation is the ingress of carbon dioxide into concrete, which reacts with calcium hydroxide to form calcium carbonate, thereby reducing the pH of concrete. The lowered pH is conducive for the release of some of the bound chloride in concrete. Not only this, but it also leads to destruction of the passivation layer which leaves the steel vulnerable to corrosion (Broomfield, 2007).

Carbonation does not occur when the concrete is completely dry or fully saturated. Leaching also reduces the chloride binding capability of the concrete (Ballim et al., 2009). However, even without carbonation occurring, the presence of enough free chlorides at the reinforcement can also cause corrosion, despite it being only of the localized kind. It is interesting to note that

the effect of carbonation on the penetration resistance of chloride ions is more prominent in blended cements than PC (Ngala and Page, 1997). Nevertheless, carbonation also has the effect of improving and refining the pore structure of the surface concrete if it is unreinforced (Ballim et al., 2009).

2.2.5.4 Influence of moisture, time

Diffusion of the chloride ions into the concrete will only occur in the presence of moisture or in saturated or partially saturated conditions. The higher the levels of moisture in the concrete, the easier it will be for chloride ions to diffuse into the concrete (Ballim et al., 2009). As the hydration process continues, the moisture levels in the concrete decrease and chloride ingress is less likely. This is consistent with results that have shown that older concrete have lower diffusion coefficients than younger concrete (Song et al., 2008). In a marine environment, the surface chloride concentration increases with time as seen previously. Similarly, the diffusion coefficient has been identified as being time dependent.

2.2.5.5 Influence of aggregates

Aggregates are known to have a significant effect on the properties of concrete. Hobbs (2000) sought to prove that the aggregate in the concrete is as influential on the diffusion coefficient as the cement paste. Using saturated concrete, he managed to show that the diffusion coefficient of the aggregate could influence that of the concrete. However, this result is limited to instances where the diffusion coefficient of the aggregate is between 0.2 and 10 times that of the concrete; when this is the case, the diffusion coefficient of concrete can increase by a factor of ten (Hobbs, 2000).

If the aggregate diffusion coefficient is lower than the diffusion coefficient of the cement paste, the result is concrete with a diffusion coefficient lower than that of the cement paste (Hobbs, 2000). The volume of aggregates in the concrete also affects the diffusion coefficient. Reasons for this could be porosity of the aggregates, which is linked to their ability to resist chloride ingress and other deleterious species (Grieve, 2009a).

2.2.5.6 Influence of exposure environment

Structures in marine environments are more prone to deterioration due to chloride-induced corrosion than inland structures. For this reason, the EN 1992-1-1 and the South African standard (SANS, 1992) both classify environments depending on the extent of exposure to seawater or de-icing salt. Marine structures exposed to tidal and splash zones are particularly susceptible to chloride-induced corrosion. Consequently, some of the most stringent requirements are specified for these structures. At the other end of the spectrum are marine structures that are considerably further away from the sea and therefore subject to much less salt exposure. Specifications for these structures allow for the use of less conservative values

for cover and water/binder ratios. In a marine environment, the surface chloride concentration increases with time. In contrast, the diffusion coefficient decreases with time (Song et al., 2008). Both effects are intuitive considering the increased hydration and the subsequent loss in moisture as well as the abundance of chloride ions in the marine environment.

2.2.5.7 Influence of water/binder ratio

The water/binder ratio of the concrete also factors into the rate of chloride ingress (Hobbs and Matthews, 1998). Generally, increasing the water/binder ratio adversely affects performance. Hobbs and Matthews (1998) analysed a number of field results from marine structures around the world. Their analysis revealed that when plotted on a linear-linear basis the effective diffusion coefficient and the water/cement ratio showed no distinct pattern. However, when plotted on a log-linear scale, it was apparent that the diffusion coefficient increases with increasing water/binder ratio. Their study included a wide range of water/binder ratios from 0.3 to 0.9. Although these values are much higher than those used in industry nowadays, studies done in the last few years with a smaller range of water/binder ratios, 0.4 to 0.6, still reflect these trends (Bertolini et al., 2011).

Another example is the findings by Song et al. (2008) who conducted a recent but similar analysis of a number of studies on the diffusion coefficient and the water/binder ratio. They found that in most of the studies, chloride ingress measured using the diffusion coefficient, increased with the water/binder ratio. In addition, they noted an increase in the chloride diffusion coefficient with increased water/binder ratio. Similar results were found by Bijen (1996) as shown in Table 2.1.

Table 2.1: 6-month diffusivities of chloride ions in concrete in 10^{-12} m^2/s

(Bijen, 1996)

w/c	*Portland cement*	*Portland blast furnace slag cement (30/70)*	*Portland fly ash cement(75/25)*
0.4	4	0.1	0.2
0.55	10	0.3	0.5

2.2.6 Diffusion tests

Various test methods are used to measure concrete diffusivities based on the chloride concentration at different depths of a concrete specimen. The purpose of the measurements is to establish the influence of parameters as discussed in the previous sections as well as determine the potential durability. Most diffusion tests simulate the conditions expected in service or an accelerated version to obtain results in short periods. The underlying principles of these tests are the transport mechanisms described previously.

2.2.6.1 AASHTO T259 – salt ponding

The American Association of State Highway and Transportation Officials (AASHTO) have developed a salt ponding test called AASHTO T259 (1980). AASHTO T259 is a long-term test usually used to validate results of rapid chloride diffusion tests. The test procedure requires covering the sides of square specimens that have been moist cured for 14 days before drying for 28 days. Then the tops are dosed with a 3% NaCl solution while the bottom remains in 50% relative humidity for 90 days, allowing the diffusion process to occur as depicted in Figure 2.11.

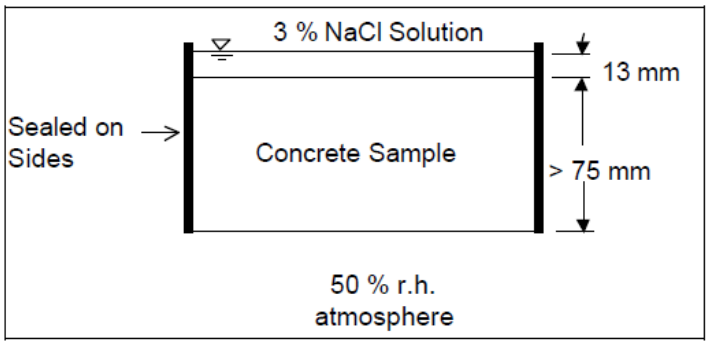

Figure 2.11: Schematic of AASHTO T259

After the 90 days, thin slices are cut from the specimen and their chloride concentration is measured. It is important to note that the test only measures the average chloride concentration at a certain depth and not the variation (Stanish et al., 2002). Additionally, the drying process before the test and differences in moisture between the top and bottom surfaces during the test implies that instead of pure diffusion, sorption and wicking occur. Nevertheless, unlike the ASTM C1202, it can be used even when concrete contains admixtures and for high quality concrete even though these take longer than the recommended 90 days (Cho and Chiang, 2006; Stanish et al., 2002).

2.2.6.2 NT Build 443 – Bulk diffusion

Similar to the AASHTO T259 (1980) is the Bulk Diffusion test (Nord Test) or NT Build 443 (1995). A version of this test modified for American standards is called the ASTM C1556 (2011). Although all three tests undergo 14-day moist curing, unlike AASHTO T259, AASHTO T259 and ASTM C1556 have the sides and the bottom covered to limit the influence of absorption and permeability. Additionally, rather than drying after moist curing, concrete specimens are saturated with limewater to prevent sorption before being immersed in 2.8M NaCl solution for at least 35 days (NT Build 443, 1995; ASTM, 2011). Thereafter, small increments (0.5mm) along the depth of the specimen, from the exposed surface, are ground into powder and tested for chloride content. This enables the measurement of the chloride

profile across the depth of the specimen. The error function *(erf)* is fitted to the chloride contents (profile) to get the diffusion coefficient and surface chloride concentration from Crank's solution of Fick's second law. This is achieved using non-linear regression analysis (Stanish et al., 2002; Kessler et al., 2008).

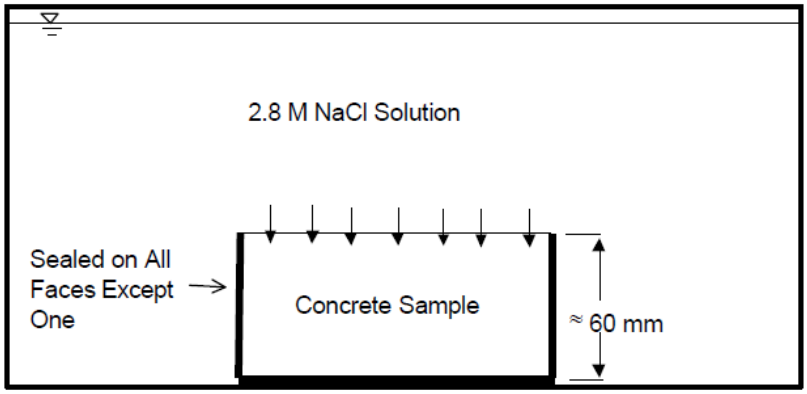

Figure 2.12: Schematic of NT Build 443 set-up

2.2.7 Rapid chloride transport tests

It is generally agreed that a rapid test for chloride ingress in concrete is necessary because the diffusion process is considerably long (Streicher and Alexander, 1995; Stanish et al., 2006; Rear et al., 2010). Consequently, while the tests described above may be a good representation of the diffusion process of chloride ions in concrete, they remain impractical due to the length of time required. Although the two test durations are rather long, ultimately they allow the measurement of the natural diffusion process. The tests are a common means of comparison and assessment of the accuracy of rapid chloride tests such as the ones described subsequently. Any glaring disparity between results from these tests and short-term results from the rapid tests is a reason enough to disregard the short-term tests. The main reason is that the rapid tests do not actually measure the natural progression of the chloride through the concrete.

Rapid Chloride Tests are based on the transport process of migration explained previously in this section. They require the speeding up of the movement of chloride ions through concrete by application of a potential difference. The tests are a measure of mechanisms that can be related to the degree of resistance of concrete against the ingress of chloride ions.

2.2.7.1 NT Build 492 – Rapid Chloride Migration

The NT Build 492 is a rapid chloride migration test that can be completed within 24 hours (CHLORTEST, 2005). Although the NT Build 492 test is related to chloride diffusivity (Romer, 2005), the parameter obtained from the test is the so-called non-steady state migration coefficient rather than the diffusion coefficient. The procedure requires at least three cylindrical

concrete specimens of 100 mm diameter and 50 mm thickness, placed in the setup shown in Figure 2.13.

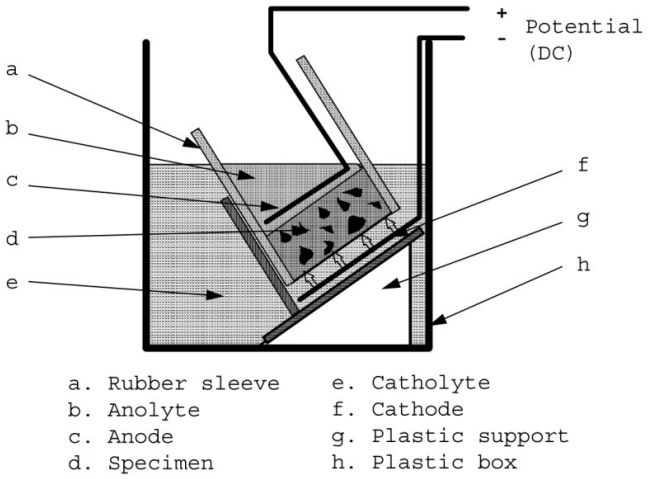

Figure 2.13: NT Build 492 migration setup

(NT Build 492, 1999)

Each concrete cylinder has a voltage applied axially and the initial current measured to allow the migration of chloride ions. The duration of voltage application depends on the initial current and can vary between 6 to 96 hours. As seen previously, the anolyte is NaOH and the catholyte is NaCl conducive for the transport of chloride ions. The cylinder is split axially and one exposed circular surface is sprayed with silver nitrate, revealing the depth of chloride penetration, which can then be measured. Thereafter, the non-steady state migration coefficient is calculated using a variation of the Nernst-Einstein equation (Equation 2.6). The diffusion coefficient from the rapid chloride migration is used as an input parameter for the calculation of the corrosion initiation period in DuraCrete.

2.2.7.2 ASTM C1202 – Rapid Chloride Penetrability Test

The ASTM C1202 whose AASHTO counterpart is the T277 is sometimes referred to as the rapid chloride penetrability test (RCPT). It is a migration-based chloride test used to measure the charge (Coulombs) through the concrete by voltage application. The charge is then related to the concrete's penetrability (CHLORTEST, 2005). The actual chloride penetrability testing occurs after a 28-day moist curing regime. The moist curing can be extended until 56 days or accelerated for a period of only 7 days. The general procedure for both versions of the test is as follows (ASTM, 2012).

Firstly, the specimen is pre-conditioned by being placed in a vacuum for three hours. Secondly, it is immersed in water and then vacuum saturated for another hour. Thereafter, it is soaked in water for 18 hours. This ensures that all specimens have the same moisture content at the start of the test (Suprenant, 1991). Then the specimen is placed between 2 reservoirs of 0.3 *M* NaOH

and 3% NaCl. It is tested by applying a potential difference of 60 V of direct current for 6 hours as shown in Figure 2.14. The current through the specimen is measured over the six-hour period and the results plotted. The area under the graph is the number of Coulombs.

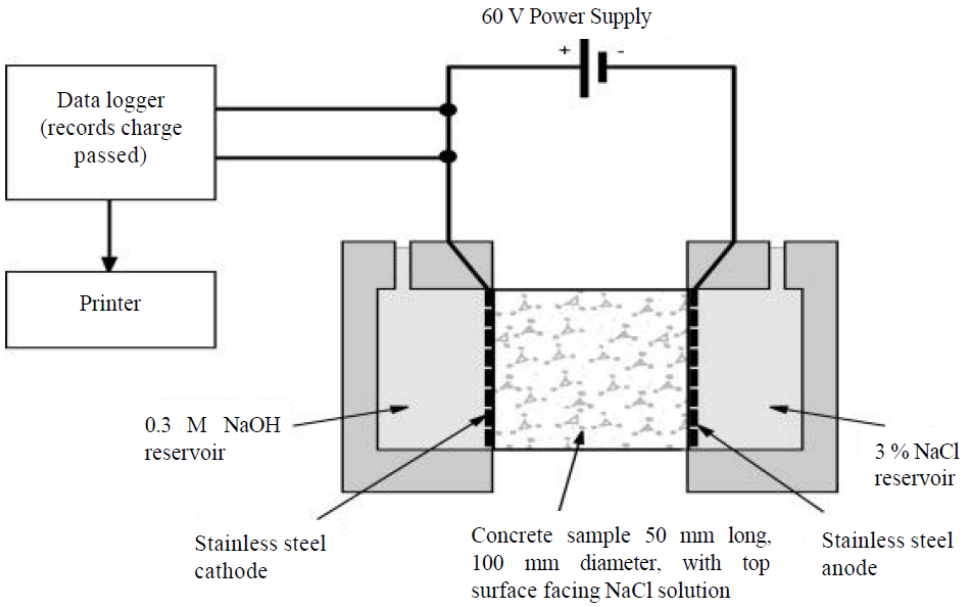

Figure 2.14: ASTM C1202 test setup

(ASTM, 2012)

Subsequently, the ability of concrete to prevent chloride ingress is assessed using Table 2.2, established by Whiting (1981). The table relates the total charge passed to the chloride ion permeability of the specimen.

Table 2.2: Chloride ion penetrability based on charge passed

(ASTM, 2012)

Charge passed (Coulombs)	***Chloride ion penetrability***
> 4000	High
2000 - 4000	Moderate
1000 - 2000	Low
100 - 1000	Very Low
< 100	Negligible

Even though Table 2.2 values are used to obtain the permeability of the tested concrete, Pfeifer et al. (1994) argue that some low permeability concretes can have charge passed exceeding 5000 Coulombs. Results from research conducted by Liu and Beaudoin (2000) also suggest that the decrease in the number of Coulombs due to the addition of admixtures does not match the reduction in permeability. This is consistent with the ASTM C1202 standard, which advises the use of the ponding test for concrete with admixtures. Moreover, the test method is limited to concrete types for which there is a proven correlation between this test and chloride ponding

tests such as *AASHTO T259* (1980). Despite this, few users of the method ensure the restriction is adhered to by carrying out the *AASHTO T259* or other similar long-term tests (Pfeifer et al., 1994). In summary, the major shortcomings of the test include:

1) The high voltage increases the temperature thereby affecting the conductivity in what is known as the Joule effect. However, this is not accounted for.

3) The charge measured is also a function of other ions and is not an exclusive measure of chloride ions.

4) The test is not under steady state conditions meaning Fick's laws of diffusion cannot be used to analyse the results for service life prediction.

5) The test cannot be used for concretes with admixtures.

This has caused authors such as Stanish et al. (2002) to question why it is still in use. Nonetheless, Pfeifer et al. (1994) defend its use and put the blame on contractors and researchers who fail to fully comprehend what it was designed for and what it measures before testing. A study on the RCPT, done by Feldman et al. (1994, 1999) offers a comprehensive and critical analysis of the test.

2.3 PART 2: THE CHLORIDE CONDUCTIVITY TEST

2.3.1 Background

Conductivity (σ) is an electrochemical process (measured in *mS/cm*) that reflects the ionic strength of the pore liquid as well as the ease with which ions can move unimpeded through the microstructure of the concrete. The chloride conductivity test (CCT) is a Durability Index test (DI) developed in South Africa at the Universities of Cape Town and Witswatersrand (Streicher 1997). It is used in the performance-based approach for the design of durable reinforced concrete structures. The test can also be used for quality control and assessment during and after construction. The development of the CCT was led by Mackechnie (1996) and Streicher (1997). Their study and subsequent implementation of the test was necessitated by the need for an accurate rapid chloride test. Streicher assisted in the development of the actual CCT, while Mackechnie was instrumental in the creation of the service life prediction (SLP) model for chloride ingress in the DI.

The development of the test included statistical analysis to establish the precision of the test. In addition, a standardisation process was performed using a ruggedness test to establish the accuracy of the results in the event of slight deviations from the recommended procedure (Streicher 1997). The development of the SLP model used a combination of CCTs and case studies of old structures in the marine environment. The former was used to establish short-term properties, which were linked to the latter or long-term properties of reinforced concrete

structures. Long-term tests such as the Bulk diffusion test were used for validation purposes of the proffered prediction model (Mackechnie, 1996).

Currently, the CCT is used for quality control purposes during construction, as well as service life prediction during the design process. Specifically, the CCT is used to determine the cover quality with respect to chloride ingress and estimate the chloride diffusion coefficient in a relatively short time. In addition, the test is valid over a range of materials and environments, a move away from the prescriptive approach, which did not account for these properties. Furthermore, it has been proven repeatable and reproducible and has good correlation with other rapid chloride tests and longer-term tests that directly measure diffusion (Stanish et al., 2006; Mackechnie and Alexander, 2000b; Beushausen and Alexander, 2008).

2.3.2 Theoretical basis of the CCT

The test measures the conductivity of the concrete and relates it to its diffusibility for two reasons. Firstly, this stems from studies that have shown that the electrical conductivity of concrete is related to concrete porosity (Brace et al., 1965). Secondly, other researchers have shown that the diffusibility of cement-based materials is dependent on the porosity (Garboczi and Bentz, 1992). Since both conductivity and diffusion are dependent on the porosity, which is a function of the microstructure, it is tenable that the two are related. Using the Nernst-Einstein equation it can also be shown that the conductivity of a porous solution and that of a porous material saturated with the pore solution are related by the same material constant or diffusibility Q. This was confirmed through experiments conducted by Brace et al. (1965) culminating in Equation 2.7 or the diffusibility equation.

$$\frac{D}{D_0} = \frac{\sigma}{\sigma_0} = Q \qquad (2.7)$$

where σ is the conductivity of the sample saturated with the electrolyte or porous medium (concrete) *[mS/cm]*; σ_0 is the conductivity of electrolyte or pore solution *[mS/cm]*; D is the diffusion coefficient of the porous medium; D_0 is the diffusion coefficient of the pore solution

Atkinson and Nickerson (1984) also illustrated electrical conductivity of a porous material saturated with a strong solution can be used to rapidly determine the permeability of the porous material. However, the diffusibility of chloride ion is difficult to isolate because of the simultaneous interactions of other ions and their own diffusion in concrete.

Nevertheless, the use of the conductivity relation to the diffusibility negates the use of the complex Nernst-Einstein equation and the ideal conditions that are difficult to replicate in the laboratory. Q is then multiplied by the diffusivity of the chloride ions to get the diffusivity of the porous medium or in this case the concrete specimen (Streicher and Alexander, 1995).

Results from the CCT confirm that the chloride conductivity of concrete is linearly related to the diffusibility (Mackechnie and Alexander, 2000a).

2.3.3 Test method and practical basis of the CCT

The CCT quantifies the 28-day electrical conductivity of a concrete specimen following an 8-day preconditioning regime (Alexander et al., 1999b). The test requires four concrete discs with a diameter of 70 ± 2 mm and a thickness of 30 ± 2 mm. These discs are heated in the oven at a temperature of 50 ± 2℃ for a period of 7 days ± 4 hours and weighed. Thereafter, they are immediately placed in a desiccator to cool for 2 – 4 hours. This is followed by a 3-hour ± 15 minutes period of vacuum saturation with the cores placed on their sides, along their circumferences.

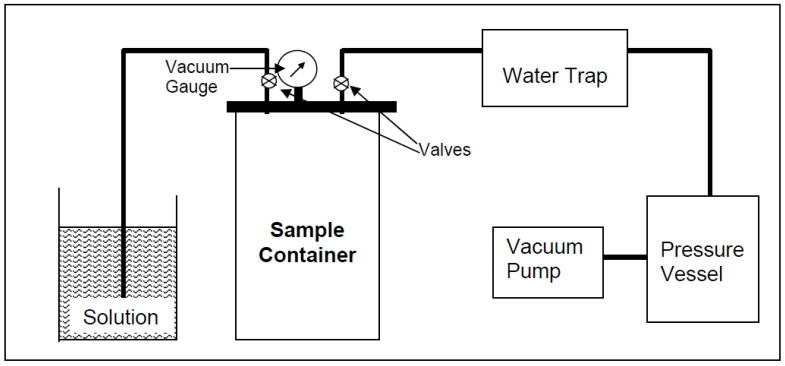

Figure 2.15: Vacuum saturation facility for CCT

(Alexander, 2009)

Afterwards, the salt solution is allowed into the vacuum saturation apparatus (Figure 2.15) for up to 1 hour ± 15 minutes. Air is then allowed in and the discs are allowed to soak in the salt solution for 18 ± 1 hours. When this period elapses, the discs are weighed once more and then the actual testing begins. The CCT is carried out at a room temperature of 23 ± 2℃ in the setup shown in Figure 2.16 below.

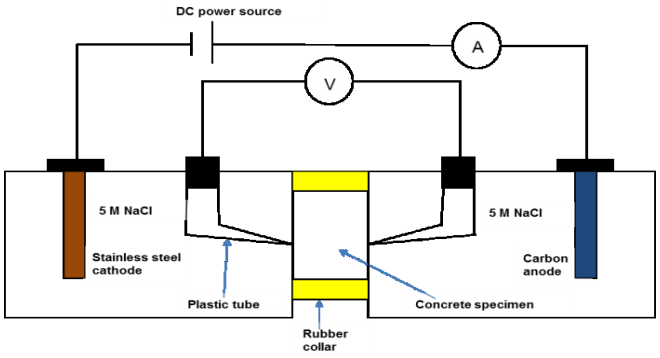

Figure 2.16: The chloride conductivity test (CCT) apparatus

(Alexander et al., 1999b)

The current through the sample is measured simultaneously with the voltage once the DC power source reading is adjusted to 10 V (Alexander et al., 1999b). A low voltage is maintained during the test, between 5 and 10 V to prevent heating up of the concrete specimen under measurement. This precaution also eliminates the possibility of chloride oxidation at the anode (Prince et al., 1999).

From the results of the test, the conductivity of the concrete specimen can be computed with the following equation (Streicher and Alexander, 1999):

$$\sigma = \frac{i}{V} \cdot \frac{t}{A} \qquad (2.8)$$

where σ is the conductivity of the sample *[mS/cm]*; i is the electric current *[mA]*; V is the potential difference *[V]*; t is the specimen thickness *[cm]*; A is the specimen cross-sectional area *[cm^2]*

The correlation of the initial current and conductivity relationship in Equation 2.8 was confirmed with tests done at a number of concrete ages by Feldman et al. (1999, 1994). Other researchers such as Nokken et al. (2008) have also used this relationship. Typical results of the CCT are shown in Figure 2.17, exhibiting the versatility of the test. It is evident that the test varies quite drastically with binder type and water/binder ratio. On the one hand, high w/b ratio results in high CCT values. On the other hand, higher quality cement with fly ash or slag has much lower CCT values than PC.

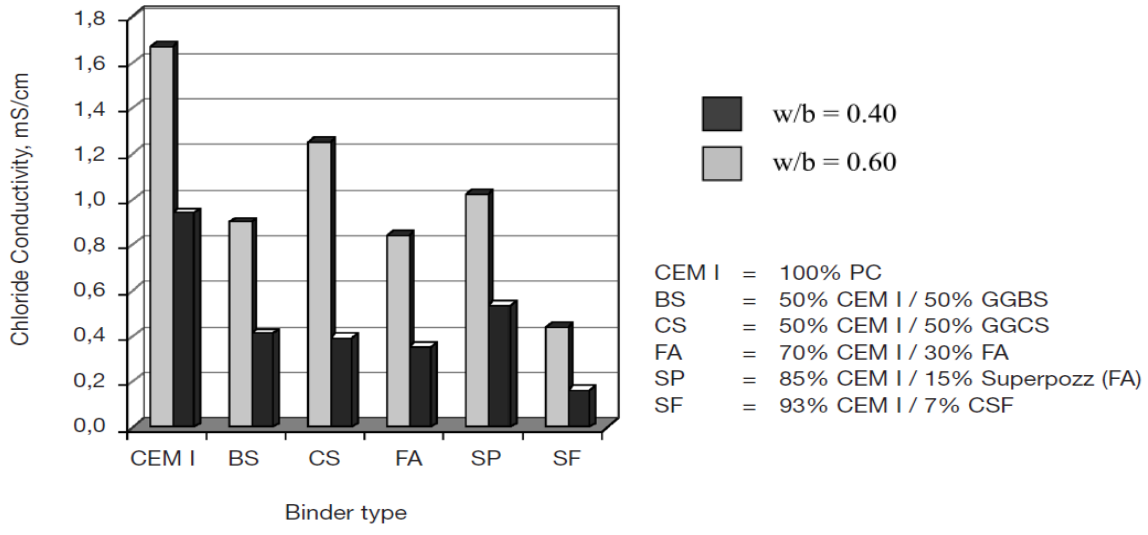

Figure 2.17: Typical test results for CCT, in relation to w/b ratio and binder type
(Ballim et al., 2009)

2.3.4 Reasons for CCT specifications and assumptions

The ideal thickness was selected from tests that examined the change in conductivity with specimen thickness. The conductivity increased with thickness when measured at the same age, for thicknesses of up to 20 mm. However, the specimen thickness had no effect on the conductivity for specimens thicker than 25 mm as these were prone to imperfect saturation (Streicher and Alexander, 1999). In addition, the aggregates had greater influence on the conductivity results in thinner specimens than the thicker ones (Streicher and Alexander, 1999). This observation necessitated the use of specimens with a minimum thickness of 25 mm to ensure the repeatability and reproducibility of results for tests performed in different labs.

The temperature at which the specimens are oven dried and tested is an important consideration. For instance, conductivity increases with increasing temperature, hence the requirement of a prescribed standard test temperature of 25 ℃ (Streicher and Alexander, 1999). The reason for this value is that it is close to room temperature and easily attainable in any laboratory. Furthermore, drying of the samples at 50 ℃ rather than 100 ℃ prevents drying damage occurring and dilution of the chloride by any leftover moisture (Streicher and Alexander, 1995).

In addition, the conductivity of the concrete pore solution is taken to be that of the 5 *M*, NaCl solution used to saturate the sample. The specification of NaCl was selected for its high ionic strength, as with most diffusion and migration tests. Saturation was essential to ensure that the primary transport mechanism is electrical conduction of the chloride ion and not diffusion.

Streicher (1997) made the decision to use a concentration of 5 *M* based on experimental work. The effect other ions in the concrete pores have on the conductivity of varying concentrations of the NaCl solution was investigated. Results showed that irrespective of the concentration of other ions in the solution, conductivity of the pore solution remains closest to that of the NaCl solution. In fact, at concentrations higher than 5 *M*, other ions had virtually no effect on the conductivity of the pore solution (Alexander et al., 1999b). The diffusibility ratio also remained constant at 5 *M* NaCl and higher, regardless of the increase in concentration of other ions. Therefore, the assumption that the conductivity of the concrete pore solution mirrors that of the saturating solution of 5 *M* NaCl is valid.

2.3.5 Evaluation of CCT and comparison with other rapid chloride tests

The chloride conductivity test is sensitive to the exposure environment, water/binder ratio, cement type, age and curing regime (Alexander et al., 1999b). Thus, it meets the requirements for a standard durability test. However, inadequate saturation of high strength concrete and heat damage caused by the drying process have been highlighted as major causes for concern (Mackechnie and Alexander, 2000b). The developers of the CCT have addressed the imperfect

saturation. They advise testing specimens with varying thickness. When thicker specimens result in low conductivity, this is a sign of ineffective saturation and such concrete should not be used for the test (Streicher and Alexander, 1999). Nonetheless, it is unclear how to consider this under normal chloride conductivity testing circumstances.

Another challenge is the 7-day oven drying procedure. This may induce drying cracks into the concrete thereby distorting the actual diffusion coefficient of the concrete specimen (Liu and Beaudoin, 2000). The rationale is that heating introduces significant changes in the pore structure and therefore the conductivity increases (Atkinson and Nickerson, 1984). A similar problem is associated with the Rapid Chloride Permeability Test (RCPT), which includes a 6-hour application of 60 V (ASTM, 2012). Consequently, it has been found that not only does the RCPT change the resistivity properties of the measured concrete but it also instigates changes in the pore structure (Feldman et al., 1994).

Even though the CCT is meant for new structures, researchers sometimes use it to characterise concrete specimens from older structures. However, older structures may have surface treatments, carbonation and exposure to marine salts all of which distort the CCT. The test also cannot be conducted on concrete with either steel reinforcement or aggregate sizes exceeding 26.5 mm (Alexander, 2009).

Issues identified with the CCT procedure include the pre-conditioning phase, which takes 7 days. This is rather lengthy compared to the RCPT pre-conditioning which takes about a day (Liu and Beaudoin, 2000). Nevertheless, unlike the CCT, there is no criterion for concretes with admixtures in the RCPT. Apparently, this important consideration of concrete materials was not implemented into the test method (Liu and Beaudoin, 2000; ASTM, 2012).

Another study comparing the RCPT and the CCT conducted in Australia by Sharfuddin et al. (2008) concluded that the latter was a better test than the former in terms of ease of use and rapidness. In addition, whereas confidence in the use of the CCT is on the rise (Beushausen and Alexander, 2008) the RCPT is being replaced with the surface resistivity test in certain areas (Kessler et al., 2008). Reasons for this change include results that have shown that the surface resistivity test is less costly, non-destructive and easier to implement than the RCPT (Riding et al., 2008).

The reproducibility and repeatability of the CCT was confirmed in an extensive study on the South African DI tests (Stanish et al., 2006). The study tested ten mixtures in ten different labs resulting in a repeatability of 9.1% and reproducibility of 21.1 %. Despite this, it is worth noting that the researchers recommended improved clarity of specifications for the test procedure. This came out of results from some laboratories that had to be discarded because the test was

not performed in a satisfactory manner. Perhaps because of this recommendation, the previous procedural manual was revised (Alexander, 2009).

The CCT showed good results compared with other tests measuring rapid chloride ingress and diffusion into concrete around the world (Beushausen and Alexander, 2008; Mackechnie and Alexander, 2000b). In particular, there was a good correlation with the RCPT as well as the NT Build across six concrete mixes. This correlation is depicted in the figures below with test results of CCT increasing with increasing Coulombs and diffusion coefficient.

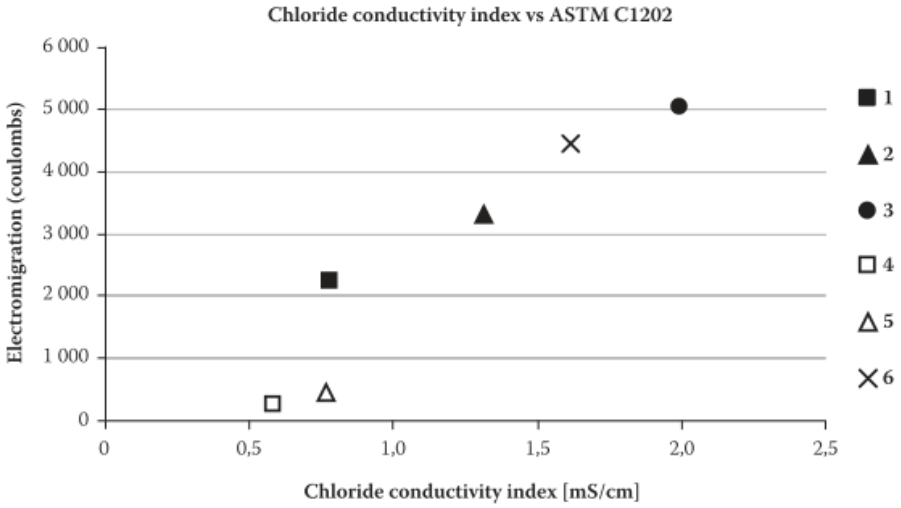

Figure 2.18: Correlation between CCT & ASTM C1202 test results

(Beushausen and Alexander, 2008)

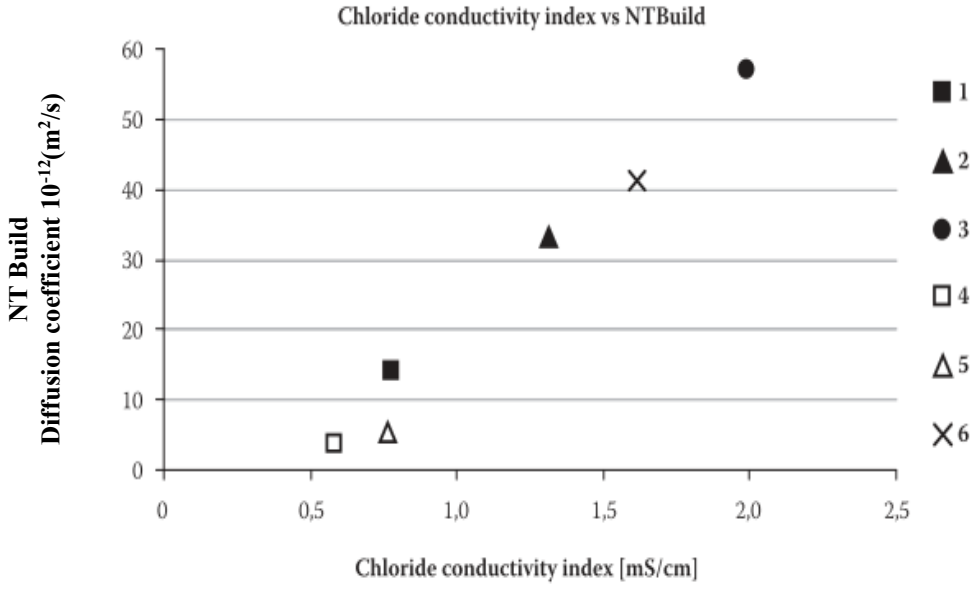

Figure 2.19: Correlation between CCT & NT Build 443 test results

(Beushausen and Alexander, 2008)

The linear relationship was based on test results of six different concrete mixes (1-6) suggesting its wide-ranging validity. The correlation with the NT Build 443 is predictable, considering that both the tests have been found suitable for the prediction of long-term chloride levels in concrete (Mackechnie and Alexander, 2000b). However, the relationship with the RCPT is less obvious considering the various issues that have been raised about it.

2.3.6 The use of CCT for performance-based specifications

Prior to the inception of the performance-based approach, it was assumed that concrete strength measurements were adequate to ensure the durability of concrete via the prescriptive approach. However, with the advent of other cementitious materials and the growing number of structures not reaching their service life it became clear that strength did not always equal durability (Rear et al., 2010).

Performance-based specifications provide a more flexible means to assess the potential durability of reinforced concrete at an early age than prescriptive-based specifications (Alexander et al., 2011). Rather than w/b ratios and binder content, performance-based specifications are more robust and classified based on actual concrete cover quality or durability test results. Performance-based specifications are available for both the CCT and surface concrete resistivity due to their relationship with chloride ion diffusion in concrete, which is a durability indicator.

2.3.6.1 CCT specifications

In earlier work, Alexander et al. (1999b) recommended Table 2.3 (see below) for durability classification of reinforced concrete using CCT results. The durability class *Excellent* referred to the best quality concrete while *Very poor* is associated with poor quality concrete.

Table 2.3: Durability classification using CCT values

(Alexander et al., 1999b)

Durability class	***CCT (mS/cm)***
Excellent	< 0.75
Good	0.75 - 1.50
Poor	1.50 - 2.50
Very poor	> 2.50

However, this did not consider other factors such as binder type and exposure environment, which also have an effect on the durability of a RC structure. It is evident that a more comprehensive method of durability classification that included these factors and the required service life was necessary.

Consequently, a more comprehensive CCT durability classification system was developed depending on the project level, required quality, as-built quality and material potential. It

specifies not only binder type, environmental exposure and service life but also, structural type and cover depth as shown in Table 2.4. The table is exclusively for 28-day CCT values for concrete structures located in marine environments (Alexander et al., 2011).

Table 2.4: Maximum CCT values for 100 year service life as-built structures (cover = 50mm)

(Alexander et al., 2011)

EN 206 Class	*70:30 CEM I: Fly Ash*	*50:50 CEM I: GGBS*	*50:50 CEM I: GGCS*	*90:10 CEM I: CSF*
XS1: Exposed to airborne salt but not in direct contact with seawater	2.50	2.80	3.50	0.80
XS2a: Permanently submerged	2.15	2.30	2.90	0.50
XS3a: Tidal splash and spray zones	1.10	1.35	1.60	0.35
XS3b: XS3a + exposed to abrasion	0.90	1.05	1.30	0.25

Portland cement (CEM I) is not in the table as it has been shown to have inadequate resistance against chloride ingress in a marine environment (Alexander et al., 2008). A further modification of this system checks the concrete mix's probability of failure with the allowable probability of failure at the durability limit state (Muigai, 2008). This allows for inclusion of the variability of the basic model parameters in Mackechnie's (1996) Fickian model. Alternatively, the CCT can be used for prediction of a concrete's long-term resistance against deterioration using a SLP model (Alexander et al., 1999b).

2.3.7 Prediction of the corrosion initiation period

The prediction of reinforced concrete durability using the CCT is based on an empirical performance-based SLP model developed by Mackechnie (1996). The model makes use of early-age concrete properties from the CCT results to characterise concrete. The test results are related to an empirical model for the prediction of long-term diffusion coefficients of marine concrete structures. The diffusion coefficient is then used as an input parameter in Crank's solution to Fick's second law of diffusion (Equation 2.4) to estimate the corrosion initiation period. The model is based on a study conducted on marine structures, which revealed the decrease of the diffusion coefficient with time irrespective of binder type (Mackechnie, 1996). Mackechnie (1996) was able to show that the 28-day CCT has a distinct linear relationship when plotted against measured 2-year diffusion coefficients (Figure 2.20).

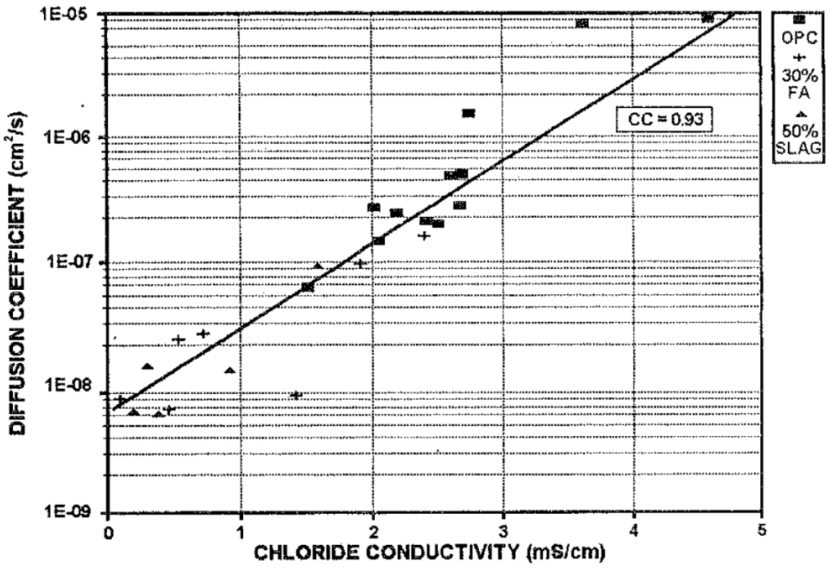

Figure 2.20: CCT versus diffusion coefficient, after two years marine exposure

(Alexander et al., 1999b)

As seen previously, Mangat and Molloy (1994) also showed that the diffusion coefficient depends on the period of exposure. From Equation 2.5 and using differential equations, they derived the following equation, which accounts for the variation of the diffusion coefficient with time:

$$\log D_c = \log D_i - m \log t \qquad (2.9)$$

where D_i and D_c are the initial instantaneous and integrated diffusion coefficients; m is the reduction coefficient; t is the time in seconds

From various case studies conducted abroad and in South Africa, it was deduced that the reduction factors shown in Table 2.5 were the best representations of long-term conditions (Mackechnie, 1996).

Table 2.5: Reduction factors of diffusion coefficients for different binder types

(Mackechnie, 1996)

Concrete type	*Reduction factor (m)*
100 % OPC	0.29
30 % Fly Ash	0.68
50 % Slag	0.68

Equations for the initial instantaneous diffusion coefficient were similarly derived from case study results such as Figure 2.20. The equations link 28-day CCT measurements to 28-day diffusion coefficients, depending on exposure condition and binder type, as seen in Table 2.6.

Table 2.6: Equations for Initial instantaneous Diffusion coefficients D_c from 28-day CCT results

(Mackechnie, 1996)

	Diffusion coefficients (D_o) (cm^2/s)		
Exposure	***OPC***	***50% SLAG***	***30% FA***
Extreme	$2.8 \times 10^{-9}(2.718^{1.6CCI})$	$5.2 \times 10^{-9}(2.718^{1.2CCI})$	$6.0 \times 10^{-9}(2.718^{1.3CCI})$
Very severe	$3.6 \times 10^{-9}(2.718^{1.1CCI})$	$5.5 \times 10^{-9}(2.718^{0.9CCI})$	$6.8 \times 10^{-9}(2.718^{0.95CCI})$
Severe	$4.0 \times 10^{-9}(2.718^{0.9CCI})$	$5.0 \times 10^{-9}(2.718^{0.75CCI})$	$6.0 \times 10^{-9}(2.718^{0.75CCI})$

*where CCI is the 28-day chloride conductivity

The 28-day diffusion coefficients are in turn used to determine the 2-year diffusion coefficients as follows. Based on his studies, Mackechnie (1996) took the time *t* in Equation 2.9 as 2 years so that the second term became:

$$m \log t = m \log (2 \times 365 \times 24 \times 60 \times 60) = 7.7998m \quad (2.9a)$$

$$\log D_i = \log D_c + 7.7998m \quad (2.10)$$

where D_i and D_c are the 2-year and 28-day diffusion coefficients; *m* is the reduction coefficient, *t* is the time in seconds

From Equation 2.10 and the equations in Table 2.6, one can get the 2-year diffusion coefficient for a concrete structure in any marine exposure category. The 2-year diffusion coefficient is used as an intermediate parameter for the calculation of the long-term diffusion coefficient. Once the two-year diffusion coefficient is known, it then becomes the initial instantaneous value in Equation 2.9. Taking the inverse logarithm of Equation 2.9 and the 2-year diffusion coefficient from Equation 2.10, the long-term diffusion coefficient at any age *x* is calculated as follows:

$$D_x = 10^{logD_i - m[\log(x \times 365 \times 24 \times 60 \times 60)]} \quad (2.11)$$

where D_x is the diffusion coefficient at design age *x* (years); D_i is the integrated diffusion coefficients; *m* is the reduction factor

The diffusion coefficient obtained from Equation 2.11 is then used as an input parameter in service life prediction (SLP) models such as Equation 2.4. Mackechnie summarised this procedure in two nomograms introduced below.

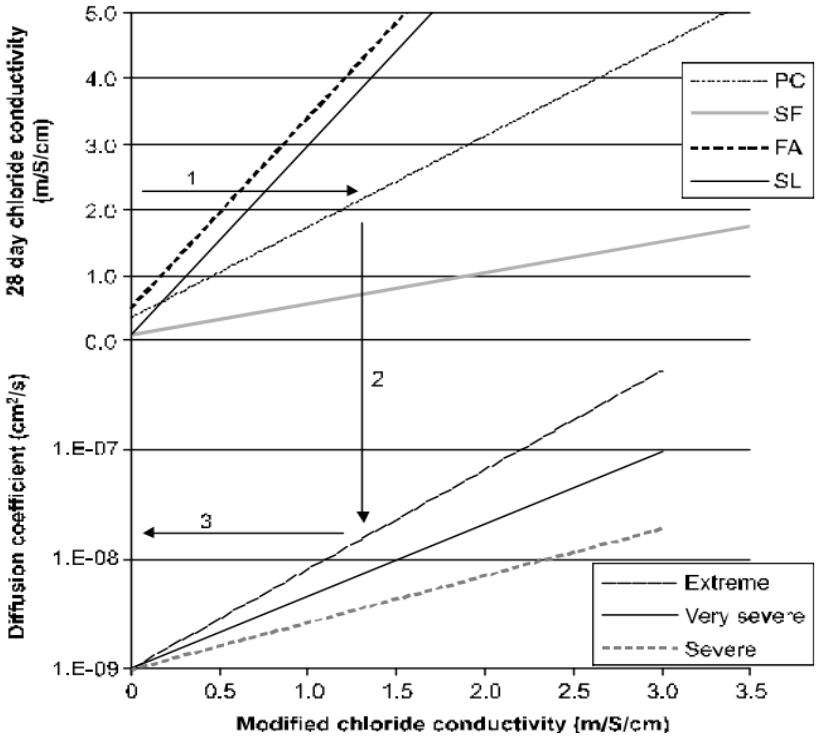

Figure 2.21: Prediction of fifty-year diffusion coefficient for marine concrete

(Mackechnie, 2001)

The nomogram in Figure 2.21 is a simplification of the model and can be used to determine the desired long-term diffusion coefficient as described above. The binder type lines in Figure 2.21 represent the different rates at which the 28-day chloride conductivity increases with time. Cement extenders such as fly ash and slag have better resistance than 100% Portland cement and so usually have lower values of modified chloride conductivity. The modified chloride conductivity is the intermediate step, which accounts for the long-term changes in the concrete due to chloride binding and continued hydration (Mackechnie, 2001; Alexander et al., 2012). The lower graph in Figure 2.21 represents the increase in diffusion coefficient with the modified chloride conductivity coefficient as seen in the diffusibility equation. The graph differs with marine exposure condition since concrete in a severe environment would have to be more resistant to chloride ingress i.e. have a lower diffusion coefficient, than one in better conditions.

Once the 28-day CCT result is determined as described previously, the value can be located in Figure 2.21. Thereafter, a line is drawn parallel to the *x-axis* until it meets the binder type line (1). The next line (2) is from the respective binder type line, to the exposure condition line. Lastly, line 3 is drawn from the exposure line to the y-axis to obtain the two-year diffusion coefficient. The diffusion coefficient can be used on its own right to compare the penetration resistance of chloride ions in concrete specimens or as an input in SLP models.

The basis for the CCT SLP model, is Crank's solution to Fick's second law of diffusion requiring inputs of cover depth, desired service life and diffusion coefficient and surface chloride concentration (Equation 2.4). The surface chloride concentration is dependent on binder type and exposure environment. Mackechnie (1996) collected data from various marine structures, which showed that they had consistent surface chloride concentrations, changing only with binder type. In addition, the research showed that the surface chloride concentration stabilized after a few years of marine exposure.

Once the diffusion coefficient is obtained using the equations or the monogram, Crank's solution to Fick's second law of diffusion is used to calculate the corrosion initiation period. Alternatively, a graphical solution of Equation 2.4 based on the CCT SLP empirical model can be used (Figure 2.22).

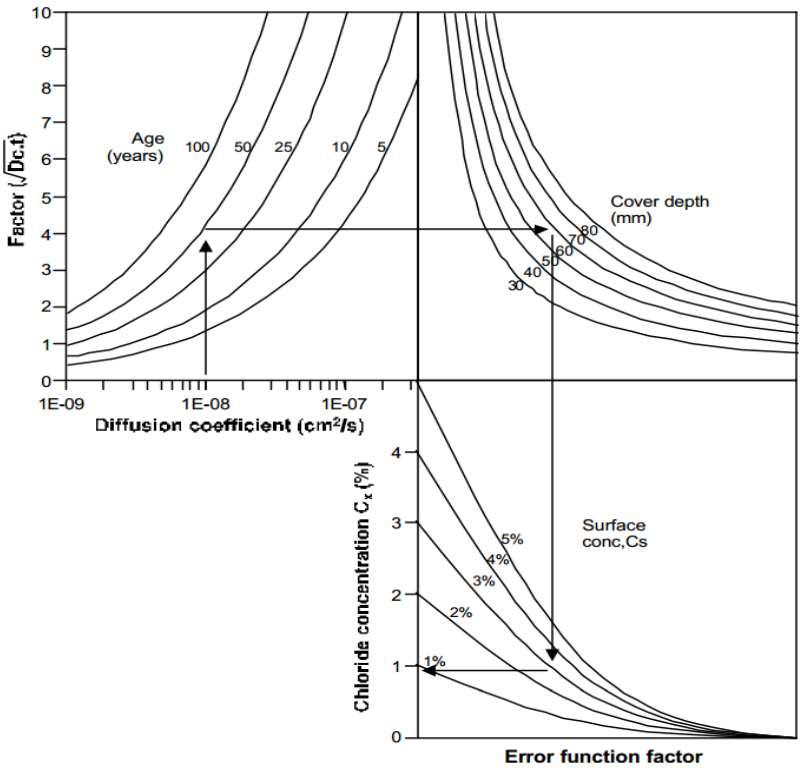

Figure 2.22: Graphical solution of Crank's solution to Fick's 2nd law of diffusion

(Mackechnie, 2001)

With this figure, designers can either obtain the chloride concentration at the desired service life or the design service life of the structure. Values for the surface chloride concentration for Crank's solution to Fick's second law can be obtained from Table 2.7. The table is based on measurements that provide values depending on binder type and exposure environment.

Table 2.7: Surface chloride concentrations (% by mass of binder)

(Mackechnie, 2001)

Concrete type	*Tidal/splash zone*	*Spray zone*
100 % PC	3.0 – 4.0	1.5 – 2.0
10% SF	2.5 – 3.0	1.3 – 1.5
30% FA	4.5 – 5.0	2.3 – 2.5
50% SL	5.0 – 6.0	2.5 – 3.0

The chloride concentration *(C_x)* obtained from Figure 2.22 can then be compared to the chloride threshold level, taken as occurring between 0.4 – 0.5% by mass of cement. The designer can then make a decision on whether or not the proposed structure will be durable enough to last as long as the desired service life (Mackechnie, 2001). This will depend on how close the calculated value is to the chloride threshold level. However, it is worth noting the variability in the literature on the chloride threshold level as seen earlier. Definitions as well as accepted values vary and authors differ even in how they define it (Glass and Buenfeld, 1997; Oh et al., 2003).

Alternatively, the diffusion coefficient and can be obtained using a spreadsheet developed at the University of Cape Town with the exposure environment, binder type, and 28-day CCT result as inputs. Other input parameters such as cover depth can be decided by the designer and input into Crank's solution to Fick's second law of diffusion to obtain the service life or corrosion initiation period of the structure.

2.3.8 Prediction of the corrosion propagation period

The corrosion propagation phase can also be modelled for purposes of service life prediction. However, many concerns regarding modelling of corrosion propagation have been highlighted by Otieno et al. (2011c). These include overestimation or underestimation of corrosion rate because of users selecting models based on input parameters at their disposal. Additionally, the corrosion propagation models are usually deficient in describing the assumptions they are based on. Moreover, the SLP of chloride-induced corrosion is usually focussed on the corrosion initiation period. The reason for this is that steel passivation quickly leads to pitting corrosion and significant loss in the rebar cross-section (Bertolini, 2008). Consequently, determining the corrosion initiation is more important than knowing the corrosion propagation period. It is for these reasons that this study was limited to corrosion initiation phase.

2.4 PART 3: SURFACE CONCRETE RESISTIVITY

Resistivity is a measure of the susceptibility of a material to the flow of ions or an electric current. A high resistivity implies that the material make-up and connectivity is not conducive for the flow of ions. In concrete, this means the composite materials that make up the microstructure and the interconnection of the pores highly influence the resistivity. Both corrosion and resistivity are electrochemical in nature. Therefore, resistivity reveals the capacity of the concrete to allow corrosion to occur, but does not indicate whether corrosion is taking place (Broomfield, 2007).

According to Polder (2001), the concrete electrical resistivity measurements of a structure exposed to chlorides are used:

- To estimate the risk of corrosion if depassivation of the steel rebars has occurred.
- To identify the most permeable parts of the structure for further investigation or rehabilitation.
- To locate spots most severely exposed to water and aggressive species.
- For the design of cathodic protection systems and other treatments.

The list above provides a starting point of the fundamentals on how the measured surface concrete resistivity is related to the properties of the RC structure. Nevertheless, in this study, the focus is on surface concrete resistivity and its use for design purposes and quality conformity of new structures. For this reason, the section that follows focusses on the concrete resistivity test methods on concrete specimens in the laboratory.

2.4.1 Surface concrete resistivity test methods

Most concrete resistivity tests require the application of a current and measuring the resulting voltage. For the most part, the tests are conducted with alternating current. The use of an alternating current as opposed to a direct current was identified and has been advised for many years (McCarter et al., 1981; Gowers and Millard, 1999). The scientific reasoning for this was the need to prevent the polarization phenomenon that occurs on the electrode-concrete interface when a direct current is used. The resistivity (ρ) equation is as follows:

$$\rho = kV \,/\, I \qquad (2.12)$$

where ρ is the resistivity; I is the alternating current *[A]*; V is the potential difference *[V]*; k is a geometrical constant

Test methods for measurement of concrete resistivity include the Wenner probe, Two Electrode Method (TEM) and Multi-ring electrode method discussed subsequently.

2.4.2 Wenner probe

The most widespread method for the measurement of surface concrete electrical resistivity is the non-destructive four point Wenner probe. The Wenner probe was initially developed as a soil resistivity test. However, it has been modified for resistivity measurements on surface concrete (Reichling et al., 2013). The Wenner probe was selected as a standard concrete resistivity test in Europe, based on its efficiency and ease of use (CHLORTEST, 2005). Other reasons included its versatility, evidenced by the fact that it can be used as both an in-situ test as well as a laboratory test. The device measures the surface concrete resistivity in a setup such as the one shown in Figure 2.23 below.

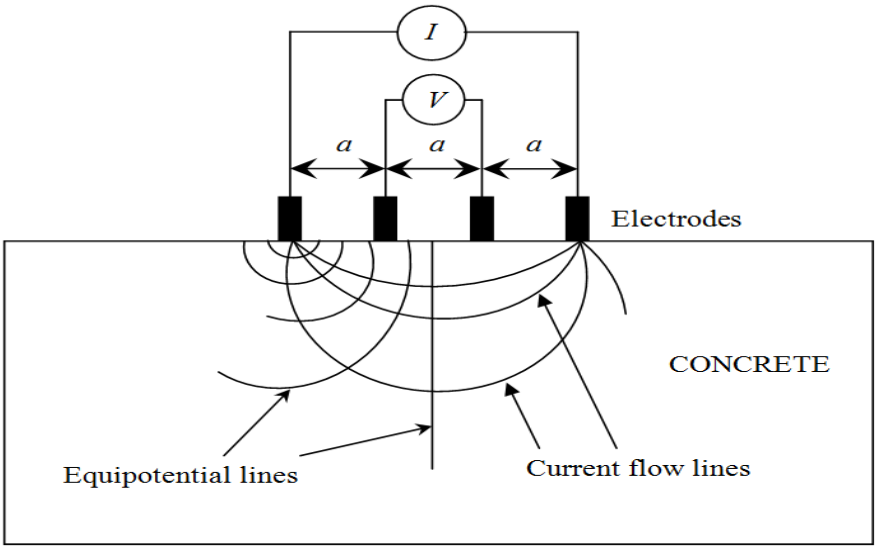

Figure 2.23: Schematic of four-electrode resistivity test, Wenner probe

(Broomfield and Millard, 2002)

To measure the resistivity, a small alternating current *(I)* is passed through the two outer probes and into the concrete specimen. Thereafter, the resulting potential difference *(V)* is measured from the two inner electrodes (Broomfield and Millard, 2002). The resistivity is calculated with geometric constant $k = 2\pi a$ in Equation 2.12 to give Equation 2.13.

$$\rho = 2\pi aV \,/\, I \qquad (2.13)$$

where ρ is the resistivity; I is the alternating current *[A]*; V is the potential difference *[V]*

Commercially available four point Wenner Probes automatically calculate the resistivity and display the reading as shown in Figure 2.24.

Figure 2.24: Commercially available Wenner probe

The Wenner probe test requires wetting or saturating of the concrete before measurements are undertaken in the laboratory or in-situ. In addition, the tips or probes of the electrode are also moistened in water to improve the electrical connection. DuraCrete (1999) suggests a well-defined pre-conditioning procedure to reduce the number of factors influencing the measurement of the resistivity (see Section 2.4.5 for more). The procedure includes storage of the concrete specimens in water containers at constant temperature for a period of at least 28 days before testing.

Alternatively, a recently released document by ASTM (2013) describes a less intensive method for obtaining the resistivity of cylindrical concrete specimens using the Wenner probe. The procedure requires a pre-conditioning period of at least 7 days during which time the concrete specimens must be at 100% relative humidity. After this period, three specimens are removed from the water; extra moisture wiped off and then tested at a temperature of 20 to 25 ℃ as follows.

i) Inscribe the cylinder as depicted in Figure 2.25

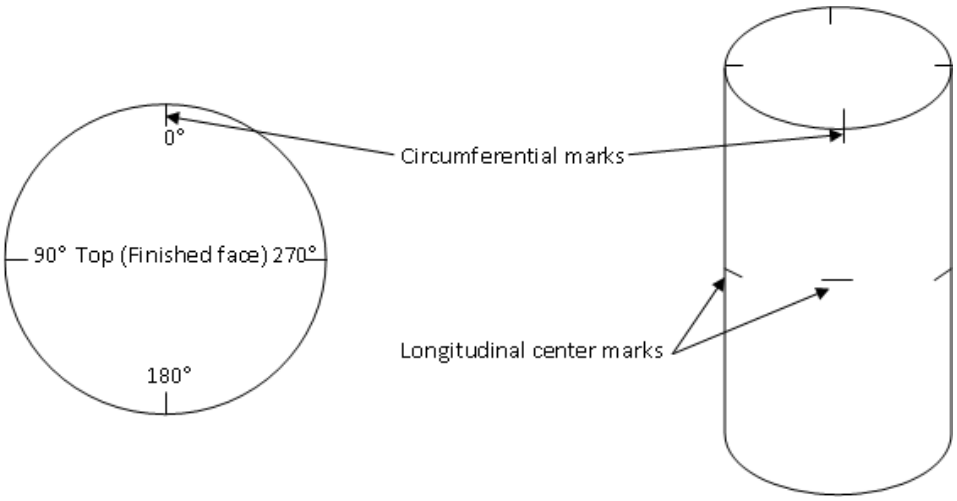

Figure 2.25: Concrete specimen marking for surface resistivity test

(ASTM, 2013)

ii) Place Wenner probe in the centre of the longitudinal side of cylinder

iii) Take measurements along the four marks in Figure 2.25 and repeat.

iv) Take the average reading of the three specimens (set) as the surface resistivity for the particular concrete mix as shown in Table 2.8.

Table 2.8: Surface resistivity readings (kΩ-cm)

(ASTM, 2013)

	1st reading				***2nd reading***				***Average***
Sample	0°	90°	180°	270°	0°	90°	180°	270°	
A									
B									
C									
	Set Average								

Table 2.9: Chloride ion penetrability based on surface resistivity *at a =38.1mm*

(Icenogle et al., 2012)

Chloride ion Penetrability	***Surface resistivity kΩ-cm 100mmx200mm***	***Surface resistivity kΩ-cm 150mmx300mm***
High	< 12	< 9.5
Moderate	12 - 21	9.5 – 16.5
Low	21 - 37	16.5 - 29
Very Low	37 - 254	29 - 199
Negligible	> 254	> 199

From the results obtained in Table 2.8, the chloride penetrability is found using Table 2.9 as recommended by Icenogle et al. (2012). Table 2.9 is in keeping with studies that have shown that the resistivity is dimension dependent and resistivity varies with change in shape and size; the thicker the specimen, the more accurate the resistivity reading (Gowers and Millard, 1999).

While 28-day moist curing is recommended for silica fume, which completes its hydrating reactions quickly, 56-day is required for fly ash and slag concrete mixes. The chloride ion penetrability obtained is then used for quality control and assurance purposes. Justification for switching from the RCPT included the low variability of resistivity results, good correlation with RCPT, and ability of concrete resistivity to identify changes in w/b ratio for the same mix (Icenogle et al., 2012). Nevertheless, it is worth noting the various factors that influence readings taken with the four-electrode setup. These are presented in detail in Sections 2.4.4 and 2.4.5.

2.4.3 Other concrete resistivity test methods

2.4.3.1 Two point test

The two point's test is a concrete resistivity test very similar to the four point Wenner probe. The main difference between the two is that for the two points test, the same two points are

used to measure both current and voltage. Gowers and Millard (1999) discourage the use of this test due to significant variation in the resistivity when the electrode diameter or contact spacing is changed. Such influence from the contact surface area is absent in the four-point test when used correctly (Broomfield and Millard, 2002).

2.4.3.2 Two Electrode Method

The two-electrode method (TEM) is a standardized test that uses two steel plates on a concrete cylinder to measure the concrete resistivity (DuraCrete, 2000). As with the Wenner probe, an alternating current is applied and the resulting voltage is measured to give the resistivity as follows:

$$\rho = RA / L \tag{2.14}$$

where A is the cross-sectional area $[m^2]$; and L the specimen length in $[m]$; *Resistance* $R = V/I$

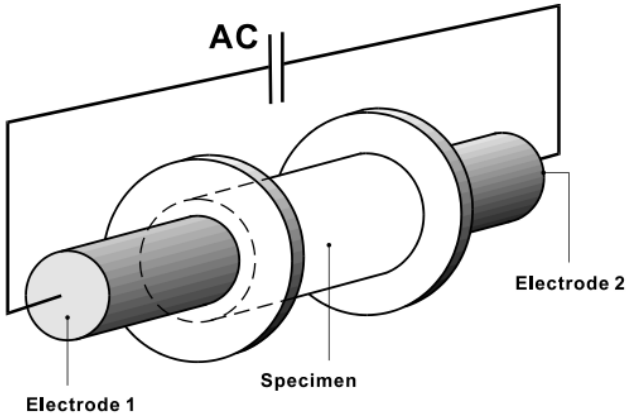

Figure 2.26: Principle of the Two-Electrode Method

(DuraCrete, 1999)

The simplicity of the TEM is illustrated in Figure 2.26. From Equation 2.14, it is apparent that precise and accurate measurements of the specimen dimensions and good electrical connection are required to obtain the correct resistivity. The recommended specimen dimensions in this case are diameter 100 mm and height 50 mm (DuraCrete, 1999). Sengul and Gjorv (2008) advise the placement of wet cloths between the concrete and the steel plates to ensure adequate electrical connection. Furthermore, 28-day storage in a chloride-free water container is suggested to lessen external influences on the resistivity, prior to the test (DuraCrete, 1999).

2.4.3.3 Multi-ring electrode method

The Multi-ring electrode method (MRE) is a sophisticated version of the TEM. As the name suggests it has multi electrodes inserted into the concrete specimen or into the structure to measure the resistivity. In addition to the properties of the TEM, it also possesses the ability to measure the time and depth-dependent resistance. However, while the cell constants for most

resistivity tests are determined through geometry, the one for the MRE has to be derived experimentally. The reason for this is that the geometrical conditions are usually difficult to determine (Büteführ et al., 2006). Moreover, the device has to be embedded into the concrete. This procedure is performed either before construction or after the structure has been built when used for in-situ placement (Weydert and Gehlen, 1999; DuraCrete, 1999).

2.4.3.4 Comparison of test methods

A comparison of the TEM and the Wenner probe is shown in Figure 2.27.

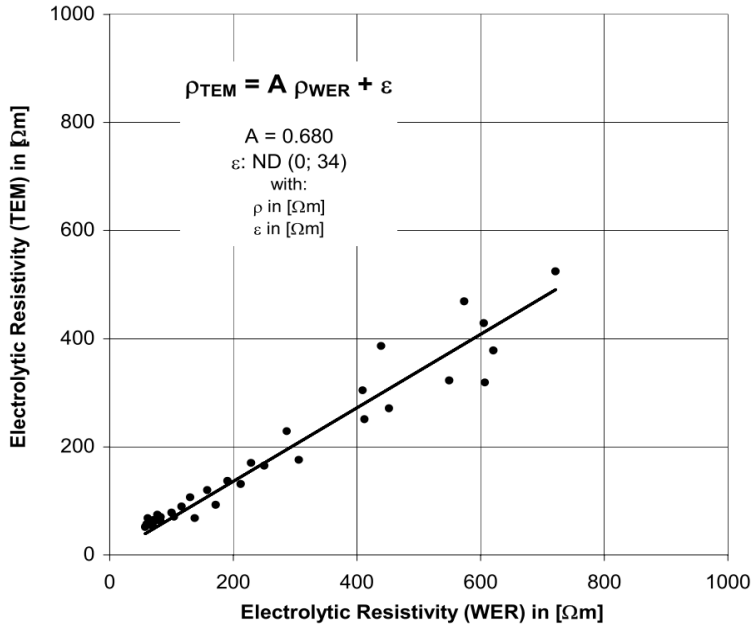

Figure 2.27: Interrelation of the TEM with the Wenner probe

(DuraCrete, 2000)

Compared to the TEM, the Wenner probe overestimates electrical resistivity by up to 1.5 times. Nevertheless, this ratio can be calculated, as it is constant provided the probe spacing and specimen type are not changing.

2.4.4 Factors influencing measurement of concrete electrical resistivity

Factors in the concrete and its environment tend to lead to variability in the test results of concrete electrical resistivity. These include the water/binder ratio, binder type and specimen shape at certain thicknesses. However, other concrete parameters such as aggregates have a low influence on the variability of resistivity results, provided a set of readings is taken over the specimen and an average reading recorded (Morris et al., 1996). Various factors and their influence on concrete resistivity are discussed in detail forthwith.

2.4.4.1 Water/binder ratio

McCarter et al. (1981) showed that the resistivity is dependent on the material mix proportions and the water/binder ratios of the concrete. These tests were carried out over a period of 4 months, which is an adequate period for the assessment of the long-term properties of concrete. According to their results, low water/binder ratios had higher resistivity than those with high water/binder ratios. The reason for this is that the degree of interconnectedness of the pores decreases as the water/binder ratio decreases (Addis, 2008). This trend was evident regardless of the mix type. Moreover, the resistivity of each mix increased slowly during the first 8 hours but increased rapidly after that and up to 24 hours. However, the increase in the longer term was minimal, with changes in resistivity no more than 0.1 *kΩ-cm* for each mix (McCarter et al., 1981). The levelling off in the long-term is possibly due to continued hydration in concrete after casting as the pore water is used up, thereby increasing the concrete electrical resistivity. As with most concrete properties, this consequence stabilizes and levels off after 28 days. This was confirmed by experiments carried out by several other researchers (Silva et al., 2006; Ferreira and Jalali, 2006; McCarter et al., 1981).

2.4.4.2 Binder type

It is generally agreed that the binder type and content has substantial influence on the concrete resistivity (Hornbostel et al., 2013; Pacheco et al., 2012). In fact, a sensitivity analysis by Pacheco et al. (2012) showed that binder type has greater influence on concrete resistivity than cover depth or w/b ratio (Figure 2.28). As the number of influencing parameters were changed, the range of resistivity was greater for binder type than for both cover depth and w/b ratio.

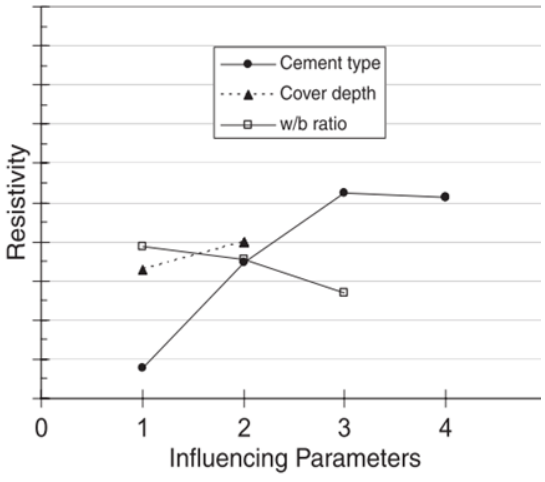

Parameter	1	2	3	4
Cement type	CEM I	CEM II	CEM III	CEM IV
w/b ratio	0.4	0.45	0.55	-
cover depth	50	10	-	-

Figure 2.28: Concrete resistivity sensitivity analysis

(Pacheco et al., 2012)

A study on concrete resistivity and binder type by Cabrera and Ghoddoussi (1994) showed that the PC concrete resistivity had a maximum increase of 50% after a year. Conversely, when Fly

Ash was added to the mix, the long-term increase in concrete resistivity was seven times more than that measured at 28 days (Cabrera and Ghoddoussi, 1994). Polder & Peelen (2002) and Smith et al. (2004) investigated the short-term (14 days) and long-term (52 weeks) characteristics of concrete with respect to concrete resistivity and supplementary cementitious materials. Increasing the percentage of silica fume showed a large initial increase in resistivity which tapered off and matched that of 100 % PC in the long-term.

In the same way, slag increased in resistivity initially and continuously increased as the concrete matured (Smith et al., 2004). The initial increase for fly ash was less than that for slag. However, the long-term increase in resistivity for fly ash was greater than that for both Slag and 100 % PC (Polder and Peelen, 2002; Smith et al., 2004). While ternary mixes with different combinations of slag, silica fume and fly ash had the highest resistivity, their use in practice would be too costly (Smith et al., 2004). It is important to note that high resistivity measurements were more prone to error due to the greater standard deviation and percentages of error. This was attributed to moisture, temperature and the closeness of the resistivity of measurement from the edge of the structure or specimen (Smith et al., 2004).

2.4.4.3 Specimen shape

Research by Gowers and Millard (1999) showed that the influence of concrete specimen geometry on resistivity measurements was minimal. This was true if the thickness and height of the specimen in question exceeded the probe spacing in the Wenner probe. This is based on a study which showed (Figure 2.29) that for any specimen for which the geometry and probe spacing ratio *b/a* exceeds two, the measured resistivity is nearly equal to the true resistivity (Gowers and Millard, 1999).

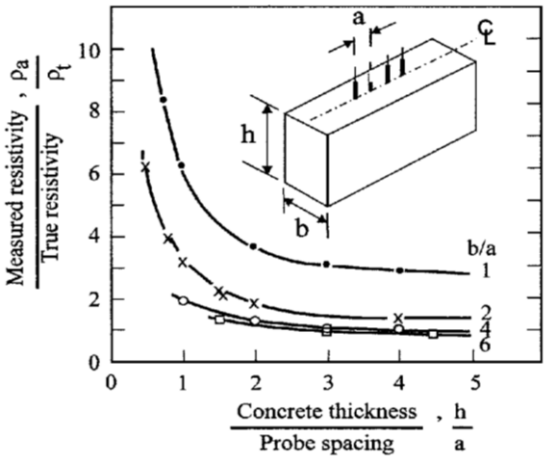

Figure 2.29: Effect of concrete section dimensions on resistivity measurement

(Gowers and Millard, 1999)

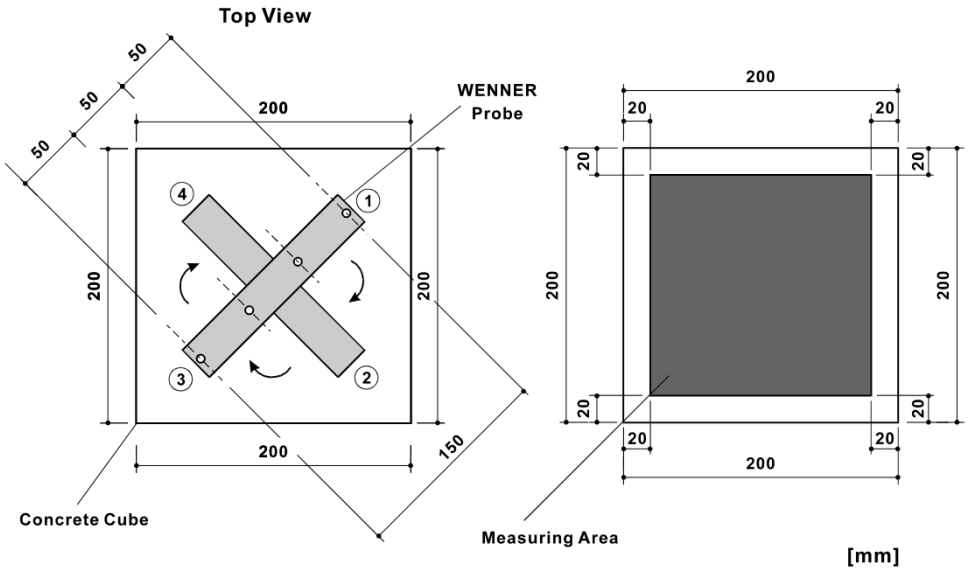

Figure 2.30: Wenner probe placement for cubic specimens

(DuraCrete, 1999)

Other research has shown that cylindrical specimens of the same concrete mix result in higher values than their cubic counterparts by up to about 30 % (Silva et al., 2006; Ferreira and Jalali, 2006). The European community uses concrete cubes for resistivity measurements, while cylinders are used in the United States of America (USA). The cylinder allows a spherical spread for the current flow. A spherical spread is also achieved when a cubic specimen is used, so long as the measurement is taken away from the edge. The recommended placement of the Wenner probe for cubic specimens is shown in Figure 2.30.

2.4.5 Challenges of site measurement of concrete resistivity

The concrete electrical resistivity test methods described above can only be used effectively if the factors that influence concrete resistivity are taken into consideration. This allows for better understanding, evaluation and interpretation of the results obtained from the test methods. According to Büteführ et al. (2006) the major environmental factors influencing the electrolytic resistivity of concrete include moisture gradients, carbonation, chloride contamination and temperature gradients. The moisture content of the concrete in particular has been highlighted as a major influence on the resistivity of the concrete. As an indication of the complexity of the interdependency of these factors, it is worth noting that the moisture content is dependent on the relative humidity of the ambient air (Osterminski et al., 2006; Weydert and Gehlen, 1999). The presence of parameters that affect the flow of ions such as sulphates and steel reinforcements also affect resistivity. These factors are investigated subsequently.

2.4.5.1 Moisture, sulphates and chlorides

Saleem et al. (1996) conducted tests to identify the effect of changes in moisture content and concentrations of sulphates and chlorides on concrete resistivity. Once cured, specimens with different moisture contents were dried and weighed. Thereafter, they were saturated, weighed and measured for concrete resistivity using a Nilsson 400 soil resistance meter, similar to the TEM. The results revealed that the electrical resistivity reduces exponentially as the moisture content is increased (Saleem et al., 1996).

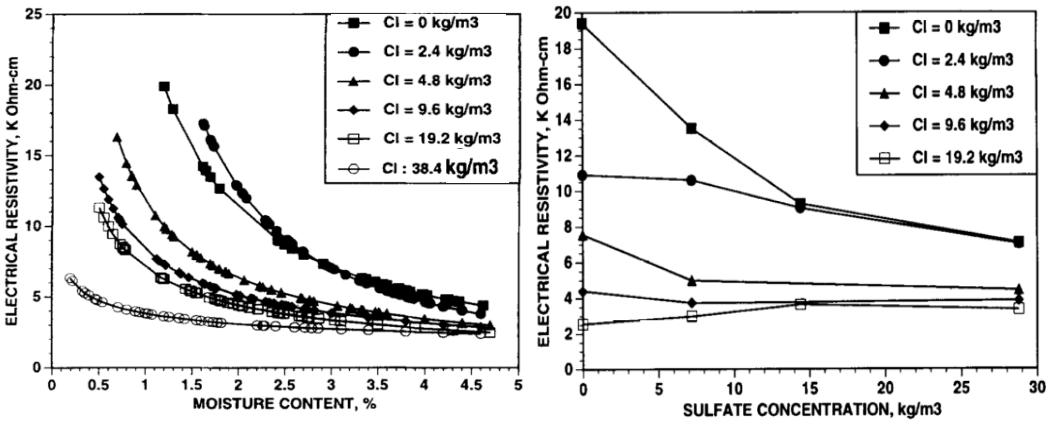

Figure 2.31: Variation of concrete electrical resistivity with moisture content and salts

(Saleem et al., 1996)

Similar results were found by Cabrera and Ghoddoussi (1994), with the resistivity decreasing rapidly at low moisture contents (1.5 – 2.5%) but levelling off at higher moisture contents. These trends were consistent even with increased chloride and sulphate concentrations in the concrete specimens (Cabrera and Ghoddoussi, 1994; Saleem et al., 1996).

Similarly, as seen in Figure 2.31, when the chloride content increased the electrical resistivity also decreased (Saleem et al., 1996; Cabrera and Ghoddoussi, 1994). This can be attributed to the increase in chloride ions facilitating conductivity. Specimens contaminated with sulphates and varying levels of chlorides showed a decrease in resistivity as the moisture content was increased. Moreover, the resistivity decreased further when a higher level of sulphate was used (Saleem et al., 1996). In the same way, specimens contaminated with chlorides and varied levels of sulphates exhibited a decrease in resistivity with increasing chloride and sulphate content. However, addition of sulphate at levels of chloride from 19.2 kg/m^3 had little effect on the resistivity; it remained consistently low at about 3kΩ-cm, regardless of the moisture content (Saleem et al., 1996).

When sulphates react with the hydrated products, destruction of the hardened cement paste occurs thereby reducing the resistivity as this allows the movement of ions (Addis, 2008). In

addition, sulphates stop the formation of Friedel's salts caused by the reaction of chlorides with aluminates. Rather the cement "prefer" to react with the sulphates so that there are more free chlorides and hence a decrease in resistivity (Thomas et al., 2012; Luo et al., 2003).

Other researchers have shown that when specimens are exposed to wet cycle periods of 1 and 2 weeks, they have better electrical connection and therefore lower concrete resistivity values. Conversely, when exposed to dry cycle periods, the electrical connectivity is lost and the concrete resistivity is high (Smith et al., 2004). Therefore, the concrete electrical resistivity is highly dependent on the moisture content. However, results from Saleem et al. (1996) show that this is less evident when the concrete has high salt concentrations.

These results are also true when specimens are left exposed to the environment and the concrete constituents changed. For instance, exposure environments high in sulphates and chlorides will lead to a decrease in electrical resistivity. Moreover, concrete resistivity measured during the rainy season is likely to be lower than in dry seasons, other conditions being constant. This is because high pore saturation makes the flow of ions easier and consequently the resistivity is less. An increased number of pores and a higher water cement ratio also decrease the resistivity (Polder and Peelen, 2002).

The resistivity also decreases with increasing porosity, depending on the degree of saturation; the higher the degree of saturation, the lower the resistivity (Cabrera and Ghoddoussi, 1994).

2.4.5.2 Temperature

Just as in most electrochemical processes, the external and internal temperatures affect the concrete resistivity. The reason for this trend is the influence temperature has on the kinetic energy of the ions; higher temperatures energise the ions. To this end, Ferreira and Jalali (2006) carried out experiments where the temperature of the concrete was controlled by immersing the concrete specimens in stabilized temperature water baths. Afterwards, the samples were removed and the electrical resistivity was measured. The results revealed that the effect of temperature is the same as that described for moisture, with the resistivity decreasing as the temperature increased (Silva et al., 2006).

Another temperature evaluation experiment was conducted on covered specimen, to prevent evaporation after casting (Manera et al., 2008). Specimens were exposed to different temperatures for 15 days and their resistivity measured and showed the same trend. In yet another attempt at classifying the temperature – resistivity relationship Riding et al. (2008) modified the RCPT to a five-minute resistivity test. The resistivity was measured after 91 days of moist curing after being placed in water at temperatures of 23, 38 and 60 ℃ to give the trend shown in Figure 2.32.

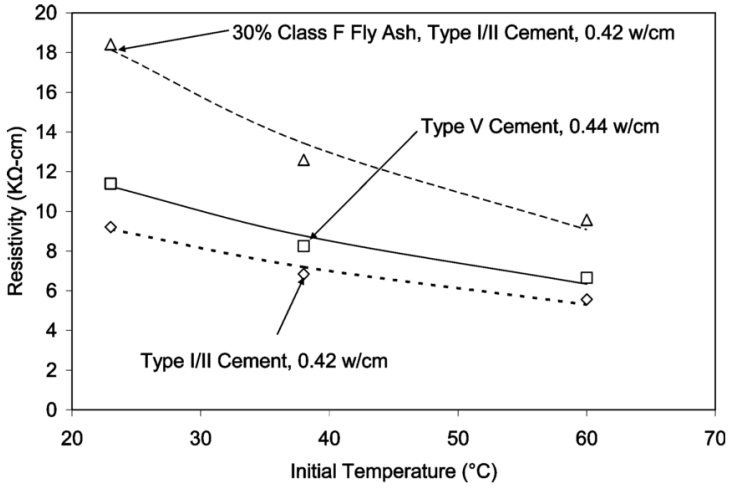

Figure 2.32: Electrical resistivity as a function of temperature

(Riding et al., 2008)

A similar experiment involving temperature versus concrete electrical resistivity also showed a linear inverse relationship between the two (Gowers and Millard, 1999). The researchers suggest adjusting resistivity measurements not taken at ambient temperature by +1k*Ω-cm* per 3 ℃ fall in temperature. However, it is worth noting that these results (Gowers and Millard, 1999) are limited to temperatures between 8 and 20 ℃. Alternatively, McCarter et al. (1981) suggested a more comprehensive method of accounting for measurements at different temperatures by means of the Arrhenius equation:

$$\rho_e(T) = \rho_0 \cdot e^{A\cdot\left(\frac{1}{T}-\frac{1}{T_0}\right)} \qquad (2.15)$$

where $\rho_e(T)$ and ρ_0 in *[Ω-m]* are the resistivities at ambient temperature T and measured temperature T_0 in *[K]* and A is the activation energy in *[K]*.

The Arrhenius equation was proven experimentally to be an accurate presentation of the relationship between concrete resistivity and temperature using an activation energy of 3270 K (Osterminski et al., 2006). Prior to this, DuraCrete (1999) had also advocated for the use of the Arrhenius equation during concrete resistivity measurements.

2.4.5.3 Steel reinforcement

The presence of steel reinforcement influences the measurement of concrete resistivity because steel is a good electrical conductor. Therefore, when measuring the resistivity in-situ, researchers have found that it is necessary to use a cover meter to determine the position of the reinforcement. Thereafter, care must be taken to take the electrical resistivity measurement away from the reinforcement when using the Wenner probe (Sengul and Gjorv, 2009). If the reinforcement cannot be avoided, measurements must be carried out perpendicular to the reinforcement rather than parallel to avoid the effect (Broomfield and Millard, 2002). This is

especially important for shallow covers, less than 30 mm (Weydert and Gehlen, 1999). However, if the probe spacing (see Figure 2.23) is much larger than the concrete cover, distortion of the measured concrete resistivity is inevitable. The recommended probe spacing is at most two-thirds the cover depth (Gowers and Millard, 1999). Moreover, it is recommended that readings be obtained at several points on the surface concrete to give a more accurate representation of the concrete resistivity (Weydert and Gehlen, 1999; Polder, 2001; Sirieix et al., 2003).

2.4.5.4 Chloride ingress and carbonation

A surface layer present on a concrete specimen interferes with the measured resistivity. This is problematic especially when a Wenner probe is used due to its requirement of closeness to the surface during measurement (Weydert and Gehlen, 1999). Gowers and Millard (1999) carried out various studies to determine the effect of chloride ingress and carbonation on the measurement of the concrete electrical resistivity. They concluded that a surface layer with a low resistivity has a considerably higher impact on the true resistivity than a higher resistivity surface layer.

For instance, chloride ingress creates a lower resistivity surface layer on concrete structures or specimen. However, its effect on the resistivity was eliminated when the electrode contact spacing was greater than eight times the surface layer thickness (Gowers and Millard, 1999). Likewise, carbonation creates a surface layer on concrete. The carbonation layer interferes with resistivity measurement such that the reading is a combination of the concrete and the carbonation layer (Weydert and Gehlen, 1999). Unlike chloride ingress, carbonation creates a high resistivity surface layer when the surface concrete is dry but a lower resistivity surface layer when it is wetted. However, the consequence of wetting carbonated concrete is difficult to predict.

Nevertheless, knowledge of the thickness and resistivity of the carbonated surface layer can be used to limit the effect. This can be achieved by using electrode spacing greater than 8 times the layer thickness just as with chloride ingress (Gowers and Millard, 1999). In cases where the carbonation surface layer exceeds the cover size, the researchers recommend taking the resistivity reading as it is. In effect, if it is thicker than the cover size, resistivity of the carbonation layer will be the same as that of the concrete. Their results revealed that this assumption is valid provided the electrode spacing is set no more than the carbonation layer (Gowers and Millard, 1999).

This presents a problem in cases where the Wenner probe is used because the commercially available version has fixed probe spacing. The carbonation effect is small enough to be ignored after 28 days of immersion in water in the laboratory but this cannot be applied to in-situ measurements (DuraCrete, 1999). To garner a measure of control, considerable wetting of the

surface of the concrete is advised when there is suspicion of layer effects. It is worth noting that this is not a problem when a Multi Ring Electrode is the instrument of choice (Weydert and Gehlen, 1999).

Concrete electrical resistivity is a reflection of the ionic strength of the pore solution and the microstructure of the concrete. As seen previously, both these properties also affect concrete durability and the corrosion rate. Therefore, electrical resistivity provides an assessment of the concrete quality and prediction of performance. The following sections describe the procedures for use of concrete resistivity for quality control and service life prediction.

2.4.6 Concrete electrical resistivity and quality control

The use of concrete resistivity in quality control is based on its relationship with the diffusion coefficient. It has been shown that measurements of concrete electrical resistivity have a good correlation with diffusion (Ferreira and Jalali, 2006; Kessler et al., 2008). In mathematical terms the correlations is a simplification of the Nernst-Einstein equation (2.6), given a certain type of concrete, constant moisture and temperature (Sengul and Gjorv, 2008):

$$D = \frac{k}{\rho} \tag{2.16}$$

where k is a constant; ρ is the concrete resistivity; D is the diffusion coefficient

The above simplification of the Nernst-Einstein equation shows that the product of the diffusivity and the resistivity is a constant value *'k'*. Empirical evidence has supported this simplification (Sengul and Gjorv, 2008; Polder, 2005; Ferreira and Jalali, 2006). For instance, Polder (1995) carried out experiments on a number of concrete mixes in the marine environment. These experiments revealed a correlation between the measured concrete resistivity and the chloride diffusion coefficient. The study was undertaken for a period of 18 months and separate tests on the mixes were conducted to establish the resistivity and the diffusion coefficient. Results showed that:

i) The diffusion coefficients for the mixes decreased in the same order as that of the increase in resistivity.

ii) The product of the resistivity and the effective diffusion coefficient was similar across the five mixes.

While the concrete tested initially was relatively young, subsequent testing of concrete samples that had been submerged in the sea for 16 years revealed the same trends (Polder, 1995). This suggests that empirical evidence agrees with Equation 2.16 and it is possible to use it for determining the diffusion coefficient provided the electrical resistivity and the constant *'k'* is known.

More recently, researchers Sengul and Gjorv (2008) as well as Polder and Peelen (2002) used the NT Build 492 to obtain the chloride diffusivity at different ages. They then used the Two Electrode Method and the Wenner probe to determine the resistivity. Thereafter, the diffusivity results were plotted against resistivity results. This is depicted in Figure 2.33 and Figure 2.34 for one concrete mix and four concrete mixes respectively. Judging by the decrease in the correlation coefficient, the relationship is less apparent when more mixes are used.

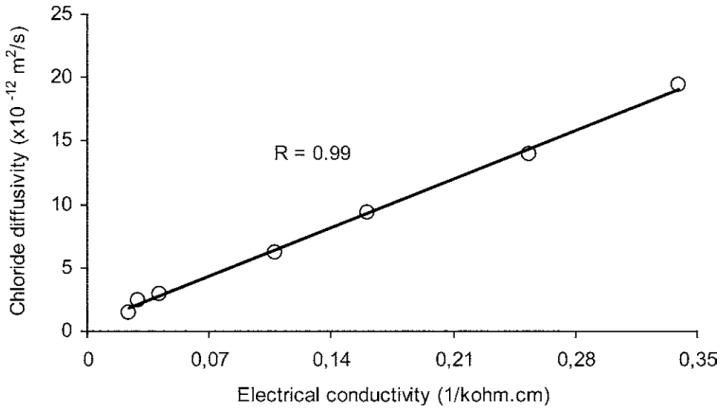

Figure 2.33: Chloride diffusivity and electrical conductivity from 3 days to 1 year

(Sengul and Gjorv, 2008)

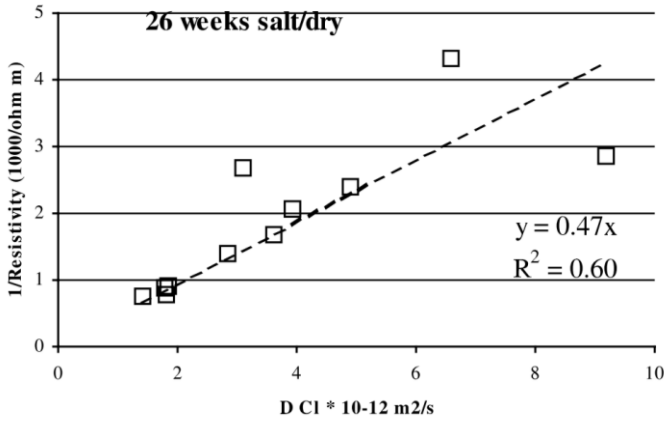

Figure 2.34: Correlation between inverse resistivity and diffusion exposed to salting and drying

(Polder and Peelen, 2002)

The linear relationship was used to obtain '*k*' from Equation 2.16. Once *'k'* is known, for a particular mix, computing the electrical resistivity negates the need to measure the diffusivity of the concrete during construction. In essence, the '*k*' value in Equation 2.16 is established in the lab beforehand, by measuring the resistivity and diffusivity for each concrete mix. The resistivity results obtained during construction are then used to gauge the degree to which these align with the previously calculated diffusivity.

The research was the basis for the creation of a performance-based approach. A similar approach was successfully implemented during the Great Heart Tunnel project. Specimen results for TEM concrete resistivity during the construction phase (28-day testing) showed good correlation with validation results using rapid chloride migration tests conducted one to three years later (Rooij et al., 2007).

Alternatively, Silva et al. (2006) have proposed the following approach. They suggest the use of early age (3-day and 7-day) concrete resistivity to predict 28-day concrete resistivity, thereby linking resistivity to long-term durability. Their research showed that values for the electrical resistivity measured after two months matched well with predicted values. The predicted values were obtained using a hyperbolic equation converted to a straight-line equation (2.17).

$$\frac{t}{\rho} = a \cdot t + b \qquad (2.17)$$

where t is the time in days; ρ is the resistivity and a and b are constants.

A graph of t/ρ versus time (t) is plotted to obtain the constants a and b. The 7-day data curve was closer to the predicted curve than the 3-day data curve. However, before the predictions are considered valid, the researchers recommend establishing whether the concrete mix in question has a good correlation with the electrical resistivity. A possible method of conducting this test is by using the procedures described above of plotting resistivity and diffusivity values to obtain *'k'*.

2.4.7 Prediction of the corrosion initiation period

Andrade and Andrea (2010) have shown that electrical resistivity measurements can be used for service life prediction by employing a series of equations. The approach they use is similar to the South African CCT service life model in its use of the cover depth, the exposure class and a durability test result. However, it does not include Fick's second law of diffusion for the estimation of the corrosion initiation period. Instead, the following procedure is followed to come up with the equation for service life prediction.

Firstly, to take into account the long-term effect of chloride binding and the aggressiveness of the environment, they replace the constant k in Equation 2.16 with constant factors K and r, so that it becomes:

$$D = \frac{K}{\rho . r} \qquad (2.18)$$

where K is a measure of the severity of exposure to the environment; reaction factor r is dependent on the chloride binding capabilities of the cement; ρ is the concrete resistivity; D is the diffusion coefficient

Experiments on real structures in environments similar with the exposure classification of the Eurocode and the Spanish multi-regime test were used to establish *K* and *r* respectively. The multi-regime test method makes use of a version of a migration cell with an anolyte and a catholyte as seen in the RCPT (see Section 2.2.7.2). The value of *r* is the ratio between steady state and non-steady test diffusion coefficients, which can both be calculated from the multi-regime test. The reaction factor also represents the retardation of the chloride profile through the concrete caused by chloride binding.

Both factors *K* and *r* can be obtained from studies conducted by Andrade and Andrea (2010) which negates their calculation for every concrete mix or cement. The values for these factors are listed in Table 2.10 and Table 2.11. However, it is worth noting that Table 2.10 are preliminary values and studies are ongoing to establish the most appropriate values for a wider range of cements (Andrade et al., 2014).

Table 2.10: Recommended values for reaction factors

Based on Andrade and Andrea (2010)		**Based on Andrade et al. (2014)**	
Cement	***r***	***Cement***	***r***
CEM I (42.5 R)	1.9	CEM I (42.5R)	1.5 - 2
CEM I + silica fume	1.5	CEM II + Pozzolans + silica fume	1.5 - 4
CEM IIA	3	CEM IIA and III	3 - 5

Table 2.11: K values for marine exposure classifications

(Andrade and Andrea, 2010)

Exposure class	***K***
XS1 (d > 500m distance to the coastline)	5000
XS1 (d < 500m distance to the coastline)	10000
XS2	17000
XS3	25000

Resistivity changes with age due to continued hydration of the concrete. This necessitated the inclusion of the aging factor q in the 28-day resistivity result ρ_0 as shown in Equation 2.19. The factor q is also dependent on the cement type and can be determined by plotting the inverse of electrical resistivity with the log of time in days. The value of q is the slope of the resulting curve.

$$\rho_t = \rho_0 \left(\frac{t}{t_0}\right)^q \qquad (2.19)$$

where t is the period for which the aging factor is calculated and t_o is the time at first measurement of the resistivity ρ_0, q is the aging factor

Note that the time-dependent resistivity equation is the inverse of the time-dependent diffusion coefficient (see Equation 2.5) since resistivity increases with time.

To determine the diffusion coefficient with a position in time, Einstein's equation for Brownian motion is used (Equation 2.20).

$$x = \sqrt{DT} \qquad (2.20)$$

where x is the cover depth *[cm]* and T is the diffusion period *[years]*.

Combining Equations 2.18 – 2.20 yields the following equation for the corrosion initiation period:

$$T = \frac{x^2 \cdot \rho_0 \left(\frac{t}{t_0}\right)^q}{K} \cdot r \qquad (2.21)$$

In summary, the following are required to predict the time to corrosion initiation of a concrete specimen:

- The surface resistivity result after 28 days of moist curing
- exposure class (K)
- service life (T), cover (x)
- binder type (r)
- aging factor (q)

2.4.8 Concrete resistivity and diffusion coefficients

There are two approaches for the calculation of diffusion coefficients based on concrete resistivity. The first approach to calculate the diffusion coefficient using resistivity is based on Archie's law (Archie, 1942) shown in Equation 2.22.

$$F = \frac{D}{D_o} = \frac{\rho_0}{\rho} = \varphi^{-c} \qquad (2.22)$$

where F is the formation factor (or diffusibility – see Equation 2.7); φ is the porosity limited to between 0.05 – 0.40; c is a constant characteristic of the type of porous medium; ρ_0 is the effective resistivity of the saturated medium and ρ is the resistivity of the pore solution; D is the diffusion coefficient of the saturated medium; D_o is the diffusion coefficient of the pore solution

The approach was derived from the oil industry where it has been validated and is used in geology (McDuff and Ellis, 1979). The principles and values for the constants are well known when applied to rocks but different values for the factors had to be determined for concrete. Tumidajski et al. (1996) found that the equation was valid for cementitious systems provided they were well hydrated. When the porosity φ and constant (c) are known then the diffusion coefficient of the saturated concrete can be determined. The use of this approach requires prior

knowledge of c and φ. However, it has been found that values for c and φ vary widely between different concrete types (Tumidajski et al., 1996; Oh and Jang, 2004; Nokken and Hooton, 2007). This means that in addition to obtaining the resistivity and diffusion coefficient of the pore solution, values for c and φ have to be found for each concrete type.

The second approach that can be used to calculate the diffusion coefficient using resistivity is similar to the one above. Although it also makes use of the diffusibility equation (2.7) as shown in Equation 2.23, less parameters are needed to establish the diffusion coefficient as explained below.

$$D_\rho = \frac{D_0}{\sigma_0} \times \frac{1}{\rho} = \frac{B}{\rho} \qquad (2.23)$$

where D_ρ is the effective chloride diffusion coefficient; D_o is the free diffusion coefficient of the chlorides in the pore solution and σ_0 is the conductivity of the pore solution; ρ is the electrical resistivity of the water saturated material.

Baroghel-Bouny et al. (2009) argue that the diffusion coefficient for chloride ions and conductivity of the concrete pore solution are constants dependent on the ionic concentration of the pore solution. The former can be found in chemistry textbooks while the latter is the subject of studies by various authors such as Rajabipour and Weiss (2006) who created a contraption for this purpose. Snyder et al. (2003) introduced the electrochemical equation summing up products of the valence, concentration and conductivity of each ionic species to get σ_0. Alternatively, the pore solution expression method can also be used which requires the squeezing out of the concrete pore solution and using chemistry analysis to determine its conductivity. More details on this and other methods can be found in a study by Buckley et al. (2007).

Alkaline solutions comparable to cementitious materials were found to have pore conductivity of 11.87 (Ω^{-1} m^{-1}). A value of 2.03 (10^{-9}) m^2/s was selected for the diffusion coefficient of chlorides ions in a 1M solution at 25 °C, as reported by Lide (2005). The value for pore solution conductivity is based on studies by Rajabipour and Weiss (2006) who used the Snyder et al. (2003) method to obtain the conductivity. It is worth noting that researchers have also shown that addition of slag and fly ash does not affect the pore solution conductivity (Nokken and Hooton, 2007). From these values, Baroghel-Bouny et al. (2009) established the following equation for the determination of an effective diffusion coefficient using resistivity measurements for blended cement concrete:

$$D_\rho = \frac{171}{\rho} \qquad (2.24)$$

where D_ρ is the effective chloride diffusion coefficient in the porous material in 10^{-12} m^2/s, when ρ is the electrical resistivity of the water saturated material in Ω-m

Note the similarity between Equation 2.16 and Equation 2.24.

The pore solution conductivity for plain PC or CEM I concrete is highly dependent on the w/c ratio and so the constant was found quite different from other binder types. Consequently, Baroghel-Bouny et al. (2009) proposed the following categories for CEM I concretes:

For w/c = 0.45 – 0.55:

$$D_\rho = \frac{207}{\rho} \quad (2.25)$$

For w/c = 0.60 – 0.70:

$$D_\rho = \frac{303}{\rho} \quad (2.26)$$

For w/c ≥ 0.80:

$$D_\rho = \frac{406}{\rho} \quad (2.27)$$

In the first category, the pore solution conductivity was equal to 9.8 (Ω^{-1} m^{-1}), second category 6.7 (Ω^{-1} m^{-1}) and the third category 5.0 (Ω^{-1} m^{-1}). Baroghel-Bouny et al. (2009) found that diffusion coefficients based on these equations were linked with diffusion coefficients calculated from non-steady state migration tests by the porosity.

$$D_\rho = \varphi D_{nss} \quad (2.28)$$

where D_ρ is the effective chloride diffusion coefficient in 10^{-12} m^2/s; φ is the porosity of the concrete; D_{nss} diffusion coefficients calculated from non-steady state migration tests

2.5 SUMMARY OF LITERATURE REVIEW

A number of durability tests currently exist for the determination of the rate at which chloride ions are transported through concrete. These are normally diffusion-based because this is the primary method for the transportation of chloride ions through concrete. Some of the tests are long-term such as the pure diffusion 90-day salt ponding test that allows the chloride ions to diffuse naturally through the concrete. Quicker tests are necessary to lessen the waiting period before owners and designers are informed of the quality of the concrete to be used for construction.

For this reason, other tests incorporate migration or the application of an electric field to speed up the movement of chloride ions, which drastically reduces the testing period. Migration test results are usually related to diffusion using relationships such as the Nernst-Einstein equation or the diffusibility equation. The equations also have test parameters such as voltage or current as input parameters and the diffusion coefficient as the output. The diffusion coefficient is then

used as an input parameter in Fick's 2nd law of diffusion during the service life design process. Alternatively, it can be used as a quality control parameter during construction.

The most commonly used short-term chloride diffusion test is the rapid chloride penetrability test (RCPT), a migration test that takes 6 hours. However, its theoretical basis and relationship with chloride diffusion continues to be disputed. In addition, the high voltage applied during testing has been shown to cause damage to the concrete microstructure. Moreover, the RCPT is not suitable for high performance concrete. In DuraCrete, the rapid chloride migration test is used which gives results within 6 to 96 hours but requires a complex setup.

An alternative to the RCPT is the chloride conductivity test (CCT), which is part of the South African Durability Index approach. With the application of an electric field through the concrete, the CCT can be conducted rapidly (up to 20 samples per hour) to characterise the quality of concrete. It also has a good correlation with long-term diffusion tests. In addition, testing in multiple labs revealed good reproducibility and repeatability. Even though a lower voltage than that of the RCPT is used, research has shown that concrete samples may suffer microstructural damage during the pre-conditioning process that involves oven heating. The CCT is used for quality control during construction and for corrosion initiation prediction during the design process. The CCT service life prediction (SLP) model is based on Fick's second law of diffusion with a time-dependent diffusion coefficient requiring input of the 28-day CCT result.

Another test that has recently been gaining prominence in durability design and quality control of reinforced concrete is the surface concrete resistivity test. Resistivity is a measure of the ability of concrete to resist penetration of deleterious species such as chloride ions. There are a number of test methods used to measure surface resistivity in concrete. Most of them can be conducted within minutes as they usually involve the application of an electric field to a concrete specimen. The two-electrode method and the four-point Wenner array probe are the most user-friendly, the easiest to use and quickest there is.

One limitation with measuring concrete resistivity either on site or in the laboratory is the variation in results with changes in testing conditions. Some of these changes include temperature, presence of steel reinforcement, surface layers, salts and moisture. However, if the influence of the changes on the surface concrete resistivity is known, the correct resistivity can be determined using equations that account for these influences (Gowers and Millard, 1999; Sirieix et al., 2003).

Surface concrete resistivity is used as an input parameter for service life design of RC structures as well as to obtain the diffusion coefficient and for quality control purposes during construction. Resistivity results are used for construction quality control in two ways. Either

resistivity is related to chloride ion penetrability as is done with RCPT results, or researchers use its inverse proportionality with the chloride diffusion coefficient. The 28-day resistivity is used as in input variable to predict the corrosion initiation period based on a model by Andrade. The resistivity diffusion coefficient is obtained from equations by Baroghel-Bouny et al. (2009), also based on its inverse proportionality with resistivity. The equations depend on binder type and water binder ratio.

With the implementation of surface concrete resistivity test standards in Europe (Rooij et al., 2007) and North America (Kessler et al., 2008) for quality control and service life prediction, surface concrete resistivity is worth investigating. The literature review did not reveal any attempts to compare the surface concrete resistivity with the CCT, as is the focus of this study. From the literature review, it can be deduced that the CCT and surface concrete resistivity can be compared as follows:

- Using SLP models for prediction of *corrosion initiation periods* and *diffusion coefficients.*

These will be explored further in the chapter that follows.

3 METHODOLOGY OF RESEARCH

3.1 Introduction

The purpose of this chapter is to describe the methodology used in this study to compare surface concrete resistivity and the CCT. Background research was carried out in the previous chapter in the form of a literature review as a guide to the study. Scientific method was used in this study to compare the CCT and surface concrete resistivity and ascertain a relationship between the two as summarized in Figure 3.1.

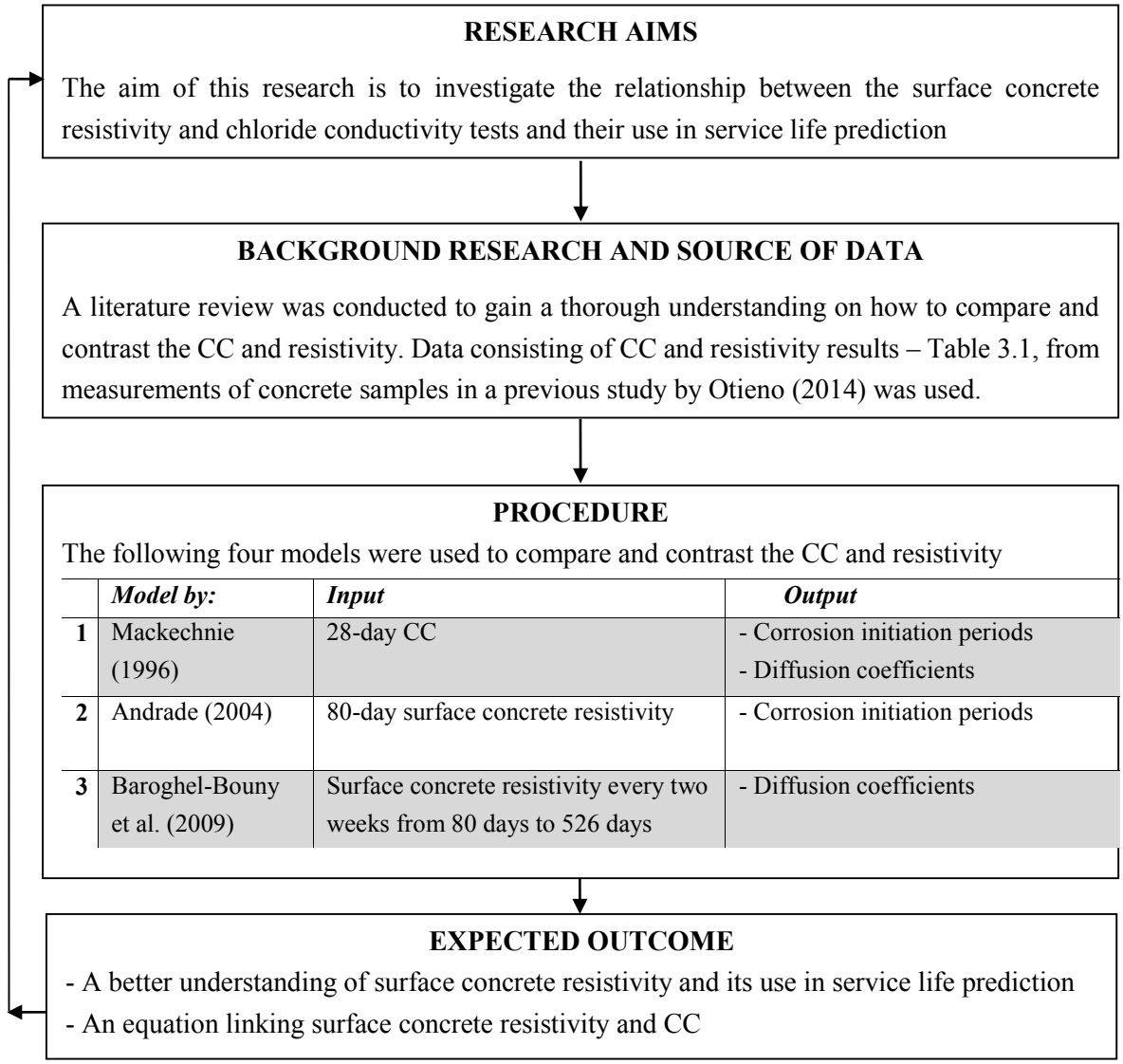

Figure 3.1: Summary of the research methodology

This chapter describes Otieno's (2014) test results, service life prediction (SLP) models and the statistical tests used in the next chapter to compare CCT and surface concrete resistivity. Results for both CCT and surface concrete resistivity were available from an on-going study

being carried out by Otieno (2014). For resistivity, models by Andrade (2004) and Baroghel-Bouny et al. (2009) were used to calculate the corrosion initiation period and diffusion coefficient respectively. For CCT, the service life prediction (SLP) model by Mackechnie was used.

3.2 Data used in the study

The data used in this study is from a project conducted by Otieno (2014) on the effect of cover depth, concrete quality and crack width on corrosion rate. It involved exposing reinforced concrete (RC) beam specimens (120 x 130 x 375 mm) to both field and laboratory environments. Measurements included corrosion rate, half-cell potential surface resistivity and concrete quality following the South African Durability Index tests. In this study, only the CCT and resistivity test results from uncracked specimens will be used, as the focus is to compare and contrast the two. Otieno's (2014) project investigated five concrete mixes as illustrated in Table 3.1.

Table 3.1: Concrete mixes for Otieno's study

Binder composition	**100 % PC**	**50/50 PC/GGBS**		**70/30 PC/FA**	
w/b ratio	**0.40**	**0.40**	**0.55**	**0.40**	**0.55**
Material(kg/m^3) Mix label	**PC-40**	**SL-40**	**SL-55**	**FA-40**	**FA-55**
PC (CEM I 42.5N)	500	231	168	324	236
GGBS	-	231	168	-	-
FA	-	-	-	139	101
Fine aggregate: Klipheuwel sand (2 mm max.)	529	749	855	749	855
Coarse aggregate: Granite (13 mm max.)	960	1040	1040	1040	1040
Water	200	185	185	185	185
Superplasticizer (SP) (litres/m^3)	2.1[a] (0.4)[b]	1.8 (0.4)	0.3 (0.1)	0.4 (0.1)	-
28-day compressive strength (MPa)	58 (3.0)	48 (2.0)	35 (0.9)	51 (0.9)	29 (1.9)

[a]: Percentage of SP by mass of total binder

[b]: Standard deviation

The mix design for the project consisted of three binder types GGBS, FA and PC with a high (0.55) and low (0.40) w/b ratio. Otieno (2014) accounted for other factors such as the exposure conditions by conducting the resistivity measurements in varied environments i.e. field and laboratory (Figure 3.2). Field specimens were placed along the Cape Town harbour two weeks before the first measurement, which was conducted 80 days after casting. Laboratory specimens were kept at a constant temperature of 25 °C. They were also exposed to three-day

cyclic wetting with 5% NaCl solution to induce accelerated corrosion. This was followed by four days of air-drying.

Figure 3.2: Laboratory and field concrete specimens from Otieno's study

The four-point Wenner probe was used to measure surface resistivity at a probe spacing of 50 mm. Surface concrete resistivity measurements for both field and laboratory environments were carried out every two weeks for 1.7 years. The CCTs were carried out at 28 and 90 days. The results from the tests were used as input parameters for the comparison of CCT and surface concrete resistivity as described in the sections that follow.

3.3 Procedures and models used for data analysis

3.3.1 Prediction of corrosion initiation period using CCT

The 28-day CCT is used in a service life prediction model (SLP) for the determination of the corrosion initiation period. The CCT SLP model entails using Equation 3.1 or Crank's solution to Fick's second law of diffusion, shown below.

$$t = \frac{x^2}{4D\left[erf^{-1}\left(1-\frac{C_x}{C_s}\right)\right]^2} \qquad (3.1)$$

where t is the corrosion initiation period *[years]*; x is the cover depth *[cm]*; D is the diffusion coefficient *[cm^2/year]*; C_s refers to the surface chloride concentration *[%]*; C_x refers to the chloride concentration at the cover depth *[%]*, erf^{-1} is the inverse error function

In calculation of the corrosion initiation period, the chloride concentration at the cover depth is the chloride threshold level. The chloride threshold level at the cover depth is taken as 0.4% in the CCT SLP model (Mackechnie, 2001). The other values required for Equation 3.1 were obtained as follows.

3.3.1.1 Diffusion coefficient and surface chloride concentration

The diffusion coefficient and surface chloride concentration were obtained from the equations and procedure described in Section 2.3.7. This is based on work by Mackechnie (1996) specific to binder type and exposure category for prediction of chloride ingress in reinforced concrete. The procedure is simplified in a spreadsheet in Table 3.2 developed at the University of Cape Town (UCT). Of the binder types listed in Table 3.2 (100% PC, 30% FA and 50% BS respectively), 1, 3, and 4 were used in Otieno's (2014) project.

Table 3.2: Screenshot of inputs and outputs in UCT spreadsheet for CCT SLP model

(Mackechnie, 1996)

							Binder type	
INPUTS			***OUTPUTS***				1	100% PC
							2	10% SF
28-day CCI	2.00		**Cs**	5.00	%		3	30% FA
Age (years)	50		**Dc (2yr)**	8.2E-08	cm^2/s		4	50% BS
Binder	4		**m**	0.68			5	50% CS
Exposure	20		**log Di**	-1.78			***Exposure category***	
			Dc (age)	9.2E-09	cm^2/s		10	Extreme
							20	Very severe
							30	Severe

3.3.1.2 Marine exposure categories

The marine exposure categories listed in the spreadsheet are based on the BS 8110 presented in Table 3.3.

Table 3.3: Marine exposure categories for use in CCT SLP

(BS 8110, 1992)

Marine exposure category	***Marine tidal and splash zones***	***Marine spray zone***
Extreme	Structures exposed directly to sea water with heavy wave action and/or abrasion	N/A
Very severe	Structures exposed directly to sea water under sheltered conditions with little wave action	Structure within 500m of shore exposed to heavy wave action and onshore wind
Severe	N/A	Structure located near shore (>500m) in an exposed marine location
Moderate	N/A	Structure in a sheltered location within 1km of shore or anywhere within 30km of coast

3.3.1.3 Cover depth

Cover depths were obtained using the South African concrete design code SANS 10100-2 (1992). The cover depth depends on the exposure environment and the type of concrete as shown in Table 3.4.

Table 3.4: Minimum cover for normal-density and low-density concrete

(SANS 10100-2, 1992)

Concrete	***Minimum cover (mm)***				
	Conditions of exposure				
	Mild	***Moderate***	***Severe***	***Very severe***	***Extreme***
Normal-density	20	30	40	50	60
Low-density	20	40	50	60	70

Normal-density concrete was used so the results and the effect of changes in cover depth between 20 mm and 60 mm was investigated.

3.3.2 Prediction of corrosion initiation period using surface concrete resistivity

The corrosion initiation period was also calculated using Andrade's SLP model with a surface concrete resistivity value as an input parameter. This calculation was carried out to assess the degree to which the model's results (corrosion initiation period) agreed with that of the CCT SLP model.

The surface concrete resistivity SLP model used is based on Andrade's work. The reason for this is that the model in question was the only one found in the literature. Although the model includes a corrosion propagation period due to the issues discussed in Section 2.3.8, only the corrosion initiation period was calculated. Equation 3.2 (Equation 2.21 repeated below for convenience) was used for the calculation of the corrosion initiation period using Andrade's resistivity-based SLP method.

$$T = \frac{x^2 \cdot \rho_0 \left(\frac{t}{t_0}\right)^q}{K} \cdot r \qquad (3.2)$$

where T is the corrosion initiation period *[years]*; q *[-]* is the aging factor; t_o is the time *[years]* at first measurement of the resistivity; t is the time *[years]* of the final measurement of resistivity ρ_0*[Ω-cm]*; x is the cover depth *[cm]*; r is the reaction factor *[-]*; K is the exposure classification factor *[cm^3Ω/year]*

Because of the guidelines in Table 3.4, the cover depths investigated for the input parameters were between 20 mm and 60 mm. Otieno's (2014) first surface concrete resistivity measurements were carried out at t_0 of 80 days while the last measurement t was at 626 days. The reaction factor (r) is a measure of the chloride binding abilities of a particular concrete.

Values chosen for *r* were 1.5 for CEM I, 3 for the slag concretes and 3.5 for the fly ash concretes based on Table 2.10 and a study showing that the reaction factors are higher for fly ash than for slag concretes (Andrade et al. 2014). The values for the exposure classification and aging factors used in Equation 3.2 are described subsequently.

3.3.2.1 Environmental classification factor (K)

Table 3.5 (Table 2.11 repeated here for convenience) lists the environmental classification factors for the resistivity-based corrosion initiation SLP model.

Table 3.5: K values following EN 206 exposure classifications

(Andrade and Andrea, 2010)

Exposure class (EN 206)	***K***$(cm^3\Omega/year)$
XS1 (d > 500m distance to the coastline	5000
XS1 (d < 500m distance to the coastline	10000
XS2	17000
XS3	25000

The exposure categories for CCT SLP model are based on BS 8110 whereas the exposure classes for Andrade's resistivity-based model are on EN206 (2002). The exposure categories needed to reflect Cape Town marine environments where the tests were carried out for a valid comparison between the two models. However, there was no way to determine how one exposure classification was related to the other. Therefore, the following reasoning was used to establish a relationship between the two.

The *K* values increase with the severity of the marine environment. As shown in Table 3.3, the *extreme* and *very severe* categories are separated by "tidal and splash" zones whereas the *very severe* and *extreme* categories are separated by "spray" zone. Studies have shown that the former zone is prone to drying and wetting and lowers the durability more than the latter (Ferreira, 2004). For these reasons, estimated values of *K* were selected to match the marine exposure categories of the CCT SLP model as follows. *XS3* has been described as being in the tidal, splash and spray marine zones, similar to the *very severe* exposure category. Consequently, the *XS3* value of *K* from Table 3.5 is 25000 and this was taken as being equivalent to the *very severe* classification. The *extreme* classification factor was selected assuming a 30% increase from *very severe* as shown in Table 3.6.

Table 3.6: k values based on BS 8110 marine exposure categories

Marine exposure category (BS 8110)	***K*** $(cm^3\Omega/year)$
Severe	17000
Very severe	25000
Extreme	32500

3.3.2.2 *Aging factor (q)*

The aging factor for concrete resistivity is similar to the reduction factor in the CCT SLP model. Both account for the improvement of concrete microstructure with time and link short-term results to long-term values. The value for the resistivity-aging factor was calculated as proposed by Andrade with t_0 and t equivalent to 80 and 626 days respectively, as discussed previously. Thereafter, the inverse values of all resistivity measurements were plotted against the corresponding measurement age on a log-log graph (Andrade and Andrea, 2010). The resulting exponent from the best-fit line was taken as the aging factor. The procedure is shown in Figure 3.3, where the aging factor is the index of the equation = 0.824, was repeated for each of the five mixes.

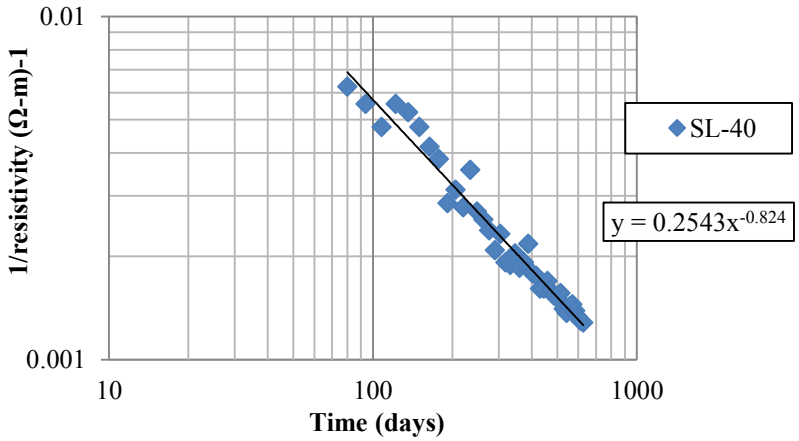

Figure 3.3: Example of calculation of concrete resistivity aging factor

3.3.3 *Prediction of diffusion coefficients using surface concrete resistivity*

As with the corrosion initiation period, the diffusion coefficient provides a means of comparison of not only the predicted durability but also the change in concrete properties with time. Therefore, this study compared the diffusion coefficient calculated using the CCT result with that of the surface concrete resistivity. The diffusion coefficient for the CCT SLP model is incorporated in the calculation of the corrosion initiation period. However, Andrade's surface resistivity SLP is not associated with a diffusion coefficient. Nevertheless, as was seen in the literature review, Baroghel-Bouny et al. (2009) produced a model for calculation of the diffusion coefficient with surface resistivity. The model is based on the diffusibility equation and calculations involved are Equations 2.24 to 2.27 (Baroghel-Bouny et al., 2009).

4 RESULTS AND DISCUSSION

4.1 Introduction

In this chapter, the results from the work carried out are presented and discussed. The objectives of this chapter were to:

i) Compare the surface concrete resistivity and CCT focussing on service life prediction (SLP) models for corrosion initiation periods and diffusion coefficients
ii) Find a relationship between surface concrete resistivity and the CCT.

To meet these objectives, firstly, the test results for surface concrete resistivity and CCT are presented. Secondly, the results for the corrosion initiation periods from the surface concrete resistivity and the CCT models are compared and contrasted. Thereafter, diffusion coefficients from the surface concrete resistivity and the CCT models are compared to identify a relationship between the two. This includes an analysis of how their ratio changes with time.

4.2 Comparison of concrete resistivity and CCT results

Surface concrete resistivity and CCT results from a study by Otieno (2014), were compared in terms of how they are influenced by age, binder type and w/b ratio. Surface concrete resistivity measurements from both the field and laboratory were taken at two-week intervals, with the first measurement occurring 80 days after casting. In comparison to resistivity, CCT measurements were only carried out in the laboratory at 28 and 90 days after casting. The graphs for each of the tests and exposure environments are presented in Figure 4.1, Figure 4.2 and Figure 4.3.

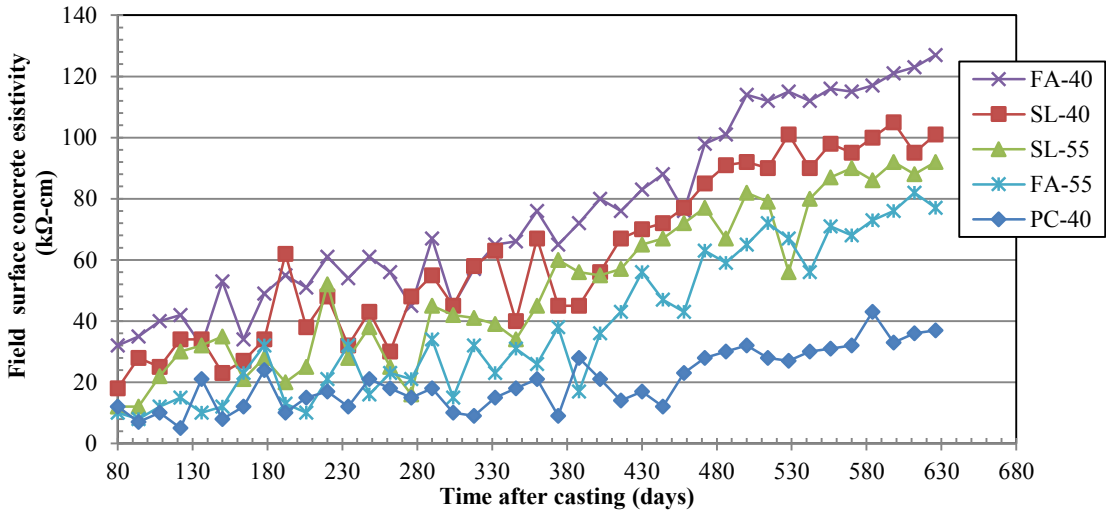

Figure 4.1: Influence of w/b ratio, binder type and age on resistivity for field specimens

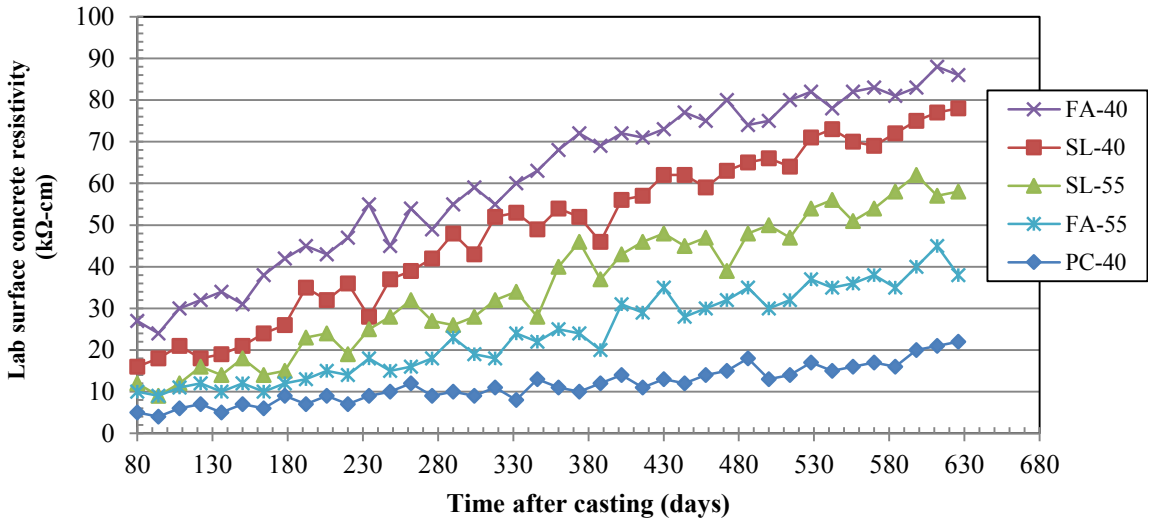

Figure 4.2: Influence of w/b ratio, binder type and age on resistivity for lab specimens

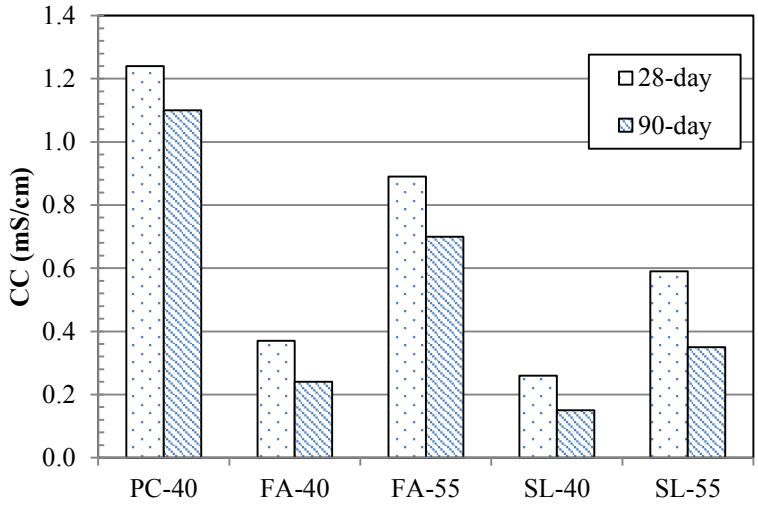

Figure 4.3: Influence of w/b ratio, binder type and age on CCT lab specimens

4.2.1 General discussion of results

Figure 4.1 to 4.3 show that the surface concrete resistivity increases whereas the chloride conductivity decreases as the concrete ages. Similar trends are reported by other researchers (Ballim et al., 2009; Smith et al., 2004). The general increase in resistivity and reduction in chloride conductivity with age could be attributed to curing. Laboratory specimens were cured through the wetting and drying regime and field specimens from the action of the tidal waves. The curing led to hydration making concrete less permeable over time. With continued hydration more voids close up and the concrete becomes less porous and permeable, improving the properties of concrete (Addis, 2008). This leads to concrete with higher penetration resistance and subsequent decrease in the chloride conductivity and increase in the surface resistivity, as seen in the three figures.

4.2.2 The influence of exposure environment on surface concrete resistivity

Figure 4.1 shows that the rate at which the field resistivity increases is higher after 350 days. In contrast, there is less change in the rate at which the lab resistivity increases after the same period (Figure 4.2). Furthermore, the field resistivity values are considerably higher than the lab resistivity (Figure 4.2). In addition, while the field resistivity evidently increases with time, some earlier measurements were higher than later measurements. For instance, for SL-40, the 200th day and the 300th day measurements fluctuate between 30 and 62 kΩ-cm. In contrast, the laboratory measurements only vary between 25 and 48 kΩ-cm. The lab resistivity measurements are more consistent and almost follow a smooth curve.

The higher field resistivity results are due to two factors. Firstly, although both sets of specimens were exposed to chlorides, the laboratory specimens were exposed to a higher concentration of chlorides than found in seawater. Therefore, the laboratory concrete specimens had increased chloride content in the pore solution. The higher chloride content resulted in lower concrete resistivity readings for laboratory specimens.

Secondly, the field specimens had higher but inconsistent resistivity than laboratory specimens due to the temperature. Laboratory specimens were kept at a fixed temperature of 25 ºC while the field specimens' temperature fluctuated with changes in weather. The temperature where the field specimens were placed can go as low as 7 ºC and as high as 27 ºC (South African Weather Service - Cape Town, 2010). The low temperatures led to high concrete resistivity readings while high temperatures led to low readings.

Because of the inconsistency of the field resistivity readings, the values used for the prediction of durability in this study were the laboratory resistivity readings. Laboratory resistivity readings are also better to compare with the CCT, which is also laboratory based.

4.2.3 The influence of binder type and w/b ratio on surface concrete resistivity and CCT

The results show that CCT is influenced by age, binder type and w/b ratio. For instance, PC-40 had the highest chloride conductivity followed by SL-55, FA-55, SL-40 and FA-40. Low chloride conductivity signifies good quality concrete due to its direct proportionality with diffusivity, as seen in the simplified Nernst-Einstein equation. Therefore, from these results, FA-40 and SL-40 had the best quality concrete, in terms of diffusivity. The reason for this is that cement extenders such as fly ash and slag make the concrete microstructure denser (Addis, 2008).

In addition, CCT results are low at a lower w/b ratio, for the binary blends. This can be expected as lower w/b ratios are synonymous with good quality concrete (Mehta and Monteiro, 2006; Addis, 2008). This is due to the increased hydration and densification of the concrete and consequent reduction in the diffusivity of the microstructure. The chloride conductivity of the

slag concrete is lower than that of the fly ash concrete at the same w/b ratio (Figure 4.3). These results are in line with the literature, which shows that at the same w/b ratio, slag has lower chloride conductivity than fly ash (Ballim et al., 2009; Mackechnie, 1996).

Table 4.1 and 4.2 compare the effect of changing the w/b ratio and binder type on the chloride conductivity of the concrete. It is evident that for blended cement concrete, changing the w/b ratio has a greater influence on the chloride conductivity than changing the binder type.

Table 4.1: Influence of change in w/b ratio on chloride conductivity

	w/b ratio *(28-day chloride conductivity in mS/cm)*		
Binder type	***0.4***	***0.55***	***% change***
GGBS	0.26	0.59	56
FA	0.37	0.89	58

Table 4.2: Influence of change in binder type on chloride conductivity

	Binder type *(28-day chloride conductivity in mS/cm)*		
w/b ratio	***GGBS***	***FA***	***% change***
0.4	0.26	0.37	30
0.55	0.59	0.89	34

The binder type and w/b ratio are also highly influential in the determination of the surface concrete resistivity. PC-40 had the lowest surface concrete resistivity for both field and laboratory results. FA-40 had the highest surface concrete resistivity followed by SL-40, even though FA-55 had lower resistivity than SL-55. This indicated that at low w/b ratio, addition of fly ash led to much less interconnectedness of the pores than addition of slag. However, at high w/b ratio, the fly ash concrete pores are more interconnected than the slag concrete pores. The concrete mixes with higher w/b ratios had more moisture in the pore solution and therefore lower resistivity values.

Table 4.3 and 4.3 compare the effect of changing the w/b ratio and binder type on the surface concrete resistivity.

Table 4.3: Influence of change in w/b ratio on surface concrete resistivity

	w/b ratio *(avg of 570 to 612 day resistivity in kΩcm)*		
Binder type	***0.4***	***0.55***	***% change***
GGBS	73.3	57.8	21
FA	83.8	39.5	53

Table 4.4: Influence of change in binder type on surface concrete resistivity

	Binder type *(avg of 570 to 612 day resistivity in kΩcm)*		
w/b ratio	***GGBS***	***FA***	***% change***
0.4	73.3	83.8	13
0.55	57.8	39.5	32

It is evident that change in w/b ratio has a greater effect on the resistivity for fly ash than GGBS concrete. Moreover, changing the binder type is more effective in influencing the resistivity at high than low w/b ratio.

For the blended cement concrete, the following can be surmised:

- w/b ratio has a greater influence on chloride conductivity than binder type
- changing the w/b ratio for GGBS concrete is more effective than changing it for FA concrete in influencing the surface concrete resistivity
- changing the binder type has a greater influence on surface concrete resistivity at a high w/b ratio than a low one

4.3 Input variables and calculations of corrosion initiation periods

The CCT SLP is an empirical model that is being used in the South African construction industry for the prediction of chloride-induced corrosion initiation (Mackechnie, 1996). Andrade's (2004) surface concrete resistivity SLP model is also an empirical model but its use is so far restricted to Europe. This section presents the input variables and equations for the corrosion initiation period (CIP) as calculated using the resistivity model and those of the CCT SLP model.

4.3.1 CCT model: corrosion initiation period calculations and input variables

The CCT SLP corrosion initiation period was calculated, using Excel,for each mix and exposure category using Crank's solution to Fick's second law of diffusion as follows:

$$t = \frac{x^2}{4D\left[erf^{-1}\left(1-\frac{C_x}{C_s}\right)\right]^2} \qquad (4.1)$$

where t is the corrosion initiation period *[years]*; x is the cover depth *[cm]*; D is the diffusion coefficient *[cm^2/year]*; C_s refers to the surface chloride concentration *[%]*; C_x refers to the chloride concentration at the cover depth *[%],* erf^{-1} is the inverse error function

Values for the 28-day CCT, from Otieno's results, were input into the equations described in Section 2.3.7 to obtain the diffusion coefficient. These two variables are dependent on exposure conditions and binder type. The chloride threshold level was assumed to be 0.4% for all five

mixes and cover depths 20, 30, 40, 50 and 60 mm were used. For extreme exposure category, the values used for input into Equation 4.1, are presented in Table 4.5.

Table 4.5: CCT SLP model: CIP (t) Input parameters - Extreme exposure

	CONCRETE MIX				
Variable	***PC-40***	***SL-40***	***SL-55***	***FA-40***	***FA-55***
28-day CCI (mS/cm)	1.24	0.26	0.59	0.37	0.89
D_{50} (10^{-8} cm^2/s)	0.800	0.0796	0.118	0.109	0.210
D_{50} (cm^2/yr)	0.252	0.0251	0.0373	0.0343	0.0674
C_s (%)	3	5	5	4.5	4.5
C_x (%)	0.4	0.4	0.4	0.4	0.4

4.3.2 Surface concrete resistivity model: CIP input variables

The CIP's for surface concrete resistivity was calculated, using Excel, from the laboratory results for each concrete mix using the following equation:

$$T = \frac{x^2 \cdot \rho_0 \left(\frac{t}{t_0}\right)^q}{k} \cdot r \qquad (4.2)$$

where T is the period *[years]* for which the aging factor q *[-]* is calculated; t_o is the time *[years]* at first measurement of the resistivity; t is the time *[years]* of the final measurement of resistivity ρ_0*[Ω-cm]*; x is the cover depth *[cm]*; r is the reaction factor *[-]*; k is the exposure classification factor *[cm^3Ω/year]*

The 80-day resistivity for laboratory specimens was used as the first measurement and 626-day resistivity as the final measurement. The reaction factor was taken as 1.9 for PC-40, 3 for slag and 3.5 for fly ash concrete as recommended by Andrade (see Table 2.10). Similar to the CCT model, the CIP for surface concrete resistivity was calculated for cover depths 20, 30, 40, 50 and 60 mm. The values used for surface concrete resistivity CIP calculations, extreme exposure type are presented in Table 4.6.

Table 4.6: Resistivity model: CIP (T) Input parameters - Extreme exposure

	CONCRETE MIX				
Variable	***PC-40***	***SL-40***	***SL-55***	***FA-40***	***FA-55***
reaction factor (r)	1.5	3	3	3.5	3.5
aging factor (q)	0.689	0.824	0.909	0.635	0.81
t (yrs) at 626 days	1.715	1.715	1.715	1.715	1.715
exposure class k *(cm^3Ω/year)*	32500	32500	32500	32500	32500
80-day lab resistivity ρ *(Ω.cm)*	5000	16000	12000	27000	10000
t_0 (yrs) at 80 days	0.219	0.219	0.219	0.219	0.219

The aging factor (q) was the exponent in the resulting best-fit line obtained by plotting the log-inverse of resistivity over log-time. The figures used are presented below.

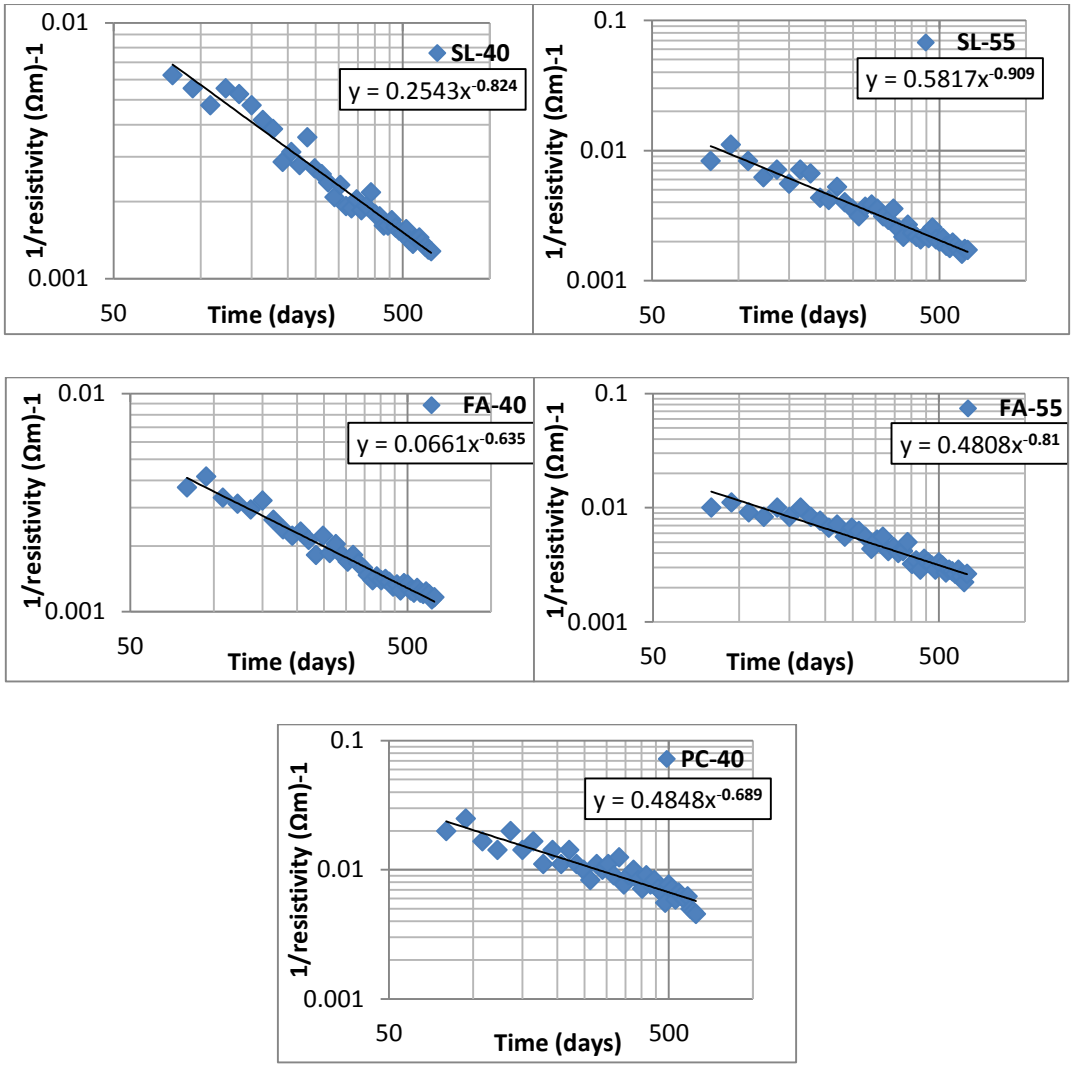

Figure 4.4: Lab surface concrete resistivity aging factors (indices)

4.4 Comparison of SLP models for corrosion initiation periods

According to Alexander et al. (2012) and Bertolini (2008) the chloride-induced corrosion initiation period (CIP) depends on the following:

- thickness and quality of concrete cover
- penetration resistance of the cover zone
- chloride threshold value

Although Bertolini (2008) concedes that adequate quality control during construction is also important, corrosion initiation can still only be controlled by knowing and designing for the CIP before construction. The chloride threshold level is taken as occurring at 0.4% for all binder types and w/b ratios in the CCT model and is not used in Andrade's resistivity model.

For this reason, this section will compare the CCT and lab surface concrete resistivity service life prediction (SLP) models based on the first two factors.

4.4.1 The influence of thickness and quality of concrete cover on the CIP

As can be expected, results from the two service life prediction models show that the CIP increases with increase in cover depth for all binder types (Figure 4.5).

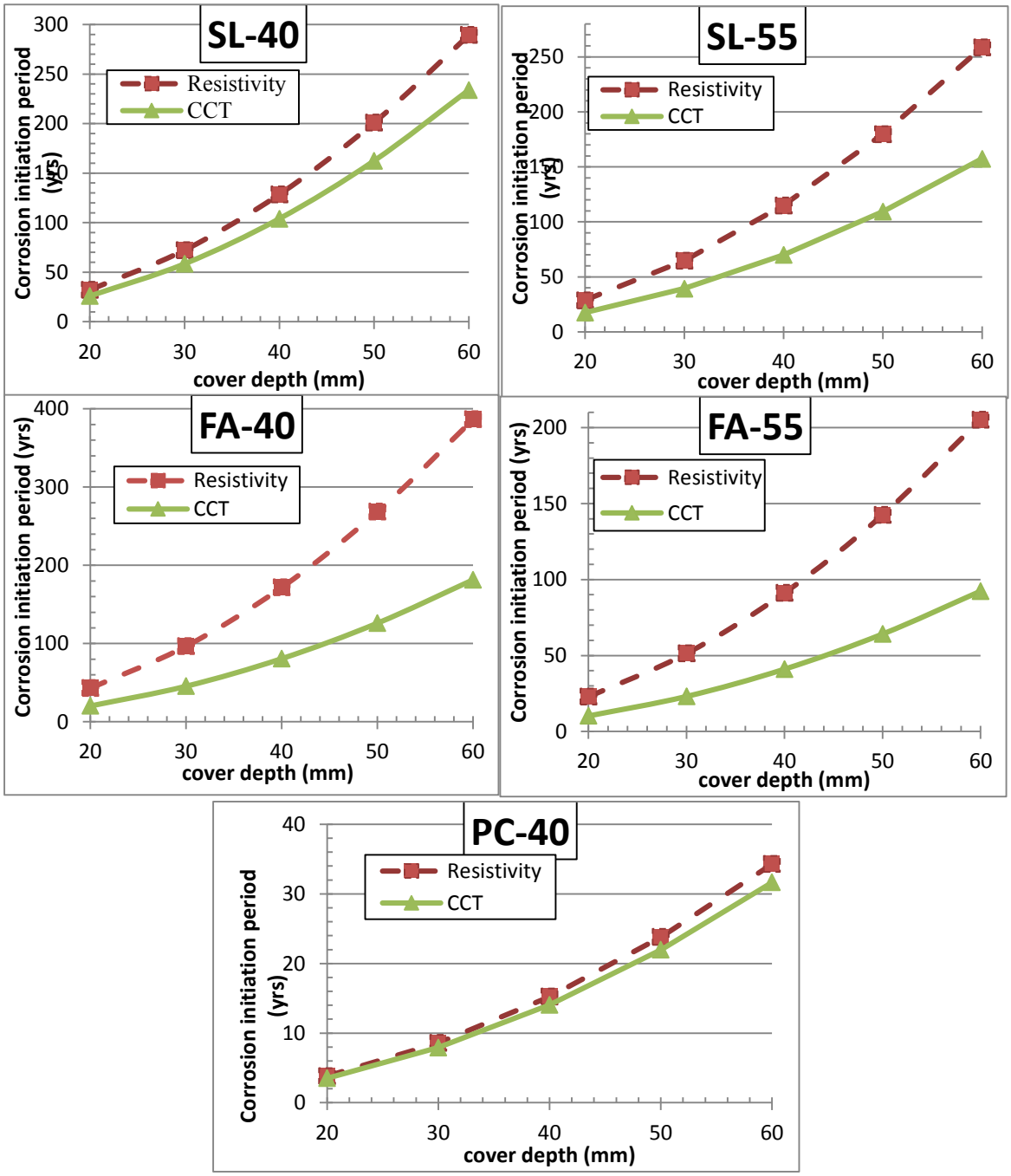

Figure 4.5: Influence of cover depth on CIP for extreme exposure category

Generally, both CIP's for the surface concrete resistivity and CCT models increase with cover depth and predict that the larger the distance to the steel rebars the longer it will take deleterious materials to reach them. However, it is clear that the surface concrete resistivity model consistently gives higher corrosion initiation periods than the CCT model. Regardless of this, the difference is also dependent on the w/b ratio and binder type. For instance, the two models overlap for concretes PC-40 and SL-40.

The CIP curves for the two models diverge as cover depth increases for all binder types, with an almost imperceptible difference at 20 mm cover. A cover depth of 20 mm would evidently be inadequate irrespective of which SLP model or binder type is used because it would give a service life of less than 50 years. The reason for this is that with a low cover, the chloride ions take less time to reach the steel reinforcement. Even blended cement concretes with 20 mm cover depth would have corrosion initiating at an unacceptable service life of less than 50 years.

The service lives from the two models at a cover depth of 40 mm, are shown in Figure 4.6.

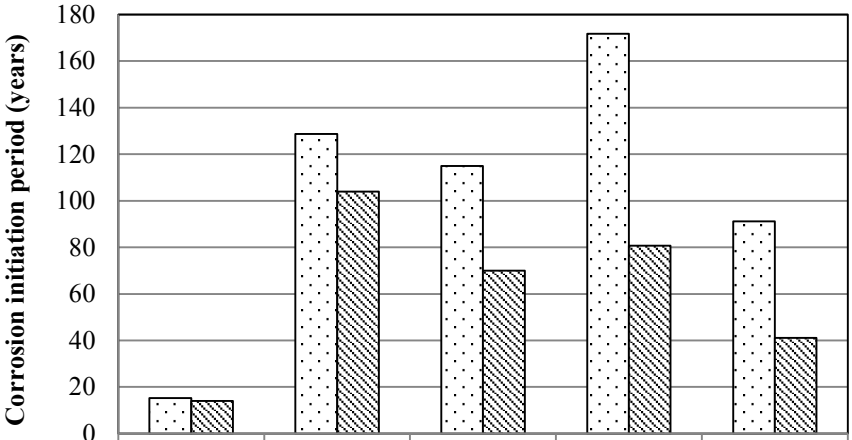

	PC-40	SL-40	SL-55	FA-40	FA-55
Resistivity model	15	129	115	172	91
CCT model	14	104	70	81	41

Figure 4.6: Comparison of CIP for extreme exposure at 40mm cover

Figure 4.6 makes it clear that the values for the resistivity model for FA-40 and FA-55 are more than twice as high as the CCT model. In addition, while the highest service life for the CCT model is from the SL-40 concrete, the highest service life for the resistivity model is FA-40. However, the service life for both models decreases with an increase in w/b ratio. Moreover, the lowest service life after PC-40 is FA-55 for both models. Additionally, from low to high w/b ratio, the slag concretes have a 33% and 11% difference between service lives, but for fly ash, the service life is reduced by 53% and 51 % for the resistivity and CCT models respectively. This is in agreement with the above suggestion that slag is less sensitive to changes in w/b ratio than fly ash.

Thus, it can be inferred that the two models result in a bigger difference with the addition of supplementary cementitious materials especially fly ash. Moreover, concrete with blended cement and low w/b ratio is best for use in the marine environment. It also suggests that fly ash at high w/b ratio and CEM I only concrete are not as adequate for use in the marine environment as the other concretes. This is because CEM I only concrete provides less resistance to the penetration of chloride ions allowing corrosion initiation to occur early such that the recommended service life is never achieved. Additionally, high w/b ratio signifies a lesser degree of hydration and less densification of the concrete, which is more favourable to the transportation of chloride ions.

4.4.2 The effect of the resistance of the cover zone on CIP

The penetration resistance or quality of the concrete cover zone will determine the rate at which chloride ions penetrate through to the steel reinforcement. This is influenced by the binder type and chemistry of the concrete microstructure whose make up is known to improve with time due to hydration reactions and chloride binding. For the CCT SLP model, these changes are characterized by the reduction factor and the surface chloride concentration (Mackechnie, 1996). In the surface concrete resistivity SLP model, they are characterised by the chloride binding (reaction) factor and the aging factor (Andrade, 2004).

4.4.2.1 The influence of reduction factor and aging factor

The reduction factor in the CCT model is a binder specific pre-determined value from Mackechnie's (1996) model for service life prediction of RC structures (see Table 2.5). The reduction factor and the 28-day CCT are used to predict the reduced long-term diffusion coefficient, which can be obtained from Mackechnie's (1996) spreadsheet. Note that the reduction factor is the same for 30% FA and 50% GGBS i.e. 0.68, suggesting that the two have similar long-term improvements in microstructural quality. The reduction factor for CEM I is lower at 0.29. Nonetheless, it is worth noting that Mackechnie (1996) did not use values from specimens in his study and resorted to other studies as the values in his study were unstable with some exceeding one.

In contrast, the aging factors for the resistivity model are calculated based on surface resistivity values measured over time, for each concrete mix. Although not yet available, a table similar to the one used for the CCT can be created depicting an aging factor for each concrete mix as shown below. The aging factor is then used to predict the increased long-term resistivity from the early-age resistivity. An aging factor close to one represents more of an increase in the penetration resistance with time than an aging factor close to zero. This would negate the need to calculate an aging factor for the same concrete mix on every project as done in this study (see Table 4.7).

Table 4.7: Calculated aging factors from resistivity measurements

Concrete mix	*Aging factor*
FA-40	0.635
PC-40	0.689
FA-55	0.810
SL-40	0.824
SL-55	0.909

The calculated values in Table 4.7 are similar with research showing that aging factors range between 0.7 and 1.2 for concrete with supplementary cementitious materials; with aging factors for GGBS being higher than those for fly ash (Thomas and Bamforth, 1999). The results suggest that there is more improvement in the impenetrability of the microstructure of GGBS than for FA and CEM I cement concretes.

4.4.2.2 The influence of surface chloride concentration and reaction factors

The surface chloride concentration depends on curing as well as binder type and content. In the CCT, the recommended surface chloride concentration based on marine exposure investigations and case studies are given in Table 2.7. Blended cement concrete with GGBS (5.0%) and FA (4.5%) have higher surface chloride concentrations than binders having only CEM I (3.0%). However, the quoted values are for the extreme exposure environments, less severe exposure environments have lower values.

The surface chloride concentration is similar to the chloride binding (reaction) factor in the resistivity model. The reaction factor introduces a complex variable which is chemistry as well as time dependent and therefore specific to binder type and content. Andrade's values for this are 1.9 for CEM I and 1.5 for CEM I with small additions of silica fume and CEM II of 3.0 (Andrade et al., 2009; Andrade, 2004). However, since the numbers are based on the measured reactivity and chloride binding capabilities from the Multi-regime migration test, it is difficult to predict what numbers these would be for GGBS and FA as used in the current study.

4.5 Diffusion coefficients calculations and results

The chloride diffusion coefficient is commonly used as an input parameter in service life prediction (SLP) models for RC structures. It represents the rate at which chloride ions are likely to proceed through the concrete. The diffusion coefficient is usually input into SLP models based on Crank's solution to Fick's second law of diffusion such as the CCT model. Alternatively, the diffusibility equation is used as with the resistivity procedure by Baroghel-Bouny et al. (2011). Diffusion coefficients were calculated for both the surface resistivity and CCT SLP methods for the duration of the measurements (80 to 626 days).

4.5.1 CCT diffusion coefficients: calculations and results

Diffusion coefficients from CCT values were determined using the spreadsheet created for the SLP model. The procedure consisted of inputting the measured 28-day CCT values for each binder type, the desired age and selecting the exposure type. The resulting values for the diffusion coefficients as established from the CCT model are presented in Appendix A.

4.5.2 Surface concrete resistivity diffusion coefficients: calculations and results

The diffusion coefficients for surface concrete resistivity were calculated as recommended by Baroghel-Bouny et al. (2009) using the diffusibility equation:

$$D = \frac{D_0}{\sigma_0 \times \rho} \qquad (4.3)$$

The diffusion coefficients were calculated using the constants given in Table 4.8 and resistivity measured at a particular age after casting.

Table 4.8: Constants used in the calculation of resistivity diffusion coefficients

(Baroghel-Bouny et al., 2009)

Constant	*PC-40*	*SL-40, FA-40, SL-55, FA-55*
D_0 (m^2/s)	2.03×10^{-9}	2.03×10^{-9}
σ_0 (S/m)	9.8	11.87
$B = D_0/\sigma_0$ (m^3/ S.s)	0.207×10^{-9}	0.171×10^{-9}

4.6 Comparison of CCT and surface resistivity

There was no discernible relationship between CCT and surface concrete resistivity test results. The exact reaction factor to use for the surface concrete resistivity was not clear and a relationship could not be established using the corrosion initiation period either. Instead, an investigation of how the two could be related with the diffusion coefficient was carried out.

4.6.1 Comparison of diffusion coefficients from CCT and surface resistivity models

The diffusion coefficient models for CCT and surface resistivity have different underlying theories and input parameters. For instance, the CCT model is empirical and based on a modified version of Crank's solution to Fick's second law of diffusion as well as the diffusibility equation. Not only does it require input of 28-day CCT, but also exposure environments and desired age for the diffusion coefficient. These values can then be input into a spreadsheet of the model, as seen in Table 3.2 in the previous chapter.

In comparison, the surface resistivity model for calculation of the diffusion coefficient is based solely on the diffusibility equation (see Section 2.4.8). The resulting diffusion coefficient is a function of the measured resistivity and assumed values for the diffusivity and conductivity of

the concrete pore solution. The surface resistivity model is more rigid in that the designer cannot select the age of the diffusion coefficient, since it is dependent on the age at which the surface resistivity is measured. Moreover, unlike in the CCT model, there is no consideration for the exposure environment of the structure. Although this severely limits the model, Baroghel-Bouny et al. (2011) found that the method gave similar results with the non-steady state migration diffusion coefficient (see Section 2.2.7.1) – making it a rapid, convenient indirect method. Therefore, one cannot expect the surface concrete resistivity and CCT models to produce the same diffusion coefficients. Both sets of diffusion coefficients (Table A. 2 and Table A. 3) were plotted to investigate their relationship as shown below.

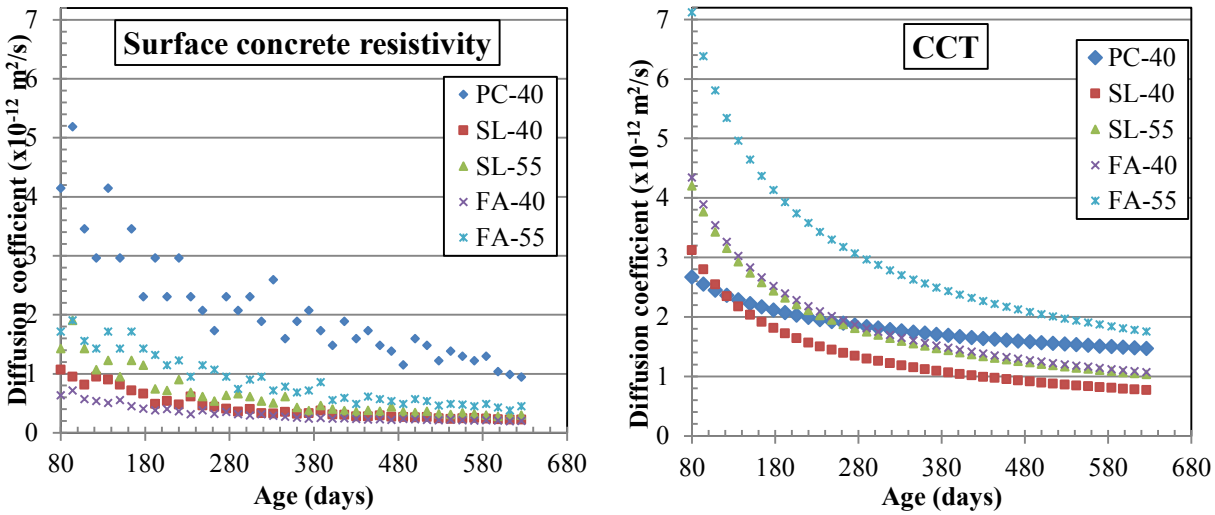

Figure 4.7: Comparison of CCT and surface concrete resistivity diffusion coefficients

A lower diffusion coefficient represents a higher densification of the concrete microstructure and greater penetration resistance to chloride ingress. From Figure 4.7, it is evident that as expected, the diffusion coefficients for both models decrease with time. In the early ages of concrete after casting, the concrete is less dense and more susceptible to diffusion. However, at later ages after longer curing periods, hydration products have developed and increased the density of the concrete microstructure. This explains why the diffusion coefficients are higher at earlier ages for both the CCT and surface concrete resistivity models.

In both the surface concrete resistivity and CCT method, the diffusion coefficient lowers with a decrease in the w/b ratio. This can be explained by the fact that low w/b ratios have more binder and less capillary pores which can be filled up with hydration products; thereby increasing the densification of the concrete microstructure. In both cases, the difference between the two w/b ratios is much greater for FA-40 and FA-55 than for SL-40 and SL-55.

In the CCT model, the diffusion coefficient for FA-55 is initially twice as much or much higher than for the other concrete mixes. However, by the end of the measurement period, the FA-55

diffusion coefficient has reduced drastically to within 0.8 x 10^{-12} m^2/s of the other concrete mixes. For PC-40, initially, the diffusion coefficient is the lowest among the five concrete mixes. Nonetheless, over time the diffusion coefficients for the other concrete mixes decrease at a higher rate than it does and it seems even FA-55 will eventually have a lower diffusion coefficient than PC-40. This is because as the concrete ages, the chloride binding ability of fly ash and slag concrete in combination with the fine filler effect supersedes the PC-40 microstructural density, which is only dependent on hydration reactions to improve.

In contrast, in the surface concrete resistivity model, it is evident initially and until the end of the measurements that the PC-40 diffusion coefficient remains higher than the other concrete mixes. The fly ash and slag concrete have almost overlapping diffusion coefficients curves at the end of the measurement period. This is similar to the CCT method and indicates that in the long-term there is little difference in the densification of the microstructure between slag and fly ash concrete. Slag and fly ash have lower diffusion coefficients than PC-40 because the penetration resistance against chloride ingress improves with the addition of cement extenders.

4.6.2 Ratio of diffusion coefficients for CCT and surface concrete resistivity

The ratio of the two diffusion coefficients over time was plotted to investigate the relationship between surface concrete resistivity and chloride conductivity. The results obtained are summarised in Figure 4.8.

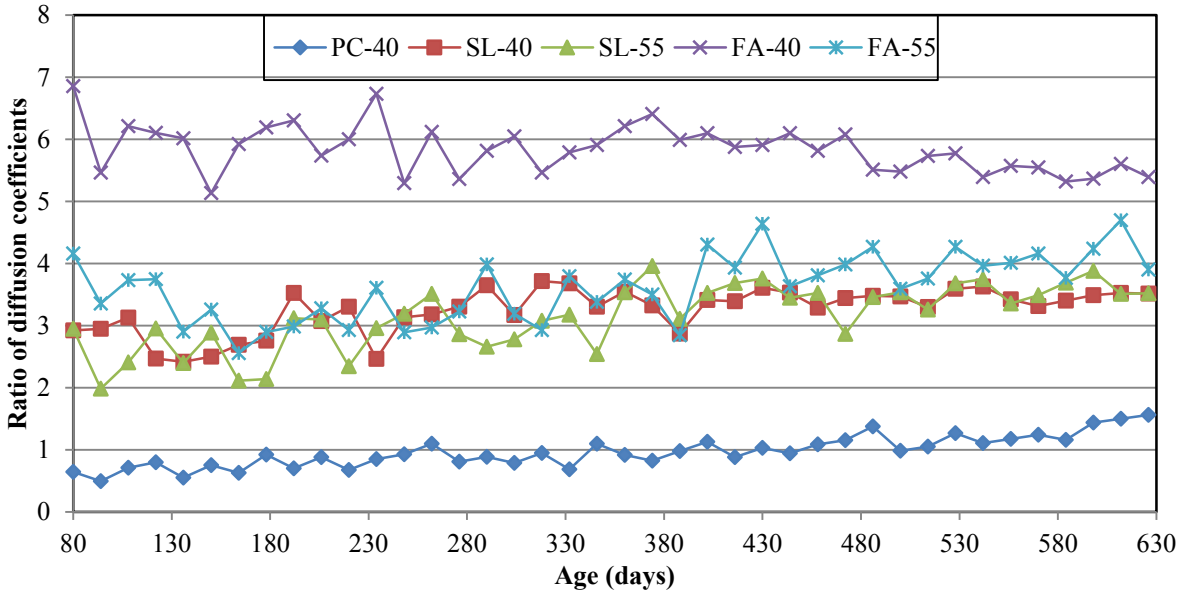

Figure 4.8: Effect of age on ratio of diffusion coefficients

In general, the ratio of the diffusion coefficients for CCT and resistivity (D_σ /D_ρ) is constant with time. The average values for the ratios for each mix are available in Appendix A.

PC-40 has an average ratio of 0.97, suggesting that without the influence of cement extenders, the diffusion coefficient calculated with the CCT is almost equal to that calculated with surface resistivity. In contrast, for FA-40 the ratio D_σ / D_ρ is equal to 5.84. The other three mixes SL-40, SL-55 and FA-55 have average ratios of 3.24, 3.14 and 3.62 respectively. The diffusion coefficient ratios for slag do not differ much with change in w/b ratio, in contrast with fly ash whose ratio is higher at the lower w/b ratio. At a 0.55 w/b ratio, the slag and fly ash have almost the same average value for the D_σ / D_ρ of 3.14 and 3.62 respectively. However, at 0.40 w/b ratio the average D_σ / D_ρ value for the fly ash (5.84) is nearly twice as high as that for the slag (3.25).

The result suggests that the two models for calculating the diffusion coefficients are related by a constant specific to binder type. Therefore, despite its limitations, the surface concrete resistivity model for diffusion coefficient can be used by relating it to the CCT diffusion coefficient.

4.6.3 Relationship between surface concrete resistivity and CCT diffusion coefficient

Surface concrete resistivity measurements were plotted against the corresponding diffusion coefficient, calculated using the CCT SLP model to investigate a trend. Note that a similar graph of CCT values with the diffusion coefficient from the surface concrete resistivity SLP model could not be plotted. This is because CCT measurements were only carried out at two ages and two points would not provide enough information to observe a trend. Plotting the surface concrete resistivity results with the CCT SLP model diffusion coefficient revealed the following trends.

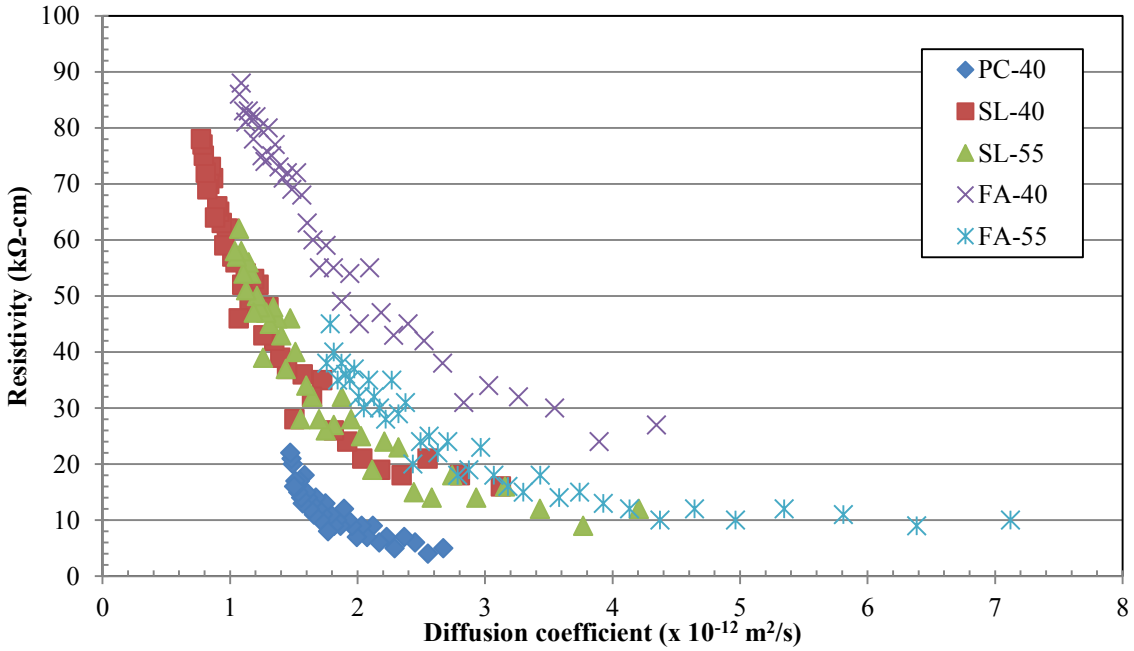

Figure 4.9: Relationship between resistivity and CCT diffusion coefficient – All mixes

Figure 4.9 shows the surface concrete resistivity and CCT diffusion coefficient relationship for all five concrete mixes. The figure indicates that the CCT diffusion coefficient reduces with an increase in resistivity, regardless of the binder type. This is consistent with the simplified Nernst-Einstein equation and work by various researchers. Other researchers present the resistivity-diffusion coefficient as the conductivity-diffusion coefficient so that a linear relationship is observed rather than a hyperbolic curve (Sengul and Gjorv, 2008; Polder and Peelen, 2002). The relationship is intuitive since concrete with a high penetration resistance against chloride ingress must also have a low diffusion coefficient as they both represent an increased density in the concrete microstructure.

The steep curve for SL-40 and FA-40 shows that surface concrete resistivity increases faster than the decrease in chloride diffusion. In contrast, chloride diffusion decreases faster than surface concrete resistivity increases for SL-55 and FA-55. The much higher resistivity and lower diffusion coefficients for the FA-40 concrete mix than for the others is an indication of its superior refinement of the pore structure. This could be caused by its low w/b ratio as well as smaller particles, which provide the "fine filler" effect. Note that the grouping of the concrete mix curves in Figure 4.9 is similar to that in Figure 4.8 i.e. 1) PC-40; 2) SL-40, SL-55 and FA-55; 3) FA-40.

4.6.4 The relationship between CCT diffusion coefficient and surface concrete resistivity

The results and analysis suggest that the ratio of the resistivity and CCT diffusion coefficients is a constant dependent on the binder type.

$$D_\sigma / D_\rho = k \qquad (4.4)$$

where D_σ is the diffusion coefficient calculated from the CCT SLP model; D_ρ is the diffusion coefficient calculated from the resistivity model by Baroghel-Bouny et al. (2011); k is a constant

From the diffusibility equation, $D_\rho = \frac{B}{\rho}$, substituting this into Equation 4.4 gives the following equation:

$$D_\sigma = \frac{B}{\rho} \times k \qquad (4.5)$$

where B is a known constant depending on w/b ratio and binder type; ρ is the resistivity in Ω-m; k is a constant

The values for B taken from the Baroghel-Bouny et al. (2011) equations were calculated for blended cements and CEM I only concrete (see Table 4.8). The constant k values have been found in this study from the ratio of diffusion coefficients. Three distinct patterns were

observed of the ratios i.e. i) PC-40 ii) SL-40, SL-55 and FA-55 and iii) FA-40. Consequently, the following three equations can be inferred:

For PC-40:

$$D = \frac{201}{\rho} \quad (4.6)$$

For SL-40, SL-55 and FA-55:

$$D = \frac{571}{\rho} \quad (4.7)$$

For FA-40:

$$D = \frac{1000}{\rho} \quad (4.8)$$

where D is the diffusion coefficient $[10^{-12}\ m^2/s]$ calculated from the CCT SLP model; ρ is the resistivity in Ω-m

The equations provide a means to link surface concrete resistivity measurements to the CCT SLP model. This implies that, resistivity measured at any age can be used to calculate the corresponding CCT SLP model diffusion coefficient. Once the diffusion coefficient is obtained, its value can be input into the CCT SLP model to obtain the remaining service life of a RC structure as described in Section 2.3.7.

4.7 Summary

Surface concrete resistivity and CCT were compared in terms of test results, diffusion coefficients and corrosion initiation periods. The results from both tests were obtained from a study by Otieno (2014) on cracked and uncracked concrete specimens. Only the uncracked concrete test results were used in this study. A model by Mackechnie (1996) in the form of a spreadsheet was used to obtain the diffusion coefficient from CCT results. The diffusion coefficient from this process was used as one of the input parameters for the determination of the corrosion initiation period. A model by Baroghel-Bouny et al. (2009) was used to calculate the diffusion coefficient from resistivity results. A model by Andrade (2004) was used as the basis for the calculation of the corrosion initiation period from resistivity results. All calculations were carried out in Excel.

5 CONCLUSIONS AND RECOMMENDATIONS

5.1 Introduction

The motivation for this study was research showing that surface concrete resistivity is increasingly being used as a rapid means to predict concrete durability. An investigation was carried out on the use of surface concrete resistivity in the durability design of reinforced concrete (RC) structures and its relationship with the chloride conductivity test (CCT).

The literature revealed two models for prediction of durability during design requiring surface concrete resistivity as an input parameter. These were Andrade's model for service life prediction (SLP) and Baroghel-Bouny et al. (2009)'s model for calculation of diffusion coefficients. The two models were compared to the SLP model requiring input of the chloride conductivity test (CCT) results as used in the South African Durability Index. The CCT SLP model is used to determine both the corrosion initiation period and diffusion coefficient. The following conclusions and recommendations can be drawn from the analysis.

5.2 Comparison of test results

The surface concrete resistivity was found to be highly sensitive to exposure environment. For the use of surface concrete resistivity results in the design of reinforced concrete structures, it is better to measure resistivity in laboratory-controlled conditions. Laboratory-controlled conditions will reduce the influence of changing factors in the field such as temperature, moisture and chloride penetration on surface concrete resistivity.

For blended cement concrete, increasing the w/b ratio has a greater influence on chloride conductivity than changing the binder type. Increasing the w/b ratio has twice the influence on the surface concrete resistivity of fly ash concrete than slag concrete. Use of a different binder type is more effective at high w/b ratio than low w/b ratio in influencing the surface concrete resistivity.

5.3 Comparison of corrosion initiation periods

The CCT model and surface concrete resistivity models give similar corrosion initiation periods for CEM I only concrete and slag concrete at 0.40 w/b ratio. For slag concrete at 0.55 w/b ratio and fly ash at 0.40 and 0.55 w/b ratio, the CCT model gives more conservative (lower) corrosion initiation period (CIP) values than the surface concrete resistivity model. The CIP's for fly ash concretes were almost twice as high for surface concrete resistivity than for the CCT model. For both the CCT and surface concrete resistivity CIP models, the use of cement extenders and low w/b ratios greatly improved the penetration resistance and corrosion initiation period.

For both models, Portland cement concretes required an impractical cover depth of more than 60 mm to achieve a service life of 50 years. Consequently, Portland cement concretes can be ruled out for use in marine environments. In both models, the use of supplementary cementitious materials resulted in a higher increase in the CIP than using a larger cover depth. Therefore, at high cover depth, the chemistry of the concrete cover zone is more important in the resulting corrosion initiation period than the distance to the rebars.

5.4 Comparison of diffusion coefficients

The chloride diffusion coefficients as calculated from the surface concrete resistivity model give lower values for blended cement concrete than the ones calculated from the CCT model. However, the ratio of the two models' diffusion coefficients is constant with time for each binder type. The average ratio of the CCT and resistivity diffusion coefficients is close to one, at 0.97, for CEM I concrete. It can be concluded that the short-term diffusion coefficients for CEM I concrete are the same for the resistivity and CCT model. Therefore, values from one model can be compared with values from the other model.

The diffusion coefficient from the CCT model reduces with an increase in the surface concrete resistivity forming a hyperbolic function, which confirms the simplified Nernst-Einstein equation. Three equations relating the two were found 1) slag at high and low w/b ratios as well as fly ash for high w/b ratios 2) fly ash concrete at low w/b ratios 3) CEM I only concrete

The equations found can be used as a means to ascertain the CCT diffusion coefficient from a surface concrete resistivity result. Thereafter, the CCT model can be used to obtain the service life of a structure.

5.5 Recommendations

- The surface concrete resistivity test is intuitive, easy to use and relatively cheap for the determination of the durability of concrete. Considering the correlation that has been found with other more established tests, it is recommended that it be used in cases where these tests (e.g. CCT) are not feasible.
- The diffusion coefficient data was limited to a period of two years. Further study is necessary to ascertain long-term surface concrete resistivity diffusion coefficients for use in SLP models.
- The data used in this study was comprehensive but second hand and it was collected for an entirely different purpose. Further study should be carried out specifically within this area of study so that the recommended pre-conditioning and measuring procedure for surface concrete resistivity can be carried out. This will provide a stronger basis for the comparison of the CCT and surface concrete resistivity.

- Andrade's surface concrete resistivity model for SLP can be used for the calculation of CIP's for CEM I only concrete and slag at low w/b ratios. These can be compared with other RC structures with CIP's calculated from the CCT SLP model.

6 REFERENCES

AASHTO Standard T259, 1980. *Standard Method of Test for Resistance of Concrete to Chloride Ion Penetration.* Washington D. C.: American Association of State Highway and Transportation Officials.

Addis, B., 2008. *Fundamentals of concrete*. Midrand: Cement & Concrete Institute, p.58.

Ahmad, S., 2003. Reinforcement corrosion in concrete structures, its monitoring and service life prediction—a review. *Cement and Concrete Composites*, 25(4-5), pp.459–471.

Alexander, M.G., 2009. *Durability Index Testing Procedure Manual*. Cape Town.

Alexander, M.G., Ballim, Y. and Mackechnie, J.R., 1999a. *Concrete durability index testing manual - Monograph 4*. Cape Town: Department of Civil Engineering, University of Cape Town, pp.1–33.

Alexander, M.G., Ballim, Y. and Stanish, K., 2008. A framework for use of durability indexes in performance-based design and specifications for reinforced concrete structures. *Materials and Structures*, 41(5), pp.921–936.

Alexander, M.G., Beushausen, H. and Otieno, M., 2012. *Corrosion of steel in reinforced concrete: Influence of binder type, water/binder ratio, cover and cracking. Monograph 9*. Cape Town: University of Cape Town.

Alexander, M.G., Santhanam, M. and Ballim, Y., 2011. Durability design and specification for concrete structures—the way forward. *International Journal of Advances in Engineering Sciences and Applied Mathematics*, 2(3), pp.95–105.

Alexander, M.G., Streicher, P.E. and Mackechnie, J.R., 1999b. *Rapid chloride conductivity testing of concrete - Monograph 3*. Cape Town: Department of Civil Engineering, University of Cape Town, pp.1–35.

Alonso, C., Andrade, C. and Gonzalez, J.A., 1988. Relation between resistivity and corrosion rate of reinforcements in carbonated mortar made with several cement types. *Cement and Concrete Research*, 18(5), pp.687–698.

Ampadu, K.O., Torii, K. and Kawamura, M., 1999. Beneficial effect of fly ash on chloride diffusivity of hardened cement paste. *Cement and Concrete Research*, 29(4), pp.585–590.

Andrade, C., 1993. Calculation of chloride diffusion coefficients in concrete from ionic migration measurements. *Cement and Concrete Research*, 23, pp.724–742.

Andrade, C., 2004. Calculation of initiation and propagation periods of service life of reinforcements by using the electrical resistivity. In: *International Symposium: Advances in Concrete through Science and Engineering*. Evanston: Northwestern University, pp.1–8.

Andrade, C. and Andrea, R.D., 2010. Electrical resistivity as microstructural parameter for the modelling of service life of reinforced concrete structures. In: K. van Breguel, G. Ye and Y. Yuan, eds., *2nd International Symposium on Service Life Design for Infrastructure*. Delft: RILEM, pp.379–388.

Andrade, C., Andrea, R.D., Castillo, A. and Castellote, M., 2009. The Use of Electrical Resistivity as NDT Method for the Specification of the durability of Reinforced Concrete. In: *Non-Destructive Testing in Civil Engineering*. Nantes.

Andrade, C., Andrea, R.D., Rebolledo, N., 2014. Chloride ion penetration in concrete: The reaction factor in the electrical resistivity model. *Cement and Concrete Composites*, 47, pp.41–46.

Angst, U., Elsener, B., Larsen, C.K. and Vennesland, Ø., 2009. Critical chloride content in reinforced concrete — A review. *Cement and Concrete Research*, 39(12), pp.1122–1138.

Anon, 2010. *South African Weather Service - Cape Town*. [online] World Weather Information Service. Available at: <http://www.worldweather.org/035/c00138.htm> [Accessed 10 Dec. 2013].

Archie, G., 1942. The electrical resistivity log as an aid in determining some reservoir characteristics. *Transactions of AIME Journal*, 146(99), pp.54–62.

Arya, C. and Xu, Y., 1995. Effect of cement type on chloride binding and corrosion of steel in concrete. *Cement and Concrete Research*, 25(4), pp.893–902.

ASTM Standard C1556, 2011. *Test Method for Determining the Apparent Chloride Diffusion Coefficient of Cementitious Mixtures by Bulk Diffusion*. West Conshohocken, PA: ASTM International.

ASTM Standard C1202, 2012. *Test Method for electrical indication of concrete's ability to resist chloride ion penetration*. West Conshohocken, PA: ASTM International.

ASTM Standard W., 2013. *Test Method for Measuring the Surface Resistivity of Hardened Concrete Using the Wenner Four-Electrode Method*. West Conshohocken, PA: ASTM International.

Atkinson, A. and Nickerson, A., 1984. The diffusion of ions through water-saturated cement. *Journal of materials science*, 19, pp.3068–3078.

Ballim, Y., Alexander, M.G. and Beushausen, H., 2009. Durability of concrete. In: G. Owens, ed., *Fulton's concrete technology*, 9th ed. Midrand: Cement & Concrete Institute, pp.155–188.

Baroghel-Bouny, V., Kinomura, K., Thiery, M. and Moscardelli, S., 2011. Easy assessment of durability indicators for service life prediction or quality control of concretes with high volumes of supplementary cementitious materials. *Cement and Concrete Composites*, 33(8), pp.832–847.

Baroghel-Bouny, V., Nguyen, T.Q. and Dangla, P., 2009. Assessment & prediction of RC structure service life by means of durability indicators & physical/chemical models. *Cement and Concrete Composites*, 31, pp.522–534.

Bertolini, L., 2008. Steel corrosion and service life of reinforced concrete structures. *Structure and Infrastructure Engineering*, 4(2), pp.123–137.

Bertolini, L., Lollini, F. and Redaelli, E., 2011. Comparison of resistance to chloride penetration of different types of concrete through migration and ponding tests. In: C. Andrade and G. Mancini, eds., *Modelling of Corroding Concrete Structures RILEM BOOKSERIES*. Madrid: Springer London.

Beushausen, H. and Alexander, M.G., 2008. The South African durability index tests in an international comparison. *The South African Institution Of Civil Engineering*, 50(1), pp.25–31.

Bijen, J., 1996. Benefits of slag and fly ash. *Construction and Building Materials*, 10(5), pp.309–314.

Brace, W.F., Orange, A.S. and Madden, T.R., 1965. The effect of pressure on the electrical resistivity of water-saturated crystalline rocks. *Journal of Geophysical Research*, 70(22), pp.5669–5678.

Broomfield, J., 2007. *Corrosion of steel in concrete - Understanding, Investigation and Repair*. 2nd ed. London: Taylor & Francis Group.

Broomfield, J. and Millard, S., 2002. Measuring concrete resistivity to assess corrosion rates. *Concrete*, 36(2), pp.37–39.

Buckley, L.J., Carter, M. A., Wilson, M. A. and Scantlebury, J.D., 2007. Methods of obtaining pore solution from cement pastes and mortars for chloride analysis. *Cement and Concrete Research*, 37(11), pp.1544–1550.

Büteführ, M. et al., 2006. On-site investigations on concrete resistivity – a parameter of durability calculation of reinforced concrete structures. *Materials and Corrosion*, 57(12), pp.932–939.

Cabrera, J. and Ghoddoussi, P., 1994. The influence of fly ash on the resistivity and rate of corrosion of reinforced concrete. In: V. Malhotra, ed., *Durability of concrete: Proceedings of the third CANMET-ACI International Conference*. Detroit, Michigan: American Concrete Institute, pp.229–244.

Caré, S., 2008. Effect of temperature on porosity and on chloride diffusion in cement pastes. *Construction and Building Materials*, 22(7), pp.1560–1573.

Castellote, M. et al., 2001. Oxygen and chloride diffusion in cement pastes as a validation of chloride diffusion coefficients obtained by steady-state migration tests. *Cement and Concrete Research*, 31(4), pp.621–625.

Castellote, M. and Andrade, C., 2009. Assessment of the behaviour of concrete in the initiation period of chloride induced corrosion of rebars. In: M.G. Alexander, ed., *Concrete Repair, Rehabilitation and Retrofitting II*. London: Taylor & Francis Group, pp.331–338.

Cerny, R. and Rovnanikova, P., 2002. *Transport processes in concrete*. London: Spon Press.

CHLORTEST, 2005. *Guideline for Practical Use of Methods for Testing the Resistance of Concrete to Chloride Ingress*. Boras.

Cho, S.W. and Chiang, S.C., 2006. Using the chloride migration rate to predict the chloride penetration resistance of concrete. In: M. Konsta-Gdoutos, ed., *Measuring, monitoring and modeling concrete properties*. Springer Netherlands, pp.575–581.

Claisse, P., 2005. Tranport properties of concrete. *Concrete International*, (January), pp.43–48.

Collepardi, M., Marcialis, A. and Turriziani, R., 1972. Penetration of chloride ions into cement pastes and concretes. *Journal of the American Ceramic Society*, 55(10), pp.534–535.

Crank, J., 1979. *The mathematics of diffusion*. Oxford university press.

DuraCrete, 1998. Modelling of Degradation. In: *Probabilistic Performance based durability design of concrete structures*. The European Union - Brite EuRam III, pp.10–38.

DuraCrete, 1999. Compliance Testing for Probabilistic Design Purposes. In: *Probabilistic Performance based durability design of concrete structures*. Gouda, Netherlands: The European Union - Brite EuRam III.

DuraCrete, 2000. General guidelines for durability design and redesign. In: *Probabilistic Performance based durability design of concrete structures*. Gouda, Netherlands: The European Union - Brite EuRam III.

FDOT, 2004. *Florida Method of Test For Concrete Resistivity as an Electrical Indicator of its Permeability*. pp.1–4.

Feldman, R., Chan, G., Brousseau, R. and Tumidajski, P.J., 1994. Investigation of the rapid chloride permeability test. *ACI Materials Journal*, 91(2), pp.246–255.

Feldman, R., Prudencio, L.R. and Chan, G., 1999. Rapid chloride permeability test on blended cement and other concretes: correlations between charge, initial current and conductivity. *Construction and Building Materials*, 13(3), pp.149–154.

Ferreira, R.M., 2004. *Pobability-based durability analysis of concrete structures in marine environment. PhD Thesis*. University of Minho.

Ferreira, R.M. and Jalali, S., 2006. Quality control based on electrical resistivity measurements. In: *ESCS-2006 : European Symposium on Service Life and Serviceability of Concrete Structures : proceedings*. Helsinki, pp.325–332.

Garboczi, E. and Bentz, D., 1992. Computer simulation of the diffusivity of cement-based materials. *Journal of materials science*, 27, pp.2083–2092.

Glass, G. and Buenfeld, N.R., 1997. The presentation of the chloride threshold level for corrosion of steel in concrete. *Corrosion Science*, 39(5), pp.1001–1013.

Gowers, K.R. and Millard, S., 1999. Measurement of concrete resistivity for assessment of corrosion severity of steel using Wenner technique. *ACI Materials Journal*, 96(5), pp.536–541.

Grieve, G., 2009a. Aggregates for concrete. In: G. Owens, ed., *Fulton's concrete technology*, 9th ed. Midrand: Cement & Concrete Institute, pp.25–26.

Grieve, G., 2009b. Cementitious material. In: G. Owens, ed., *Fulton's concrete technology*, 9th ed. Midrand: Cement & Concrete Institute, pp.1–14.

Heiyantuduwa, R., Beushausen, H. and Alexander, M.G., 2006. Prediction models for concrete durability. *Concrete Plant International CPI*, 3, pp.80–88.

Hobbs, D.W., 2000. Aggregate influence on chloride ion diffusion into concrete. *Cement and Concrete Research*, 29(1999), pp.1995–1998.

Hobbs, D.W. and Matthews, J.D., 1998. Minimum requirements for concrete to resist deterioration due to chloride-induced corrosion. In: D.W. Hobbs, ed., *Minimum requirements for durable concrete: Carbonation- and chloride-induced corrosion, freeze-thaw attack and chemical attack*. Berkshire: British Cement Association, pp.43–89.

Hornbostel, K., Larsen, C.K. and Geiker, M.R., 2013. Relationship between concrete resistivity and corrosion rate – a literature review. *Cement and Concrete Composites*.

Icenogle, P.J. et al., 2012. Evaluation of Surface Resistivity Measurements as an Alternative to the Rapid Chloride Permeability Test for Quality Assurance and Acceptance.

Johnson, R., Freund, J. and Miller, I., 2011. *Probability and Statistics for Engineers*. Boston: Prentice Hall.

Kessler, R. et al., 2008. *Surface resistivity as an indicator of concrete chloride penetration resistance*. Florida, pp.1–18.

Kropp, J. and Alexander, M.G., 2007. Transport mechanisms and reference tests. In: R. Torrent and L.F. Luco, eds., *Non-Destructive Evaluation of the Penetrability and thickness of the concrete cover RILEM TC 189-NEC: State-of-the-Art Report*. RILEM Publications SARL.

Lide, D.R. ed., 2005. *CRC Handbook of Chemistry and Physics, Internet Version*. Boca Raton, FL: CRC Press, p.940.

Lindvall, A., 1998. Duracrete – probabilistic performance based durability design of concrete structures. In: *2nd International Symposium in Civil Engineering*. Budapest, pp.1–10.

Liu, Z. and Beaudoin, J.J., 2000. The Permeability of Cement Systems to Chloride Ingress and Related Test Methods. *Cement, Concrete and Aggregates*, 22(1), pp.16–23.

Lu, X., 1997. Application of the Nernst-Einstein equation to concrete. *Cement and Concrete Research*, 27(2), pp.293–302.

Luo, R., Cai, Y., Wang, C. and Huang, X., 2003. Study of chloride binding and diffusion in GGBS concrete. *Cement and Concrete Research*, 33(1), pp.1–7.

Mackechnie, J.R., 1996. *Predictions of reinforced concrete durability in the marine environment. Ph.D. Thesis*. University of Cape Town, Cape Town, South Africa.

Mackechnie, J.R., 2001. *Predictions of reinforced concrete durability in the marine environment - Monograph 1*. Cape Town: Department of Civil Engineering, University of Cape Town.

Mackechnie, J.R. and Alexander, M.G., 1997a. Durability Findings from Case Studies of Marine Concrete Structures. *Cement, Concrete and Aggregates*, 19(1), pp.22–25.

Mackechnie, J.R. and Alexander, M.G., 1997b. Exposure of concrete in different marine environments. *Journal of Materials in Cvil Engineering*, 9(February), pp.41–44.

Mackechnie, J.R. and Alexander, M.G., 2000a. Practical considerations for rapid chloride conductivity testing. In: C. Andrade and J. Kropp, eds., *2nd International RILEM Workshop on Testing and modelling the chloride ingress into concrete*. RILEM Publications SARL, pp.451–460.

Mackechnie, J.R. and Alexander, M.G., 2000b. Rapid chloride test comparisons. *Concrete International*, 22(5), pp.40–49.

Manera, M., Vennesland, Ø. and Bertolini, L., 2008. Chloride threshold for rebar corrosion in concrete with addition of silica fume. *Corrosion Science*, 50(2), pp.554–560.

Mangat, P.S. and Molloy, B.T., 1994. Prediction of long term chloride concentration in concrete. *Materials and Structures*, 27(6), pp.338–346.

Marchand, J. and Samson, E., 2009. Predicting the service-life of concrete structures – Limitations of simplified models. *Cement and Concrete Composites*, 31(8), pp.515–521.

McCarter, W.J., Ezirim, H. and Emerson, M., 1992. Absorption of water and chloride into concrete. *Magazine of Concrete Research*, 44(158), pp.31–37.

McCarter, W.J., Forde, M.C. and Whittington, H.W., 1981. Resistivity characteristics of concrete. *Proceedings of the Institution of Civil Engineers*, 71(2), pp.107–117.

McDuff, R.E. and Ellis, R.A., 1979. Determining diffusion coefficients in marine sediments: A laboratory study of the validity of resistivity techniques. *American Journal of Science*, 279(Jun), pp.666–675.

Mehta, P. and Monteiro, P., 2006. *Concrete*. 3rd ed. McGraw Hill.

Montgomery, D.C. and Runger, G.C., 2003. *Applied Statistics and Probability for Engineers Third Edition*. 3rd ed. New York: John Wiley & Sons, Inc.

Morris, W., Moreno, E. and Sagues, A., 1996. Practical evaluation of resistivity of concrete in test cylinders using a wenner array probe. *Cement and Concrete Research*, 26(12), pp.1779–1787.

Morris, W., Vico, A., Vazquez, M. and de Sanchez, S., 2002. Corrosion of reinforcing steel evaluated by means of concrete resistivity measurements. *Corrosion Science*, 44(1), pp.81–99.

Muigai, R., 2008. *Probabilistic modelling for durability design of reinforced concrete structures. Masters Thesis*. University of Cape Town, Cape Town, South Africa.

Muigai, R., Moyo, P. and Alexander, M.G., 2012. Durability design of reinforced concrete structures: a comparison of the use of durability indexes in the deemed-to-satisfy approach and the full-probabilistic approach. *Materials and Structures*, 45(8), pp.1233–1244.

Ngala, V. and Page, C., 1997. Effects of Carbonation on pore structure and Diffusional properties of hydrated cement pastes. *Cement and Concrete Research*, 27(7), pp.995–1007.

Nokken, M.R., Boddy, A., Hooton, R.D. and Thomas, M.D.A., 2006. Time dependent diffusion in concrete—three laboratory studies. *Cement and Concrete Research*, 36(1), pp.200–207.

Nokken, M.R., Boddy, A., Wu, X. and Hooton, R.D., 2008. Effects of Temperature, Chemical, and Mineral Admixtures on the electrical conductivity of concrete. *Journal of ASTM International*, 5(5), pp.1–9.

Nokken, M.R. and Hooton, R.D., 2007. Using pore parameters to estimate permeability or conductivity of concrete. *Materials and Structures*, 41(1), pp.1–16.

NT Build 443, N., 1995. *Hardened concrete accelerated chloride penetraton test method*.

NT Build 492, N., 1999. *Concrete, Mortar and Cement-based repair materials: Chloride Migration Coefficient from Non-Steady-State Migration Experiments*.

Oh, B.H. and Jang, S.Y., 2004. Prediction of diffusivity of concrete based on simple analytic equations. *Cement and Concrete Research*, 34(3), pp.463–480.

Oh, B.H., Jang, S.Y. and Shin, Y.S., 2003. Experimental investigation of the threshold chloride concentration for corrosion initiation in reinforced concrete structures. *Magazine of Concrete Research*, 55(2), pp.117–124.

Osterminski, K., Schießl, P., Volkwein, a. and Mayer, T.F., 2006. Modelling reinforcement corrosion – usability of a factorial approach for modelling resistivity of concrete. *Materials and Corrosion*, 57(12), pp.926–931.

Otieno, M., 2014. *The development of empirical chloride-induced corrosion rate prediction models for cracked and uncracked steel reinforced concrete structures in the marine tidal zone.* Unpublished PhD Thesis. University of Cape Town, Cape Town, South Africa.

Otieno, M., Beushausen, H. and Alexander, M.G., 2011a. Modelling corrosion propagation in reinforced concrete structures – A critical review. *Cement and Concrete Composites*, 33(2), pp.240–245.

Otieno, M., Beushausen, H. and Alexander, M.G., 2011b. Prediction of corrosion rate in reinforced concrete structures - a critical review and preliminary results. *Materials and Corrosion*.

Pacheco, J., Napoles-Morales, O. and Polder, R.B., 2012. Statistical analysis of electrical resistivity as a tool for estimating cement type of 12-year-old concrete specimens. In: M.G. Alexander, H. Beushausen, F. Dehn and P. Moyo, eds., *Concrete Repair, Rehabilitation and Retrofitting III*. Cape Town: Taylor & Francis Group, pp.701–706.

Pfeifer, D., McDonald, D. and Krauss, D., 1994. The rapid chloride permeability test and its correlation to the 90-day chloride ponding test. *Precast/Prestressed Concrete Institute*, 37 - 47(January - February).

Polder, R.B., 1995. Chloride diffusion and resistivity testing of five concrete mixes for marine environment. In: *1st RILEM workshop on chloride penetration into concrete*. Saint-Rémy-lès-Chevreuse, pp.225–233.

Polder, R.B., 2001. Test methods for on site measurement of resistivity of concrete: *Construction and Building Materials*, 15(RILEM TC-154 technical recommendation), pp.125–131.

Polder, R.B., 2005. Durability of marine concrete structures – field investigations and modelling. *HERON*, 50(3), pp.133–153.

Polder, R.B., 2009. Critical chloride content for reinforced concrete and its relationship to concrete resistivity. *Materials and Corrosion*, 60(8), pp.623–630.

Polder, R.B. and Peelen, W.H., 2002. Characterisation of chloride transport and reinforcement corrosion in concrete under cyclic wetting and drying by electrical resistivity. *Cement and Concrete Composites*, 24(5), pp.427–435.

Polder, R.B., Wegen, G. van der and Breugel, K. Van, 2010. Guideline for service life design of structural concrete with regard to chloride induced corrosion - the approach in the Netherlands. In: K. Van Breugel, G. Ye and Y. Yuan, eds., *2nd International Symposium on Service Life Design for Infrastructure*. Delft: RILEM, pp.265–272.

Poulsen, E. and Mejlbro, L., 2006. *Diffusion of chloride in concrete*. New York: Taylor & Francis Group.

Prince, W., Pérami, R. and Espagne, M., 1999. Mechanisms involved in the accelerated test of chloride permeability. *Cement and Concrete Research*, 29(5), pp.687–694.

Quinn, G. and Keough, M., 2002. *Experimental Design and Data Analysis for Biologists*. Cambridge: Cambridge University Press.

Rajabipour, F. and Weiss, J., 2006. Electrical conductivity of drying cement paste. *Materials and Structures*, 40(10), pp.1143–1160.

Rear, B.K. et al., 2010. *Report on Performance-Based requirements for concrete*. Chicago, pp.1 – 42.

Reichling, K. et al., 2013. Full surface inspection methods regarding reinforcement corrosion of concrete structures. *Materials and Corrosion*, 64(2), pp.116–127.

Riding, K.A. et al., 2008. Simplified Concrete Resistivity and Rapid Chloride Permeability Test Method. *ACI Materials Journal*, July-Augus(105), pp.390–394.

Romer, M., 2005. Recommendation of RILEM TC 189-NEC "Non-destructive evaluation of the concrete cover": Comparative test - Part I: Comparative test of "penetrability" methods. *Materials and Structures*, 38(284), pp.895–906.

Rooij, M.R. De, Polder, R.B. and Oosten, van H.H., 2007. Validation of service life performance of in situ concrete by TEM and RCM measurements. *HERON*, 52(4), pp.225–238.

Saleem, M., Shameem, M., Hussain, S.E. and Maslehuddint, M., 1996. Effect of moisture, chloride and sulphate contamination on the electrical resistivity of Portland cement concrete. *Construction and Building Materials*, 10(3), pp.209–214.

SANS Standard 10100-2, 1992. *The structural use of concrete: materials and execution of work.* Pretoria: The South African Bureau of Standards.

Scott, A., 2004. *The Influence of Binder Type and Cracking on Reinforcing Steel Corrosion in Concrete. PhD Thesis*. Univeristy of Cape Town.

Sengul, O. and Gjorv, O.E., 2008. Electrical resistivity measurements for quality control during concrete construction. *ACI Materials Journal*, 105(6), pp.541–547.

Sengul, O. and Gjorv, O.E., 2009. Effect of embedded steel on electrical resistivity measurements on concrete structures. *ACI Materials Journal*, 106(1), pp.11–18.

Sharfuddin A.M., Kayali, O. and Anderson, W., 2008. Chloride penetration in binary and ternary blended cement concretes as measured by two different rapid methods. *Cement and Concrete Composites*, 30(7), pp.576–582.

Shi, X., Xie, N., Fortune, K. and Gong, J., 2012. Durability of steel reinforced concrete in chloride environments: An overview. *Construction and Building Materials*, 30, pp.125–138.

Silva, J., Jalali, S. and Ferreira, R.M., 2006. Estimating electrical resistivity based on early age measurements. In: V. Baroghel-Bouny, C. Andrade, R. Torrent and K.L. Scrivener, eds., *International RILEM Workshop on Performance based evaluation and indicators for concrete durability*. Madrid: RILEM, pp.67–74.

Sirieix, C., Breysse, D. and Frappa, M., 2003. Improvement of electrical resistivity measurement for non destructive evaluation of concrete structures. In: *2nd RILEM Workshop, Paris*. pp.93–102.

Smith, K., Schokker, A. and Tikalsky, P., 2004. Performance of supplementary cementitious materials in concrete resistivity and corrosion monitoring evaluations. *ACI Materials Journal*, 101(5), pp.385–390.

Snyder, K., Feng, X., Keen, B. and Mason, T., 2003. Estimating the electrical conductivity of cement paste pore solutions from OH−, K+ and Na+ concentrations. *Cement and Concrete Research*, 33(6), pp.793–798.

Song, H.-W., Lee, C.-H. and Ann, K.Y., 2008. Factors influencing chloride transport in concrete structures exposed to marine environments. *Cement and Concrete Composites*, 30(2), pp.113–121.].

Stanish, K., Alexander, M.G. and Ballim, Y., 2006. Assessing the repeatability and reproducibility values of South African. *Journal Of The South African Institution Of Civil Engineering*, 48(2), pp.10–17.

Stanish, K., Hooton, R.D. and Thomas, M.D.A., 2002. *Testing the chloride penetration resistance of concrete: A literature review*. Toronto.

Stanish, K. and Thomas, M., 2003. The use of bulk diffusion tests to establish time-dependent concrete chloride diffusion coefficients. *Cement and Concrete Research*, 33(1), pp.55–62.

Streicher, P.E., 1997. *The development of a rapid chloride test for concrete, and its use in engineering practice*. University of Cape Town.

Streicher, P.E. and Alexander, M.G., 1995. A chloride conduction test for concrete. *Cement and Concrete Research*, 25(6), pp.1284–1294.

Streicher, P.E. and Alexander, M.G., 1999. Towards Standardization of a Rapid Chloride Conduction Test for Concrete. *Cement, Concrete and Aggregates*, 21(1), pp.23–30.

Suprenant, B., 1991. Testing for chloride permeability of concrete. *Concrete Construction*, pp.531–533.

Thomas, M., 1996. Chloride thresholds in marine concrete. *Cement and Concrete Research*, 26(4), pp.513–519.

Thomas, M.D.A. and Bamforth, P.B., 1999. Modelling chloride diffusion in concrete Effect of fly ash and slag. *Cement and Concrete Research*, 29, pp.487–495.

Thomas, M.D.A., Hooton, R.D., Scott, A. and Zibara, H., 2012. The effect of supplementary cementitious materials on chloride binding in hardened cement paste. *Cement and Concrete Research*, 42, pp.1–7.

Tumidajski, P.J. et al., 1996. On the relationship between porosity and electrical resistivity in cementitious systems. *Cement and Concrete Research*, 26(4), pp.539–544.

Tuutti, K., 1980. Service life of structures with regard to corrosion of embedded steel. *ACI Special Publication*, 65.

Val, D. V. and Stewart, M.G., 2009. Reliability Assessment of Ageing Reinforced Concrete Structures—Current Situation and Future Challenges. *Structural Engineering International*, 19(2), pp.211–219.

Weydert, R. and Gehlen, C., 1999. Electrolytic resistivity of cover concrete: Relevance, measurement and interpretation. In: M. Lacasse and D. Vanier, eds., *Durability of Building Materials and Components 8: Service life and durability of materials and components 1*. Vancouver: National Research Council, Canada, pp.409–419.

Whiting, D., 1981. *Rapid determination of the chloride permeability of concrete*. Skokie, Illinois.

Yuan, Q., Shi, C., Schutter, G. De and Audenaert, K., 2009. Effect of temperature on transport of chloride ions in concrete. In: M.G. Alexander, H. Beushausen, F. Dehn and P. Moyo, eds., *Concrete Repair, Rehabilitation and Retrofitting II*. London: Taylor & Francis Group, pp.345–352.

APPENDIX A: DATA AND RESULTS

The figure below was used to gauge the weather patterns that field concrete specimens were exposed to.

Figure A. 1: Cape Town temperature and precipitation means

(South African Weather Service - Cape Town, 2010)

Month	Mean Temperature °C		Mean Total Precipitation (mm)	Mean Number of Precipitation Days
	Daily Minimum	Daily Maximum		
Jan	15.7	26.1	15	5.5
Feb	15.6	26.5	17	4.6
Mar	14.2	25.4	20	4.8
Apr	11.9	23.0	41	8.3
May	9.4	20.3	69	11.4
Jun	7.8	18.1	93	13.3
Jul	7.0	17.5	82	11.8
Aug	7.5	17.8	77	13.7
Sep	8.7	19.2	40	10.4
Oct	10.6	21.3	30	8.7
Nov	13.2	23.5	14	4.9
Dec	14.9	24.9	17	6.2

All the corrosion initiation periods (CIP's) calculated from the CCT and surface concrete resistivity SLP models are presented in the table below.

Table A. 1: CIP's for resistivity and CCT, extreme exposure at 20 to 60 mm cover depth

		Corrosion initiation period (years)				
Model	***Cover (mm)***	***PC-40***	***SL-40***	***SL-55***	***FA-40***	***FA-55***
Resistivity	20	4	32	29	43	23
	30	9	72	65	97	51
	40	15	129	115	172	91
	50	24	201	180	268	143
	60	34	290	259	387	205
CCT	20	4	26	17	20	10
	30	8	58	39	45	23
	40	14	104	70	81	41
	50	22	162	109	126	64
	60	32	234	157	181	92

The diffusion coefficients calculated from the chloride conductivity measurements and model are listed in the table below.

Table A. 2: Diffusion coefficients from CCT model *($x10^{-12}$ m^2/s)*

Age (days)	*PC-40*	*SL-40*	*SL-55*	*FA-40*	*FA-55*
80	2.67	3.13	4.21	4.35	7.12
94	2.55	2.80	3.77	3.90	6.39
108	2.45	2.55	3.43	3.55	5.81
122	2.37	2.35	3.16	3.26	5.35
136	2.29	2.18	2.93	3.03	4.96
150	2.23	2.04	2.74	2.83	4.64
164	2.17	1.92	2.58	2.67	4.37
178	2.12	1.81	2.44	2.52	4.13
192	2.07	1.72	2.32	2.40	3.93
206	2.03	1.64	2.21	2.28	3.74
220	1.99	1.57	2.12	2.19	3.58
234	1.96	1.51	2.03	2.09	3.43
248	1.93	1.45	1.95	2.01	3.30
262	1.90	1.39	1.88	1.94	3.18
276	1.87	1.35	1.81	1.87	3.07
290	1.84	1.30	1.75	1.81	2.97
304	1.82	1.26	1.70	1.75	2.87
318	1.79	1.22	1.65	1.70	2.79
332	1.77	1.19	1.60	1.65	2.71
346	1.75	1.15	1.55	1.61	2.63
360	1.73	1.12	1.51	1.56	2.56
374	1.71	1.10	1.47	1.52	2.50
388	1.69	1.07	1.44	1.49	2.43
402	1.67	1.04	1.40	1.45	2.38
416	1.66	1.02	1.37	1.42	2.32
430	1.64	1.00	1.34	1.38	2.27
444	1.63	0.97	1.31	1.36	2.22
458	1.61	0.95	1.28	1.33	2.17
472	1.60	0.94	1.26	1.30	2.13
486	1.58	0.92	1.23	1.27	2.09
500	1.57	0.90	1.21	1.25	2.05
514	1.56	0.88	1.19	1.23	2.01
528	1.55	0.87	1.17	1.21	1.97
542	1.54	0.85	1.15	1.18	1.94
556	1.52	0.84	1.13	1.16	1.91
570	1.51	0.82	1.11	1.14	1.87
584	1.50	0.81	1.09	1.12	1.84
598	1.49	0.80	1.07	1.11	1.81
612	1.48	0.78	1.05	1.09	1.79
626	1.47	0.77	1.04	1.07	1.76

The diffusion coefficients calculated from the surface concrete resistivity measurements and model are listed in the table below.

Table A. 3: Diffusion coefficients from resistivity model *($x10^{-12}$ m^2/s)*

Age (days)	*PC-40*	*SL-40*	*SL-55*	*FA-40*	*FA-55*
80	4.15	1.07	1.43	0.63	1.71
94	5.18	0.95	1.90	0.71	1.90
108	3.46	0.82	1.43	0.57	1.56
122	2.96	0.95	1.07	0.53	1.43
136	4.15	0.90	1.22	0.50	1.71
150	2.96	0.82	0.95	0.55	1.43
164	3.46	0.71	1.22	0.45	1.71
178	2.30	0.66	1.14	0.41	1.43
192	2.96	0.49	0.74	0.38	1.32
206	2.30	0.53	0.71	0.40	1.14
220	2.96	0.48	0.90	0.36	1.22
234	2.30	0.61	0.68	0.31	0.95
248	2.07	0.46	0.61	0.38	1.14
262	1.73	0.44	0.53	0.32	1.07
276	2.30	0.41	0.63	0.35	0.95
290	2.07	0.36	0.66	0.31	0.74
304	2.30	0.40	0.61	0.29	0.90
318	1.88	0.33	0.53	0.31	0.95
332	2.59	0.32	0.50	0.29	0.71
346	1.59	0.35	0.61	0.27	0.78
360	1.88	0.32	0.43	0.25	0.68
374	2.07	0.33	0.37	0.24	0.71
388	1.73	0.37	0.46	0.25	0.86
402	1.48	0.31	0.40	0.24	0.55
416	1.88	0.30	0.37	0.24	0.59
430	1.59	0.28	0.36	0.23	0.49
444	1.73	0.28	0.38	0.22	0.61
458	1.48	0.29	0.36	0.23	0.57
472	1.38	0.27	0.44	0.21	0.53
486	1.15	0.26	0.36	0.23	0.49
500	1.59	0.26	0.34	0.23	0.57
514	1.48	0.27	0.36	0.21	0.53
528	1.22	0.24	0.32	0.21	0.46
542	1.38	0.23	0.31	0.22	0.49
556	1.30	0.24	0.34	0.21	0.48
570	1.22	0.25	0.32	0.21	0.45
584	1.30	0.24	0.30	0.21	0.49
598	1.04	0.23	0.28	0.21	0.43
612	0.99	0.22	0.30	0.19	0.38
626	0.94	0.22	0.30	0.20	0.45

The ratio of the diffusion coefficients calculated from the surface concrete resistivity and chloride conductivity models (from Tables A.3 and A.2) are listed in the table below.

Table A. 4: Ratio of diffusion coefficients

Age (days)	*PC-40*	*SL-40*	*SL-55*	*FA-40*	*FA-55*
80	0.64	2.92	2.95	6.85	4.16
94	0.49	2.95	1.98	5.46	3.36
108	0.71	3.13	2.41	6.21	3.73
122	0.80	2.47	2.95	6.10	3.75
136	0.55	2.42	2.40	6.02	2.90
150	0.75	2.50	2.88	5.13	3.26
164	0.63	2.69	2.11	5.92	2.55
178	0.92	2.76	2.14	6.19	2.90
192	0.70	3.53	3.12	6.30	2.98
206	0.88	3.07	3.10	5.74	3.28
220	0.67	3.31	2.35	6.00	2.93
234	0.85	2.46	2.96	6.73	3.61
248	0.93	3.13	3.19	5.30	2.89
262	1.10	3.18	3.51	6.12	2.97
276	0.81	3.31	2.86	5.36	3.23
290	0.89	3.65	2.66	5.82	3.99
304	0.79	3.17	2.78	6.05	3.19
318	0.95	3.71	3.08	5.46	2.93
332	0.68	3.68	3.18	5.79	3.80
346	1.10	3.30	2.54	5.91	3.38
360	0.92	3.55	3.54	6.21	3.74
374	0.82	3.33	3.96	6.40	3.50
388	0.98	2.87	3.11	5.99	2.84
402	1.13	3.41	3.52	6.10	4.30
416	0.88	3.39	3.69	5.88	3.93
430	1.03	3.61	3.76	5.91	4.64
444	0.94	3.53	3.45	6.10	3.63
458	1.09	3.29	3.53	5.81	3.81
472	1.16	3.44	2.87	6.08	3.98
486	1.38	3.48	3.46	5.51	4.27
500	0.99	3.47	3.53	5.48	3.59
514	1.05	3.30	3.26	5.73	3.76
528	1.27	3.59	3.68	5.77	4.27
542	1.11	3.63	3.75	5.39	3.96
556	1.18	3.42	3.35	5.57	4.01
570	1.24	3.31	3.49	5.54	4.16
584	1.16	3.40	3.69	5.32	3.77
598	1.44	3.49	3.88	5.37	4.24
612	1.50	3.52	3.51	5.60	4.69
626	1.56	3.52	3.52	5.39	3.90
Average	0.97	3.25	3.14	5.84	3.62
Std. Dev	0.25	0.36	0.52	0.39	0.53
Minimum	0.49	2.42	1.98	5.13	2.55
Maximum	1.56	3.71	3.96	6.73	4.69

The surface concrete resistivity measurements used as input parameters in the corrosion initiation period and diffusion coefficient models are listed below.

Table A. 5: Surface concrete resistivity (laboratory) results from Otieno (2014)

		Mix (kΩcm)				
	Age (days)	***PC-40***	***SL-40***	***SL-55***	***FA-40***	***FA-55***
28/07/2011	**80**	5	16	12	27	10
11/08/2011	**94**	4	18	9	24	9
25/08/2011	**108**	6	21	12	30	11
08/09/2011	**122**	7	18	16	32	12
22/09/2011	**136**	5	19	14	34	10
06/10/2011	**150**	7	21	18	31	12
20/10/2011	**164**	6	24	14	38	10
03/11/2011	**178**	9	26	15	42	12
17/11/2011	**192**	7	35	23	45	13
01/12/2011	**206**	9	32	24	43	15
15/12/2011	**220**	7	36	19	47	14
29/12/2011	**234**	9	28	25	55	18
12/01/2012	**248**	10	37	28	45	15
26/01/2012	**262**	12	39	32	54	16
09/02/2012	**276**	9	42	27	49	18
23/02/2012	**290**	10	48	26	55	23
08/03/2012	**304**	9	43	28	59	19
22/03/2012	**318**	11	52	32	55	18
05/04/2012	**332**	8	53	34	60	24
19/04/2012	**346**	13	49	28	63	22
03/05/2012	**360**	11	54	40	68	25
17/05/2012	**374**	10	52	46	72	24
31/05/2012	**388**	12	46	37	69	20
14/06/2012	**402**	14	56	43	72	31
28/06/2012	**416**	11	57	46	71	29
12/07/2012	**430**	13	62	48	73	35
26/07/2012	**444**	12	62	45	77	28
09/08/2012	**458**	14	59	47	75	30
23/08/2012	**472**	15	63	39	80	32
06/09/2012	**486**	18	65	48	74	35
20/09/2012	**500**	13	66	50	75	30
04/10/2012	**514**	14	64	47	80	32
18/10/2012	**528**	17	71	54	82	37
01/11/2012	**542**	15	73	56	78	35
15/11/2012	**556**	16	70	51	82	36
29/11/2012	**570**	17	69	54	83	38
13/12/2012	**584**	16	72	58	81	35
27/12/2012	**598**	20	75	62	83	40
10/01/2013	**612**	21	77	57	88	45
24/01/2013	**626**	22	78	58	86	38

APPENDIX B: EBE FACULTY ASSESSMENT OF ETHICS IN RESEARCH PROJECTS

Name of Principal Researcher/Student: **Lombe Mutale** Department: **Civil Engineering**

Preferred email address of applicant: **lombe.mutale@gmail.com**

If a Student: Degree: **MSc. Civil Engineering** Supervisor: **A/Prof. Beushausen**

If a Research Contract indicate source of funding/sponsorship: **N/A**

Research Project Title: **An investigation of the relationship between surface concrete resistivity and chloride conductivity tests**

Overview of ethics issues in your research project:

Question 1: Is there a possibility that your research could cause harm to a third party (i.e. a person not involved in your project)?	YES	**NO**
Question 2: Is your research making use of human subjects as sources of data? If your answer is YES, please complete Addendum 2.	YES	**NO**
Question 3: Does your research involve the participation of or provision of services to communities? If your answer is YES, please complete Addendum 3.	YES	**NO**
Question 4: If your research is sponsored, is there any potential for conflicts of interest? If your answer is YES, please complete Addendum 4.	YES	**NO**

If you have answered YES to any of the above questions, please append a copy of your research proposal, as well as any interview schedules or questionnaires (Addendum 1) and please complete further addenda as appropriate.

I hereby undertake to carry out my research in such a way that

- there is no apparent legal objection to the nature or the method of research; and
- the research will not compromise staff or students or the other responsibilities of the University;
- the stated objective will be achieved, and the findings will have a high degree of validity;
- limitations and alternative interpretations will be considered;
- the findings could be subject to peer review and publicly available; and
- I will comply with the conventions of copyright and avoid any practice that would constitute plagiarism.

Signed by:	Full name and signature	Date
Principal Researcher/Student:		

This application is approved by:

Supervisor (if applicable):		
HOD (or delegated nominee): Final authority for all assessments with NO to all questions and for all undergraduate research.		
Chair : Faculty EIR Committee For applicants other than undergraduate students who have answered YES to any of the above questions.		